Wind load on canopies attached to buildings of different heights

Faruk Ahmed Sakib

A Thesis in
The Department of
Building, Civil and Environmental Engineering

Presented in Partial Fulfillment of the Requirements
for the Degree of Master of Applied Science (Civil Engineering)
at Concordia University, Montreal, Quebec, Canada

September 2020

CONCORDIA UNIVERSITY

School of Graduate Studies

This is to certify that the thesis prepared

By: Faruk Ahmed Sakib

Entitled: Wind load on canopies attached to buildings of different heights

and submitted in partial fulfillment of the requirements for the degree of

Master of Applied Science (Civil Engineering)

complies with the regulations of the University and meets the accepted standards with respect to originality and quality.

Signed by the final Examining Committee:

Dr. Ashutosh Bagchi	Chair
Dr. Georgios H. Vatistas	Examiner
Dr. Lucia Tirca	External (to program) Examiner
Dr. Anjan Bhowmick	Supervisor
Dr. Theodore Stathopoulos	

Approved by _____

Dr. Michelle Nokken, GPD
Department of Building, Civil and Environmental Engineering

_____

Dr. Mourad Debbabi, Interim Dean
Gina Cody School of Engineering and Computer Science

Date   _____

Abstract

Wind load on canopies attached to buildings of different heights

Faruk Ahmed Sakib

Residential and industrial buildings commonly have various types of overhangs attached to their walls for the conveniences of their users. These overhangs have different names like canopy, patio cover, porch etc. Depending on their locations, canopies are very prone to wind due to the suction developing on their upper surface along with the pressure occurring on their lower surface (for most wind directions), which together may generate critical uplift forces causing lots of damage on these non-structural elements. Very limited studies have been carried out on wind loading on attached canopies. Current ASCE 7-16 provides a procedure for calculation of wind loading on attached canopies. These provisions include a chart to find out both upward and downward wind pressures on the attached canopy. It should be noted that ASCE provisions have limitations and are only applicable for buildings up to 60 ft high. Past and recent studies on this topic have also been limited to low-rise buildings only. Thus, structural engineers have long been asking for guidance for estimation of wind loads that may act on canopies in tall buildings. In addition, the effect of canopy width has not been investigated thoroughly.

This thesis presents a study on the effect of wind loading on attached canopies in tall buildings. In this study, high-rise (37 meters) buildings were tested with canopy attached to the wall at different heights. Canopy with different widths were also tested. In addition to the high-rise building (37 m), canopies attached to two other building heights (18.5 m and 7 m) were considered. The test program, which was carried out in the Wind Tunnel Laboratory of Concordia University, Montreal, shows that canopy attached at the top of a tall building may experience 70% more suction than that of a low-rise building. In addition, this thesis also presents the effect of building height, canopy height, wind angle of attack and effect of considered area on wind loading on canopy, which will help structural engineers better understand the behavior of canopies under wind loads both in low-rise and taller buildings. Design provisions for appropriate wind forces for canopies in taller buildings are also provided at the end of this thesis to help the structural engineers

ACKNOWLEDGMENTS

Contents

List of Figures

List of Table

Chapter 1   Introduction

1.1 Overview

An attached canopy is a horizontal, roof type component attached to the exterior wall of a building. The area under these are not surrounded by walls. This kind of non-structural attachments are common with low and high-rise buildings as they shield the residents from weather conditions such as direct sunlight, snow, rain and facilitate recreational purposes. Figure 1.1 shows canopy attached to the wall of a low-rise residential building. The wall to which the canopy is attached is referred to as the parent wall and the building is called as the parent building. Both upper and lower surfaces of a canopy is subjected to simultaneous wind pressure. In the worst-case scenario, the induced-wind pressure top and bottom of the overhang will generate forces in the same direction resulting in magnified net pressure acting on the overhang. Moreover, canopies are generally light weight. Thus, wind loading is the most critical loading while designing a canopy. Not only an under-designed canopy can be damaged by strong wind (see Fig. 1.2), but it can also turn into a projectile which is a strong threat to the neighboring buildings. Unfortunately, studies are limited and have been conducted to investigate mainly the wind pressures on canopies attached to buildings of relatively low height (3.5 m < h <10.5 m, where h is the building height). Also, limited design provisions for canopies are currently provided in the national wind codes and standards. Currently, there is very limited knowledge as of what the proper design loads should be for these types of structures. National Building Code of Canada 2015 (NBCC) does not have any design provision for attached canopy. American Society of Civil Engineers Standard (ASCE 7-16) has established a design provision for attached canopies for building height up to 18 meters.

Figure 1.1 Canopy attached to the wall of a low-rise residential building, source:
https://images.homedepot-static.com/productImages/cffd8836-295b-44ee-bbb6-88358a2f6200/svn/whites-integra-patio-covers-1251006701220-64_1000.jpg (27 August, 2020)

Figure 1.2 Canopy destroyed by hurricane wind (Candelario 2012)

Several codes and standards from other parts of the world do provide wind loading design guidelines for attached canopies (sometimes referred to as awnings), i.e. Australian/New Zealand Standard (AS/NZS 1170.2, 2011), Indian Standard (IS: 875, Part 3, 2015), German code (DIN 2010).

However, designs provisions for canopy from the above-mentioned codes and standards display some discrepancy and limitations when compared with each other. Also, due to lack of studies regarding canopy attached to buildings having heights more than 18 meters, designers and practitioners are looking for guidance on how to design canopy attached to tall buildings. A comprehensive study can help expanding the knowledge of wind loading on attached canopies. A thorough understanding on this topic can help effective assessment of economical and safety aspects of the design and construction of attached canopy whilst ensuring the integrity of the parent structure.

1.2 Scope and objectives

This thesis is aimed to expand our knowledge of wind loading effect on attached canopies. To fulfill this aim, model canopies attached to model buildings of different heights are tested in the Boundary Layer Wind Tunnel (BLWT) of Concordia University. The acquired data of wind pressure is analysed against various parameters, i.e. different relative dimensions of the canopy and parent building. A parametric study which aims to expand current knowledge on the wind loading design of canopies attached to low-rise buildings is also conducted. Data of wind induced pressures have been obtained at both upper and lower surfaces of the canopy for an array of geometrical configurations and wind directions. While designing the main structural part of the canopy, simultaneous pressure from both upper and lower surface is required, for designing of components and cladding, separate upper and lower pressures are used. The principal

objective of this study is to provide wind loading design guidelines for canopies attached to building of different height including taller buildings. These guidelines could be considered for implementation on future wind standards and building codes of practice. Comparisons between the findings of the present study and the available international studies and design guidelines are also presented to identify possible inconsistencies and limitations.

1.3 Thesis organisation

Chapter 2 consists of the literature review. A discussion of the pertinent studies currently available is provided as well as a justification for the present study.

Chapter 3 presents the experimental methodology performed to achieve the objectives of this thesis. The concept of a Boundary Layer Wind Tunnel (BLWT) and proper simulation of the boundary layer is explained. The features of the BLWT at Concordia University's Building Aerodynamics Laboratory and the flow properties used for the experiment are presented. Finally, the fabrication details of the building and attached canopy model as well as the parameters and configurations tested are described.

Chapter 4 presents the analyses of the experimental results for both peak local and area averaged suctions on both upper and lower surfaces of the attached canopy. The relationships between the peak pressures and the variation of critical parameters are presented. The area-averaging effect for the peak suctions obtained for every configuration are summarized for the upper and lower surfaces of the canopy.

Chapter 5 analyses the experimental results for both peak local and area averaged net pressure coefficients. The patterns observed are expanded upon by the use of contour plots. The relationships between the peak pressures and the variation of each isolated parameter are

discussed. Comparisons between the experimental data of the present study to previous studies are also presented. Consequently, the peak net pressure coefficients obtained for every configuration are summarized into one Figure.

In Chapter 6, the experimental findings are summarized into design recommendations to be considered for implementation in the building codes and standards. Subsequently, comparisons between the recommended design guidelines of the present study and the other available provisions are made.

Finally, conclusions, limitations, and recommendations for future research on the subject are presented in Chapter 7.

Chapter 2   Literature Review

There are some available studies regarding the wind loading on attached canopies. Most studies were conducted on low-rise building models. Some national building codes and standard provide design guidelines for attached canopies. In this chapter, the available design provisions for attached canopies has been described and compare with each other along with available past and recent studies regarding wind loading on attached canopies.

2.1   Past and recent studies on canopies attached to buildings

Researchers are trying to understand the wind loading effect on attached canopies by conducting studies using various buildings and canopy configurations. The available research, their brief description of methodology and results are discussed below.

2.1.1   Effect of wind on canopies attached to arch-roof industrial buildings

Paluch et al. (2003) studied the effect of canopies attached to industrial arch-roof buildings. Six scale models were used, with five types of canopies attached. Three of these canopies were instrumented and the static wind pressures were measured. The tests were done at the BLWT of the Universidade Federal do Rio Grande do Sul. The study showed that canopy plays no role on the pressure distribution on roof for 0° wind incidence; but if the wind direction has any other value, the canopy influences the pressure distribution on the roof. For the design of canopies, the study proposed pressure coefficient values for two wind direction (0 and 90 degrees).

2.1.2   Standard recording of wind effects on canopies

Hölscher et al. (2007) studied the wind loads on attached canopies in the boundary layer wind tunnel of Ruhr-Universität Bochum. They used models with various geometries, i.e. different

canopy height to width ratios. Their exposure category was suburban. The study provided net Cp

values
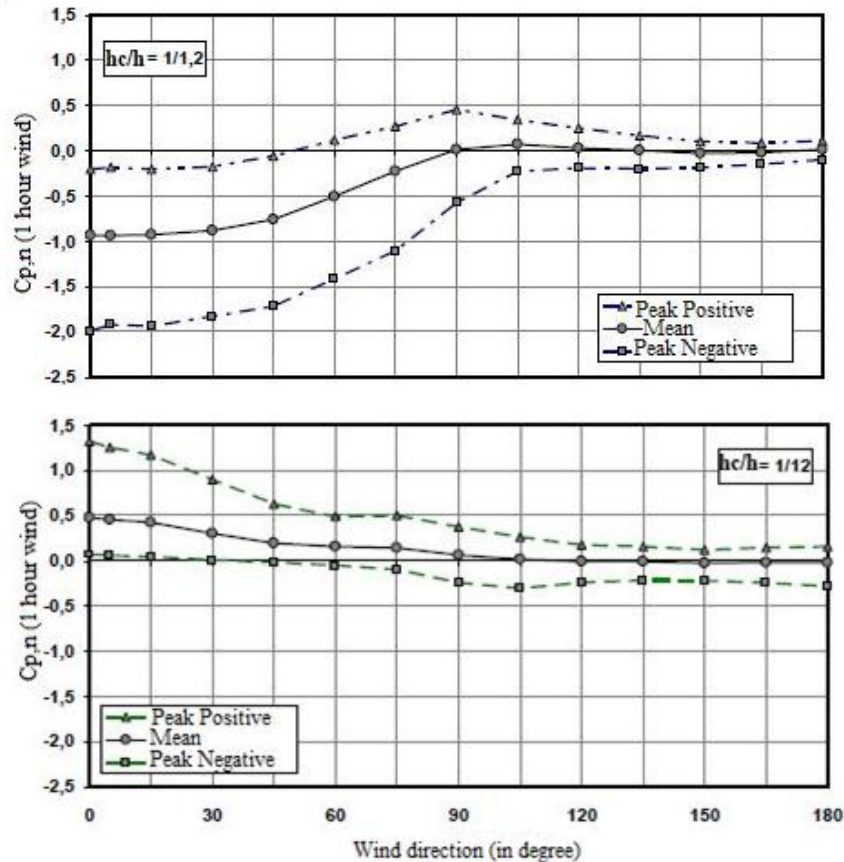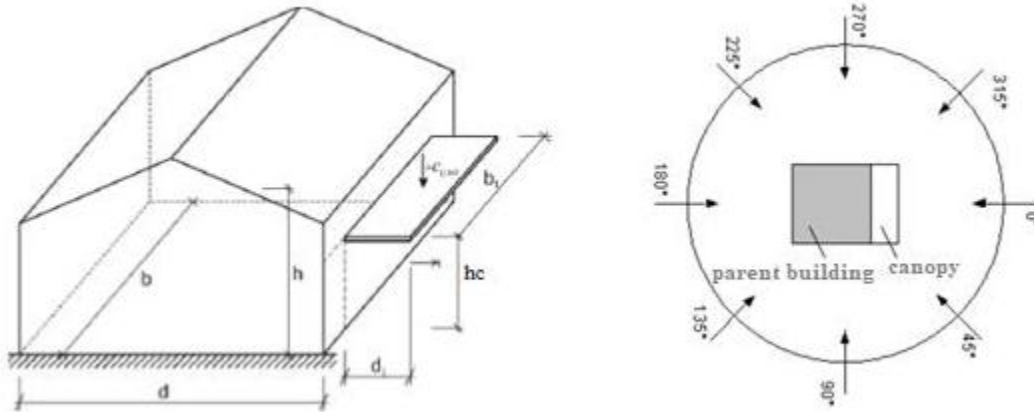
Figure 2.1 Models, wind directions and partial results from Holcher et al. (2007)

based on one-hour average wind speed and it formed the basis of the provisions for attached

canopies in the German code (DIN 2010). The model used and some results of this study are

shown in Figure 2.1, in which b_1, b, d_1 stand for canopy length, length of the wall to which canopy is attached and canopy width. Results in terms of mean and peak net pressure coefficients as a function of wind direction for low and high canopy locations show that the most critical values are found for wind blowing perpendicular to the wall with the canopy.

2.1.3 Effect of wind on patio covers

Pressure coefficients on patio covers were studied by Zisis and Stathopoulos (2010) for low rise buildings. A 1:100 geometric scale building and patio cover model was constructed and tested for
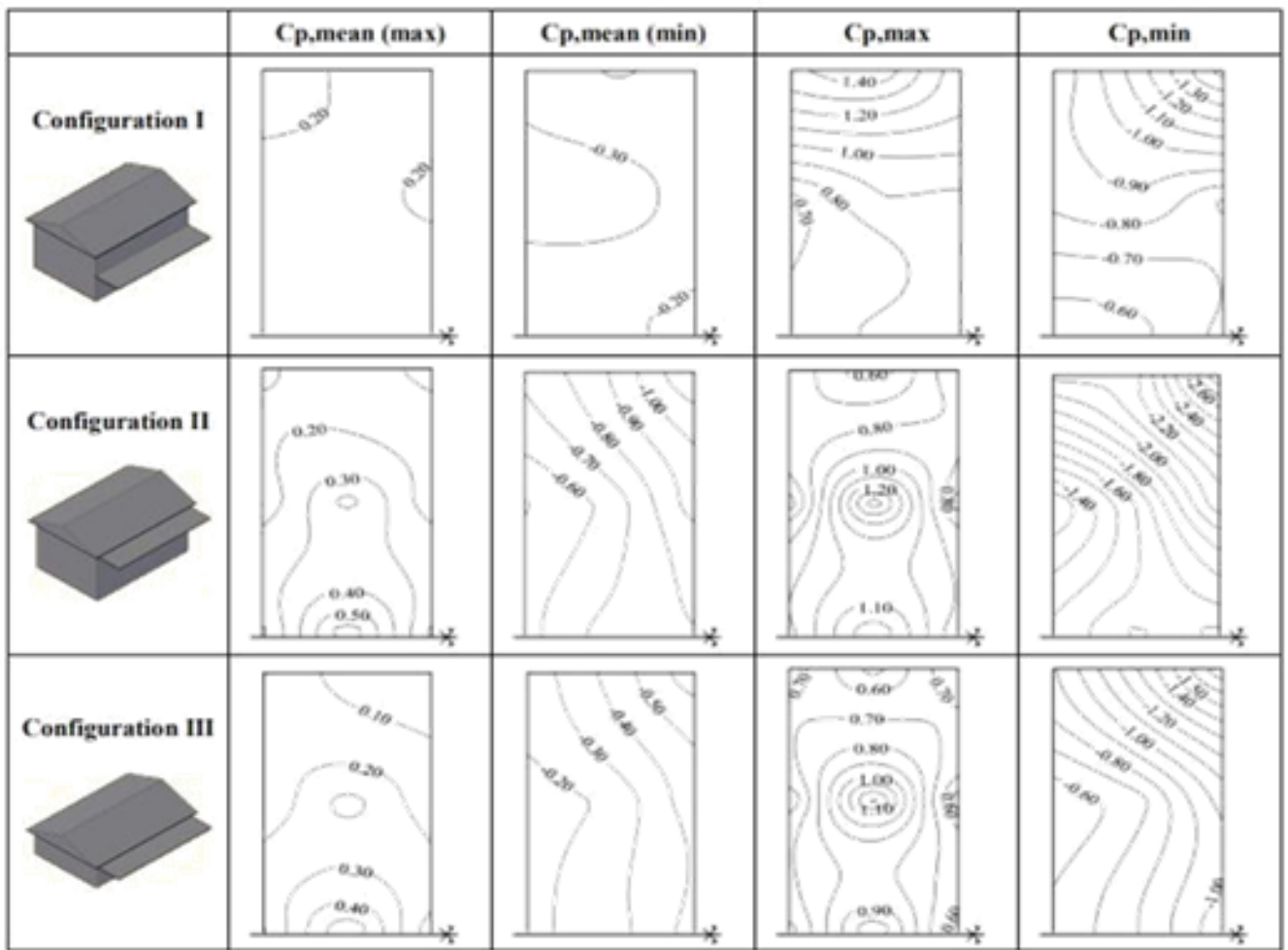
Figure 2.2 Mean, maximum and minimum values of net pressure coefficient (based on 1-hour wind speed) by Zisis and Stathopoulos (2010)

open exposure conditions. Three different models were tested to observe the effect of patio height to building height ratio. Simultaneous measurements of wind pressure/suction on each side of the patio cover was ensured by instrumenting pressure taps on both upper and lower side of the patio cover. Figure 2.2 shows some results of the study. An additional comprehensive study carried out by Candelario et al. (2014) examined 63 different model buildings with different building and canopy geometries tested for 28 wind directions. Design net pressure coefficients, GCp, for patio covers recommended for possible inclusion in ASCE-7 were proposed by these studies, which also found out that considering canopy as a free-standing roof for 90° or 270° wind direction, as stated in the Australian code, may not be correct.

2.1.4 Effect of wind on attached canopies determined by large scale wind tunnel tests

Zisis et al. (2017) used large scale models to examine the pressure coefficients on canopies attached to low-rise buildings. The study used 1:6 scaled models. The experiments were performed in the Wall of Wind (WOW) consisting of 12 fans at the research facility of Florida International University. Canopy at the top and canopy at the middle of the wall were considered for the building tested. The study only considered five wind directions i.e. 0, 15, 30, 45 and 90° and used suburban terrain exposure. The aim of the study was to provide design pressure coefficients appropriate for codes and standards. The study suggested pressure coefficients for upper surface, lower surface, as well as their net effect on the canopies, as shown in Figure 2.3, in which L_c, L, w_c and e_d are canopy length, length of the wall with the attached canopy, canopy width and distance between canopy edge to building edge, respectively. Envelope of peak Cp,net values for all cases tested as a function of hc/h are shown in Figure 2.3.

2.1.5 Computational studies

Roh and Kim (2011) studied the net pressure coefficient on canopy attached to an L-shaped tall building. No wind tunnel test was conducted; instead, Computational Fluid Dynamics (CFD) was used for the study. Numerical analysis results were obtained using ANSYS CFX 11 codes. The study used various canopy sizes with various canopy height to building-height ratios and it showed that building geometry plays a very vital role on wind loading on attached canopies. Typical results of the study are presented in Figure 2.4 and compared with the results of other studies and codes in Figure 2.10. The comparison shows that the computational study yields higher negative $C_{p,n}$ values as compared to the codes and almost all other studies, except Zisis et al. (2017) for h_c/h ratio equal to 0.5. However, for positive $C_{p,n}$ values, this study suggests lower value compared to codes and other studies for same hc/h ratio, say hc/h=0.17. It should be noted that NBCC 2015 prohibits the use of CFD for calculating wind pressures and structural loads. Since the conclusions made by Roh and Kim (2011) do not have any experimental validation, further studies are of course required.

Name		h_e	e_d	L_c	w_e & L
	AI	6.5m (21'5")	0	13.5m (44'3")	
	AII	3.5m (11'6")			
	BI	6.5m (21'5")	3.4m (11'1")		3.5m (11'6") & 13.75m (45')
	BII	3.5m (11'6")		6.75m (22'2")	
	CI	6.5m (21'5")	6.8m (22'2")		
	CII	3.5m (11'6")			
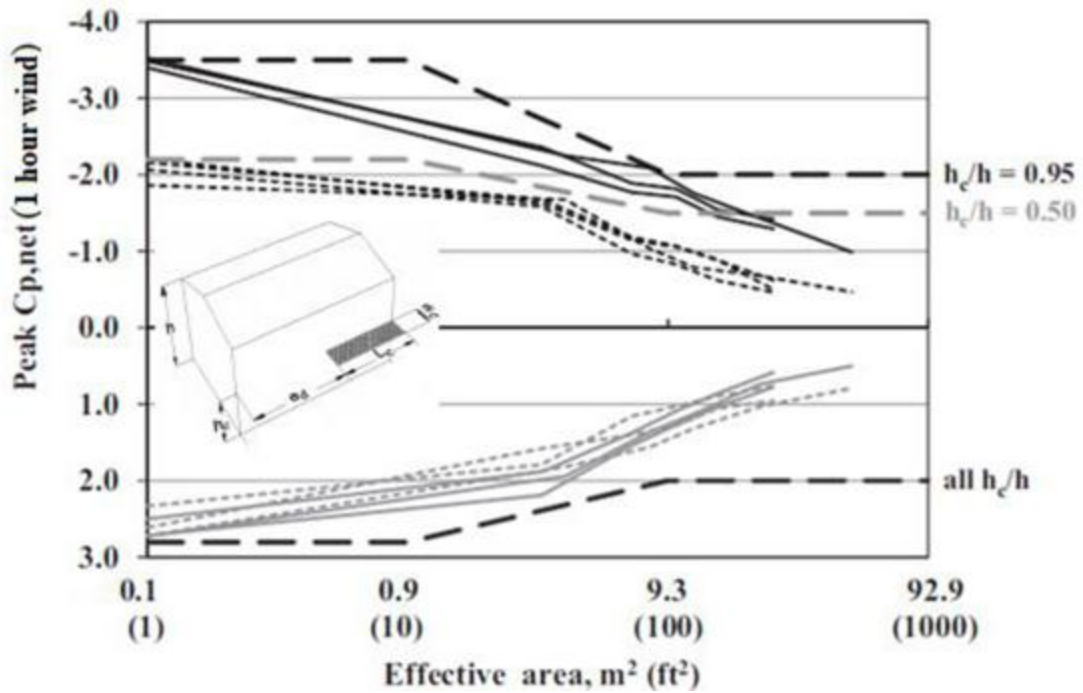
Figure 2.3 Models used and proposed values of net pressure coefficient (based on 1-hour wind speed) as a function of effective area by Zisis et al. (2017)
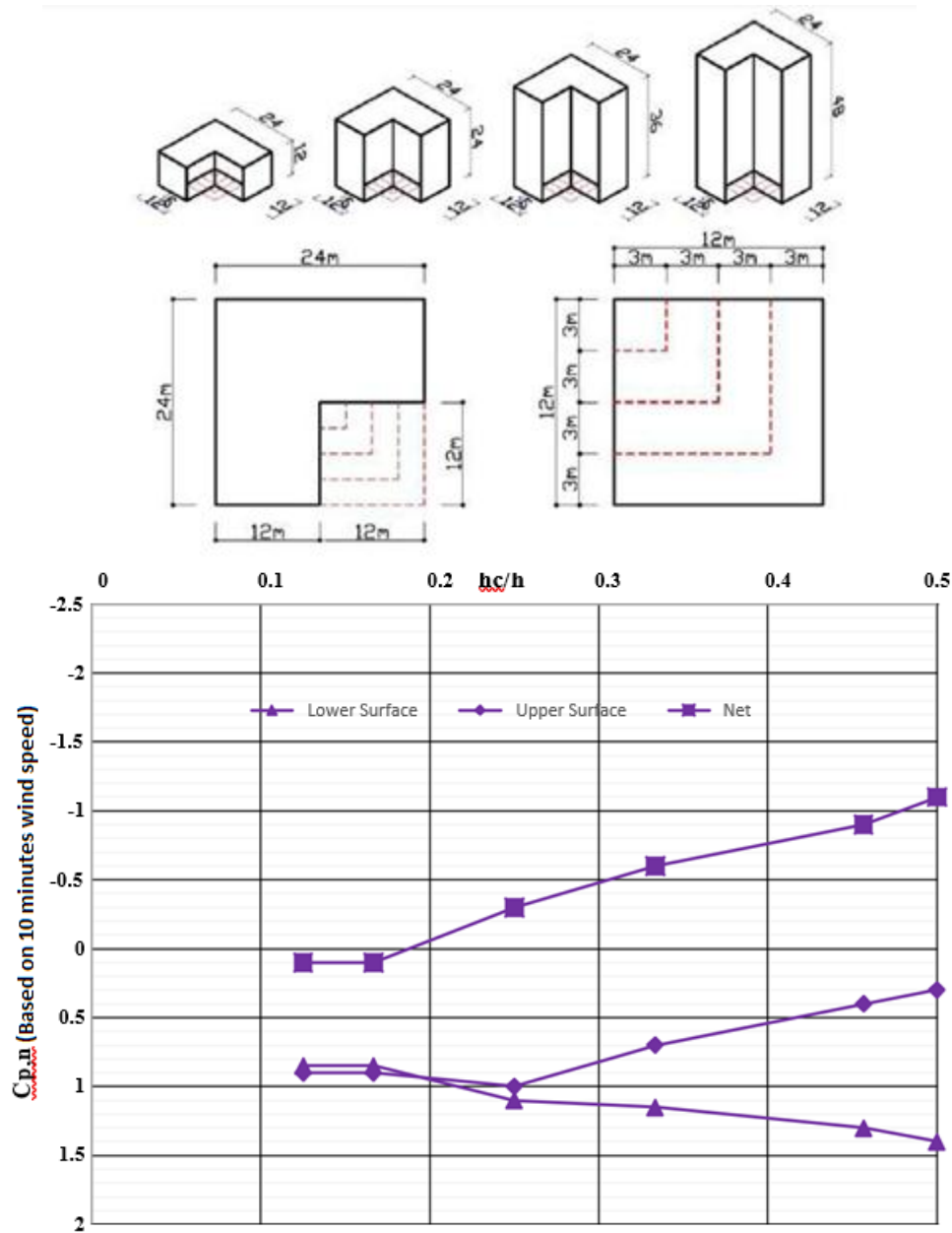
Figure 2.4 Building models used and typical results of the study of Roh and Kim (2011)

2.2 National building codes and standards

Some national building codes and standards provide guidelines for designing attached canopies. They will be discussed separately with their recommendations and limitations in the following sections.

2.2.1 Australian/New Zealand Standard (AS/NZS 1170.2, 2011)

The Australian/New Zealand Standard (AS/NZS 1170.2:2011) has provisions for attached patio covers in Appendix D. These provisions were generated based on the wind tunnel study of Jancauskas and Holmes (1985). The equation of design wind pressure according to AS/NZS 1170.2 (2011) in (N/m^2) is:

$$P = 0.6 \, [V_{des,\theta}]^2 \, C_{p,n} \, K_a \, K_l \, C_{dyn} \tag{2.1}$$

where $V_{des,\theta}$ is the design wind velocity in m/s (based on 3 second gust speed), K_a is the area reduction factor, K_l is the local pressure factor, C_{dyn} is the dynamic response factor for buildings having frequency less than 1 Hz, $C_{p,n}$ is the net pressure coefficient acting normal to the surface when the wind is perpendicular to the wall with which the canopy is attached ($\theta=0^o$), for buildings with roof angle less than 10 degrees, as shown in Figure 2.5. The recommended net pressure coefficients for various h_c/h (h: building height and h_c: canopy height) considered for the two wind directions are shown in Figure 2.5. According to the Australian/New Zealand Standard code, canopies must be designed for both net upward and downward pressure. For wind direction parallel to the wall, AS/NZS 1170.2 (2011) treats the canopy as a free roof and the design net pressure coefficients should be obtained accordingly. It should be mentioned that there is a net pressure factor of 1.5 to be multiplied with the $C_{p,n}$ to consider local effects on the small effective areas in proximity to the edge.
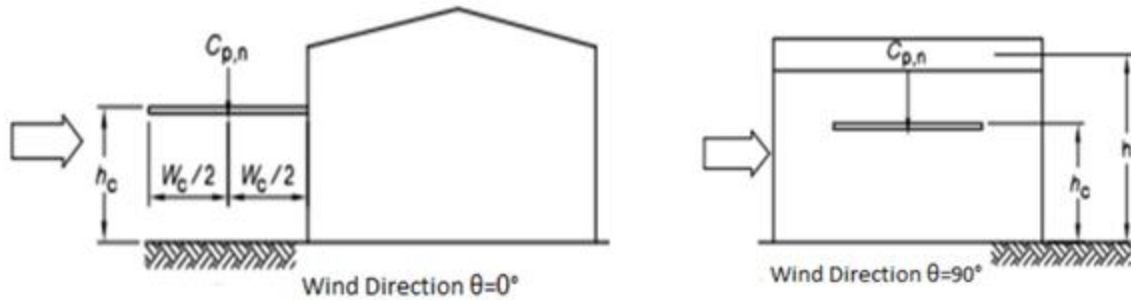
TABLE D8

NET PRESSURE COEFFICIENTS ($C_{p,n}$) FOR CANOPIES AND AWNINGS ATTACHED TO BUILDINGS FOR $\theta = 0°$ (see Figure D6(a))

Design case	h_c/h (see Note 1)	Net pressure coefficients ($C_{p,n}$)
$h_c/h < 0.5$	0.1	1.2, −0.2
	0.2	0.7, −0.2
	0.5	0.4, −0.2
$h_c/h \geq 0.5$	0.5	0.5, −0.3
	0.75	0.4, $[-0.3 - 0.2(h_c/w_c)]$ or −1.5 (see Note 2)
	1.0	0.2, $[-0.3 - 0.6(h_c/w_c)]$ or −1.5 (see Note 2)

NOTES:
1   For intermediate values of h_c/h, linear interpolation shall be used.
2   Whichever is the lower magnitude.

Figure 2.5 Cp,n values from AS/NZS 1170.2:2011 and corresponding wind directions

2.2.2   ASCE 7-16

Previously, ASCE 7-05 and ASCE 7-10 did not have any specific provisions for attached canopies, which were considered as roof overhangs and were designed accordingly. ASCE 7-16 has adopted provisions for attached canopies in Section 30.11. The equation for design wind pressure on canopies attached to the wall of buildings with roof height less than 18.3 meters is:

$$P = 0.613 K_h\, K_{ht}\, K_d\, K_e\, V^2\, (GC_p) \qquad (2.2)$$

where p is the design pressure in (N/m^2), K_h and K_{ht}, which are measured at the mean roof height, are velocity pressure exposure coefficient and topographic factor, respectively, K_d and K_e are wind directionality factor and ground elevation factor, respectively, V is the basic wind speed corresponding to a 3-s gust speed at 33 ft (10 m) above the ground in an open country exposure measured in m/s, GC_p denotes net pressure coefficients for the attached canopies and are given in Fig. 30.11-1A–B (ASCE 7-16) for contributions from both upper and lower surfaces individually and their combined (net) effect on attached canopies. In comparison to the other codes, ASCE 7-16 considers canopy area to determine design pressure and is limited to building height less than 18.3 meters. Figure 2.6 shows the overhang provisions of ASCE 7-16 in terms of net GC_p. values (both positive and negative) for different ranges of h_c/h values.

Diagram

ELEVATION

Notation
h_c = Mean canopy height, in ft (m).
h_e = Mean eave height, in ft (m).
(GC_{pn}) = Net pressure coefficients.
q_h = Velocity pressure evaluated at height $z = h$, in lb/ft^2 (N/m^2).

Net Pressure Coefficients

Notes
1. Vertical scale denotes (GC_{pn}) to be used with q_h.
2. Horizontal scale denotes effective wind area, in ft^2 (m^2).
3. Negative and positive signs signify uplifting and downward pressures, respectively.
4. Each component shall be designed for maximum positive and negative pressures.
5. Use linear interpolation for intermediate values of h_c/h_e.

Figure 2.6 Overhang GCpn provisions, after ASCE 7-16

2.2.3 Indian Standard/Code (IS: 875 (Part 3), 2015)

As per Indian Standard, wind load on canopy is obtained using the following equation:

$$F \quad = \quad 0.6 \quad (C_{pe}\text{-}C_{pi}) \quad A \quad K_d \quad K_a \quad K_c \quad (V_z)^2$$

(2.3)

where V_z is the design wind speed in m/s, based on 3 second gust, A is the surface area of the canopy, K_d, K_a, K_c are wind directionality factor, area averaging factor and combination factor, respectively, C_{pe} is pressure coefficient for the upper surface and C_{pi} is pressure coefficient for the lower surface. The Indian code provides values of pressure coefficients for only two directions: 0° (direction 1) and 180° (direction 2), as shown in Figure 2.7. The pressure coefficients for the underside surface of the canopy (C_{pi}) can be 1.25 (downward slopped canopy) or 1 (horizontal canopy) or 0.75 (upward slopped canopy) regardless of hc/h ratio (where h: eave height; hc: canopy height) and these C_{pi} values will be taken as positive if the canopy is on windward side (direction 1 in Figure 2.7). The term (C_{pe}-C_{pi}) acts as net pressure coefficient. Figure 2.7 presents the most critical overhang upper surface pressure coefficients in accordance with h/hc (called h_1/h_2). Net pressure coefficients can be produced by considering the algebraic sum of upper and lower surface coefficients.

16
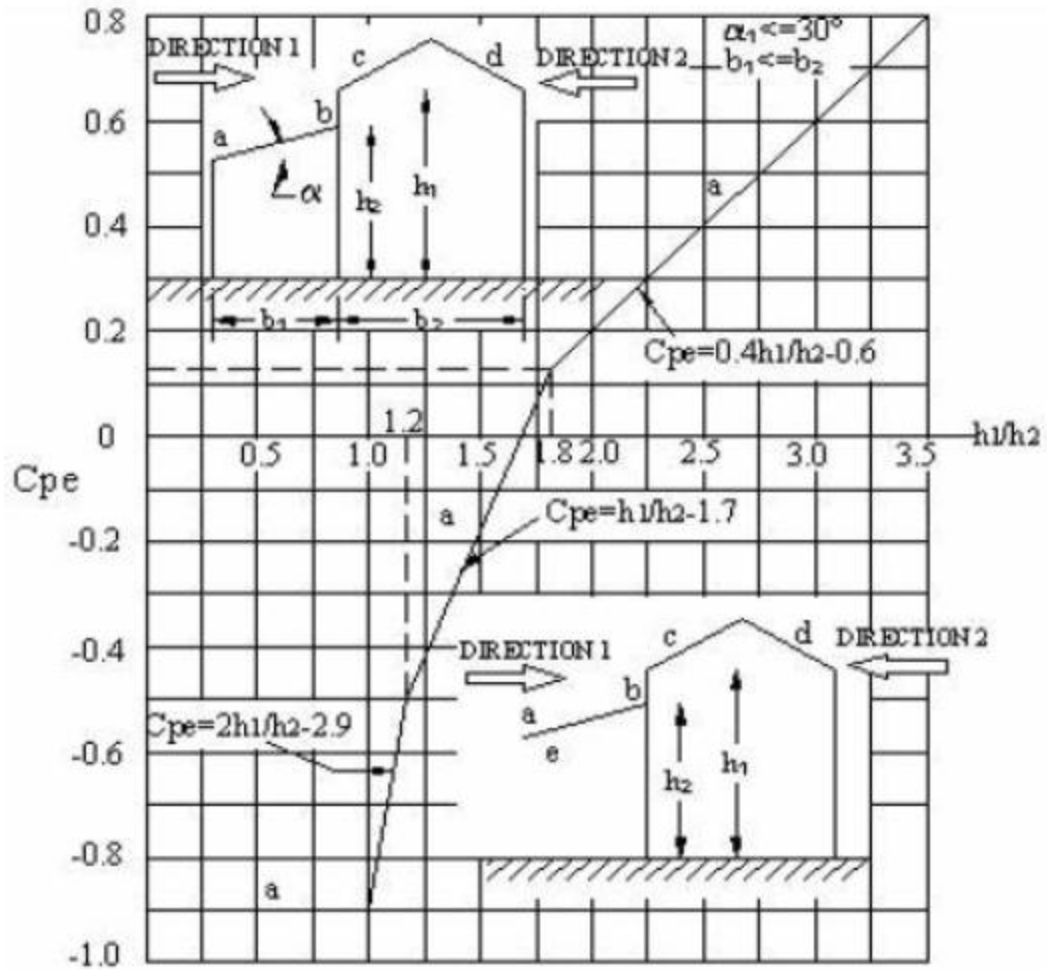
Figure 2.7 Wind directions and Cpe values from IS:875 (Part 3), 2015

2.2.4 Comparison among the above-mentioned provisions

Figure 2.8 presents a comparison among the above-mentioned provisions to understand the current solutions offered by different national building codes and standards. The Figure shows net positive and negative pressure coefficients ($C_{p,n}$ values based on 3-s gust) from AS/NZS 1170.2:2011, ASCE 7-16 and IS: 875 (Part 3), 2015 together as a function of h_c/h. Throughout this thesis, positive pressure and negative pressure on a surface indicate pressure towards the surface and
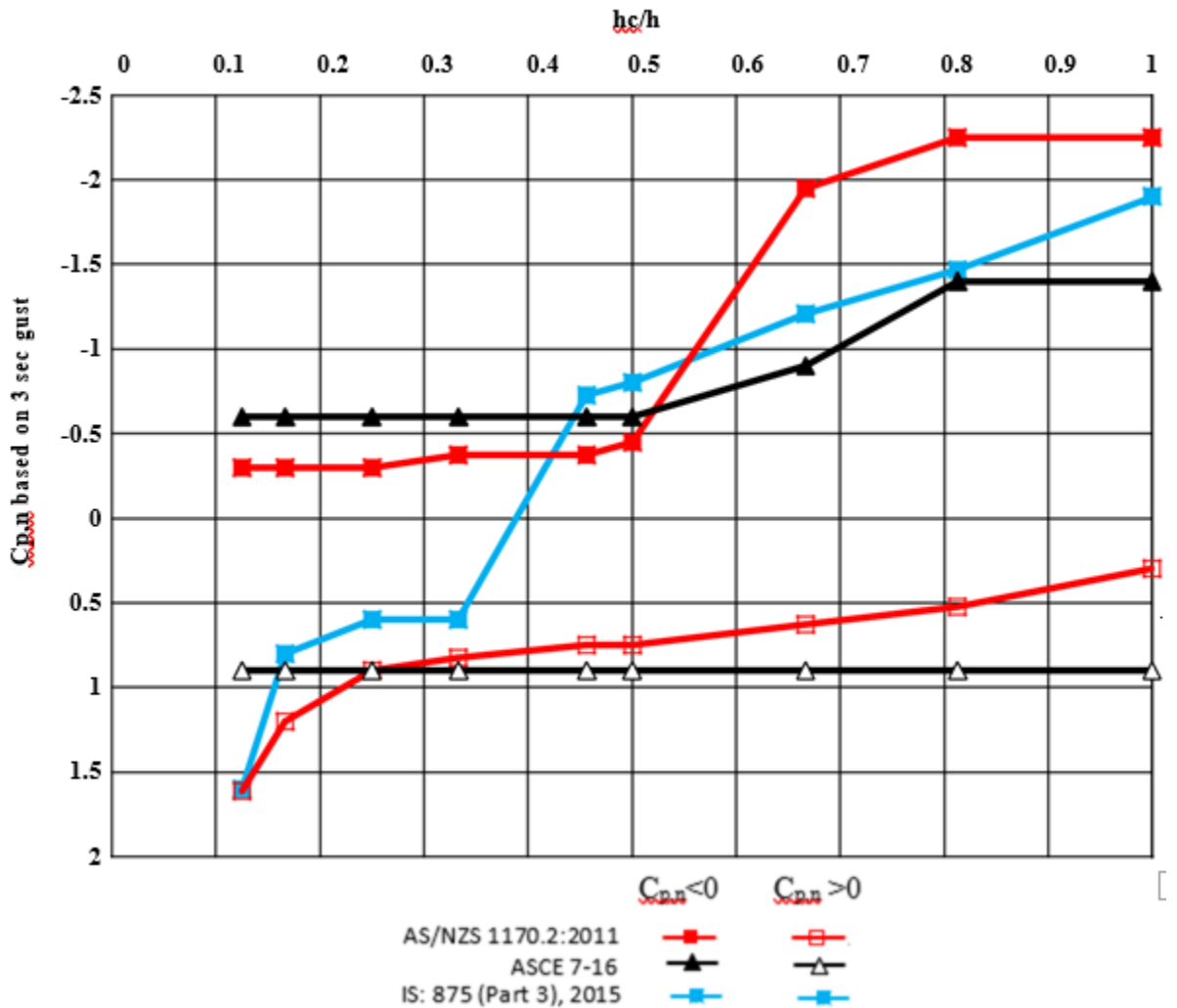
Figure 2.8 Net pressure coefficients as a function of hc/h after AS/NZS 1170.2:2011, ASCE 7-16 and IS:875 (part 3), 2015

pressure away from the surface, respectably and net positive and net negative pressure refer to downward pressure and suction (upward pressure), respectably. For simplicity, the most critical net C_p values have been shown. It is observed that the codes are suggesting different values for the two most extreme cases i.e. for $h_c/h=1$ and hc/h =0.1 (nearly). It is also clear that the Indian code does not recognize negative pressure coefficient values for canopies placed at a lower height nor positive values for canopies placed at a larger height. Besides, ASCE 7-16 provisions are limited up to building height of 18 meters, while AS/NZS and Indian code have no restriction regarding building height. These dissimilarities demand for new studies on wind loading effect on canopies at different heights.

2.3 Justification of current study

Despite the above-mentioned studies and some provisions from codes and standards, the necessity for more comprehensive study on wind loading effect on attached canopies is growing. Figure 2.9 and 2.10 can explain this necessity by illustrating the confusions and discrepancies among the provisions and results of available studies.

Figure 2.9 presents critical net C_p values (all based on 3 sec gust) on Y axis and effective canopy area on X axis. The provisions from AS/NZS 1170.2:2011 and ASCE 7-16 have been presented and compared with the studies of Zisis and Stathopoulos (2010), Candelario et al. (2014) and Zisis et al. (2017). The largest discrepancy can be observed from the pressure coefficients of AS/NZS 1170.2:2011, particularly for small effective areas (local loads). In contrast, ASCE 7-16 coefficients are more in line with the measured data both for local and area-averaged loads, positive and negative net pressures.

Figure 2.10 shows the wind load provisions for attached canopies from different wind codes, i.e. Australian (AS/NZS 1170.2:2011), ASCE 7-16, Indian (IS: 875 (Part-3)-2015), as compared with

results from past research studies (Hölscher et al. 2007, Zisis and Stathopoulos 2010, Zisis et al. 2017 and Roh and Kim 2011). Net design pressure coefficient values are expressed as functions of h_c/h ratios for small areas (local values) with appropriate modifications such as multiplication of the Cp values with the generic factor of 1.5, as suggested by AS/NZS 1170.2:2011 for small areas. Necessary scaling has been done to convert hourly wind speed data to 3 second gust data by using the correction of the Durst curve (Durst 1960). It can be observed that there are lots of dissimilarities in net pressure coefficient between the codes and values from available research. The most critical case is the uplift force (negative C_P value) as structures are mostly designed for gravity loads (downward forces). In Figure 2.10, it is observed that ASCE 7-16, AS/NZS 1170.2:2011 and IS: 875 (Part-3)-2015 all suggest different peak
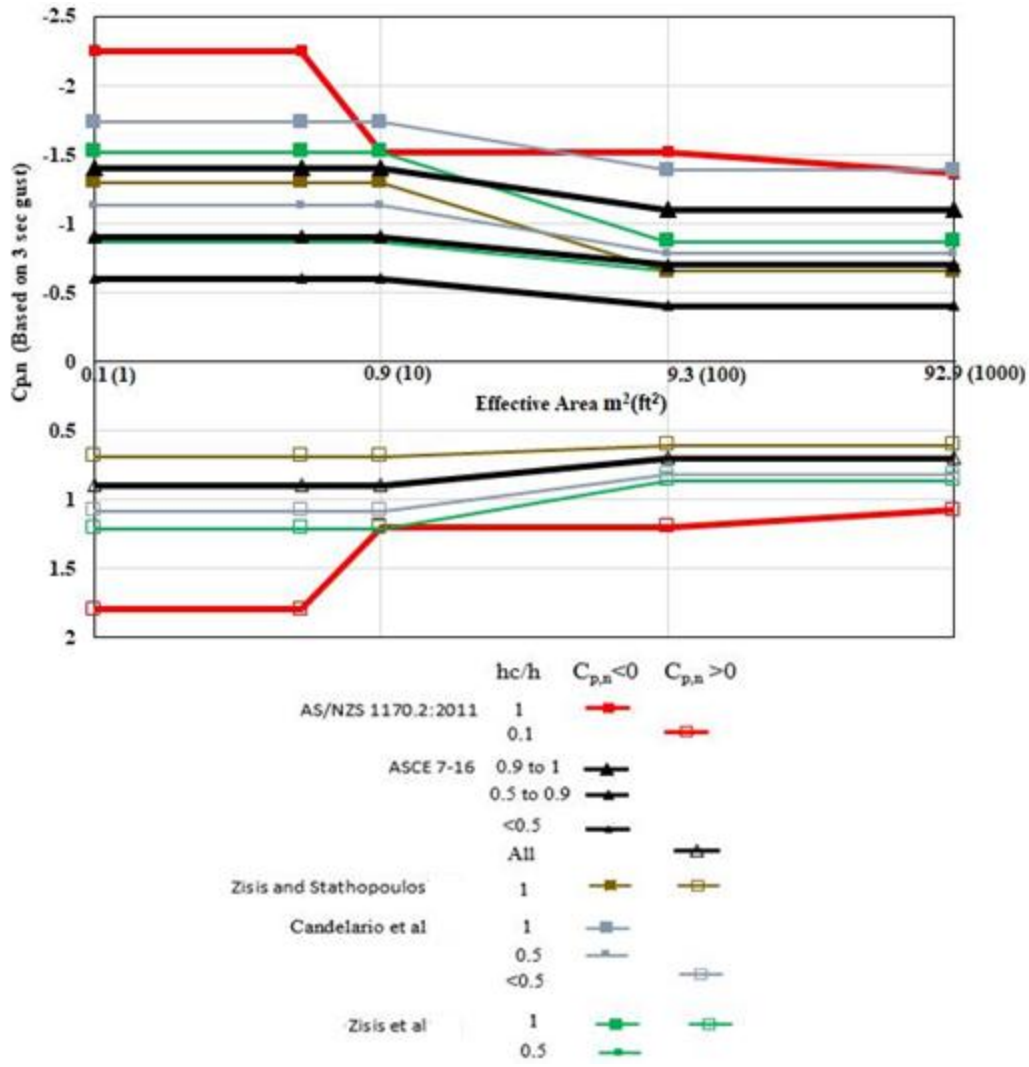
Figure 2.9 Comparison of net Cp values as a function of effective area proposed different codes

negative values for canopies at the top of the building, which is the most critical position for an attached canopy. The highest value, apart from the AS/NZS 1170.2:2011 is observed for Indian code (IS: 875 (Part-3)-2015), which is about 20% higher than the highest value of Zisis et al. (2017) and nearly 35% higher than that from ASCE 7-16. Among the wind tunnel studies, there are also significant differences between the results. For example, Zisis et al. (2017) provides 33% higher net negative C_p values than that of Zisis and Stathopoulos (2010) for the same h_c/h. It should be noted however, that the geometric scale and exposure category were different for these two studies. While comparing the positive values for C_p, ASCE 7-16 clearly provides the same positive Cp values for all

canopy heights and this results in 200% higher $C_{p,n}$ value for $h_c/h=1$ than that of AS/NZS 1170.2:2011. Also, the highest positive C_p value can be observed for the Indian and Australian wind codes, which are nearly 60% higher than the corresponding values from ASCE 7-16. These disagreements may arise from many factors such as different exposure categories, different geometries of parent buildings and canopies, consideration of different wind angles of attack. Most significant experiments for canopy loading of low buildings were carried out by Candelario et al. (2014), Zisis et al. (2017) and Zisis and Stathopoulos (2010). The differences among the studies were in the physical scaling of the models (i.e.1:100 and 1:6), terrain exposure (the power law exponent $\alpha = 0.14$ and 0.22), building and canopy geometry (i.e. building height, width, canopy width, canopy length). These studies provide different results for similar parameters, i.e. hc/h or effective area. Also, results of these studies are not always consistent with the design provisions of wind codes of practice for critical design conditions. In the case of tall buildings, no reliable data are currently available. This leads to an urge for more intensive studies and generalised results and design guidelines for canopies attached to both low and high-rise buildings to facilitate the work of designers and practitioners and ensure safety of structures and properties.
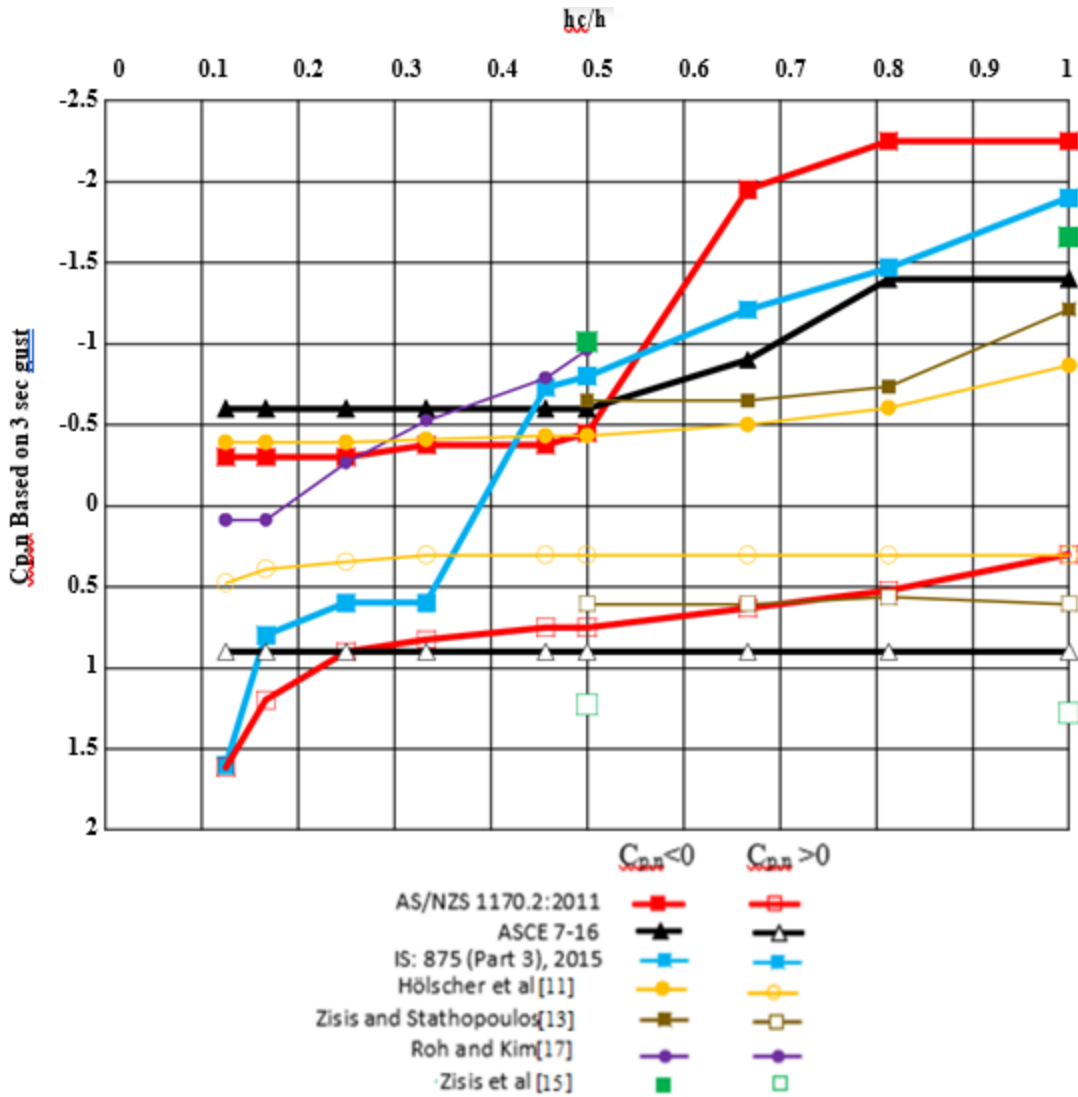
Figure 2.10 Comparison of net Cp values (based on 3 sec gust) of canopies suggested by different

Chapter 3   Experimental methodology

To investigate the effect of wind loading on attached canopies, a series of experiment was carried out at the boundary layer wind tunnel (BLWT) at Concordia University using scaled model buildings with scaled model canopies attached to them. The wind speed and loading data were collected through digitalised velocity and pressure measuring system and analysed to obtain the wind pressures on the attached canopies. In this chapter, the concept of BWLT, description of Concordia University's BWLT, velocity and pressure measuring system, description of models used, definition of terms, formulas used for the study have been presented.

3.1 Concept of BWLT

Wind encounters any submerge body's surface and friction occurs. Thus, the velocity profile becomes parabolic which means that there will be some deviation from the arithmetic average of the velocity along the vertical plane. This is called the boundary layer phenomenon and the deviation is used to define the turbulence of the flow. With higher surface roughness, turbulence is expected to be higher and the characteristics of a boundary layer flow get altered.   The atmospheric boundary layer is the result of the interaction of the wind and the surface of the earth. A boundary layer wind tunnel (BLWT), as opposed to a conventional wind tunnel, recreates the interaction between the wind and the terrain in order to simulate the natural characteristics of the wind at a defined scale. Most BLWTs today are based on the contributions of Danish engineer Martin Jensen (Jensen 1958). He observed that by building a very long wind tunnels and by modelling the surface roughness, proper simulation of the wind could be achieved. Jensen (1958) formulated scaling laws for proper wind tunnel simulations by comparing pressures on a full-scale low-rise structure to a model in a boundary layer wind

tunnel. In the current practice, the mean velocity and turbulence intensity profiles, the longitudinal scale of turbulence, and the power spectra of the longitudinal velocity are considered key features for proper simulation.

3.2 BLWT in Building Aerodynamics Laboratory at Concordia University

The BLWT in the Building Aerodynamics Laboratory (BAL) at Concordia University is of the open circuit return type and consists of a 1.8m x 1.8m (6ft x 6ft) cross section and a working section of about 12m (39.4ft) long. Top, side, and front views retrieved from the original construction plans are provided in Figure 3.1. The flow is generated by a MARK HOT double inlet centrifugal blower with a capability of providing 40 m^3/s (86400 cfm). As a result, a maximum testing wind speed of 14.0 m/sec can be attained. The wind speed can be reduced to 3 m/sec by manually adjusting the outlet control. The floor is covered with a polypropylene carpet and the ceiling consists of wooden panels of adjustable height. Different terrain exposures may be simulated by the addition of floor panels with specific roughness elements and by adjusting the ceiling to achieve a zero longitudinal pressure gradient. In this way, the proper simulation of the atmospheric flow for any exposure category can be ensured. It must be noted, however, that every experiment comprised in this study has been conducted for an open terrain exposure (low roughness), as shown in Figure 3.2. At the test section, a turntable of a 1.20m diameter has been placed to allow for the testing of models for any desired wind direction. Additionally, an acrylic glass window has been placed at the wind tunnel wall to facilitate flow visualization experimentation without having the equipment interfere with the flow.
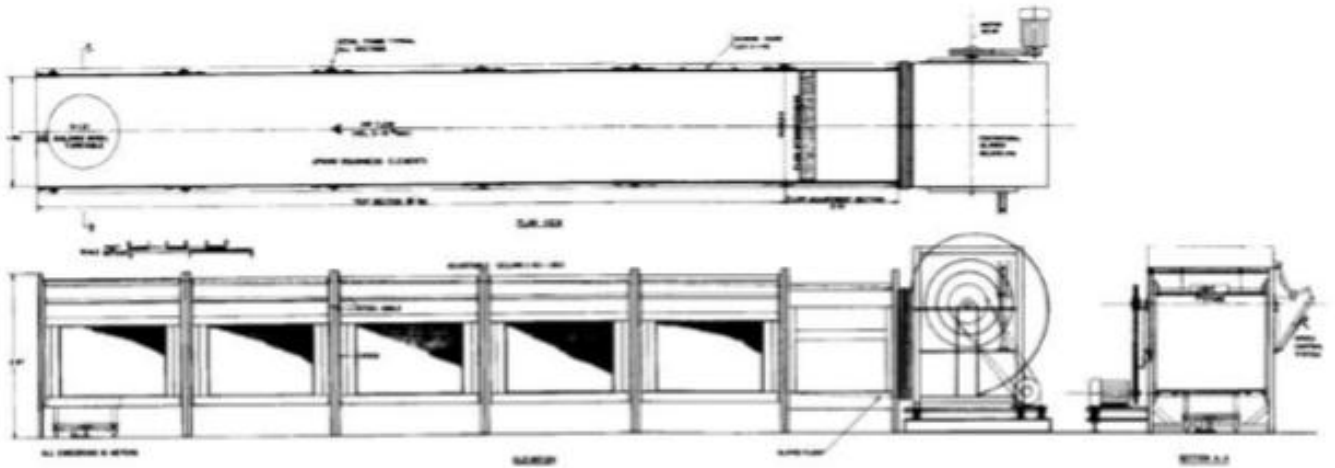
Figure 3.1 Construction Plans of Boundary Layer Wind Tunnel at Concordia University, Stathopoulos (1984-A)

Figure 3.2 Boundary layer wind tunnel at Concordia University (Front view)

3.2.1 Instrumentations

Instrumentation used for the measurement of flow phenomena in the BLWT at the Building Aerodynamics Laboratory consisted of two major independent systems for velocity and for pressure measurements. Velocity related measurements, such as wind speed and turbulence intensity profiles, were obtained using a 4-hole Cobra Probe (Turbulent Flow Instrumentation) in combination with an automated traverse system (Rotalec). Measurements were conducted at a sampling rate of 1000Hz for a duration of approximately 30 seconds. The gradient mean wind velocity was set at approximately 13.4 m/s. Pressure measurements were conducted using a Digital Service Module DSM 3400 as the Data Acquisition System (DAS) in combination with a ZOC33/64Px pressure scanner and Thermal Control Unit (TCU) system all from the Scanivalve Corp. The pressure taps in the building models are connected to the ZOC33/64Px scanners using urethane flexible tubing. Compressed air is connected to the system for purging and calibration purposes. The DAS was operated by a second computer connected to the DSM 3400 through an Ethernet network connection. A sketch of the experimental setup is shown in Figure 3.3. The scanning period was set at 50 microseconds for 64 channels resulting in a sampling frequency of 312.5 Hz. A total of 8200 frames are thus scanned in approximately 26.2 seconds, corresponding to a full-scale storm of approximately 1 hour.

3.2.2 Various aspects of simulated flow

For the pressure measurements obtained in the wind tunnel to have a physical meaning one must first be assured that the flow generated at the testing section adequately simulates the properties of the atmospheric wind. Comparisons between theoretical and experimental velocity profiles, turbulence intensity, integral scale of turbulence, and spectra of the velocity fluctuations
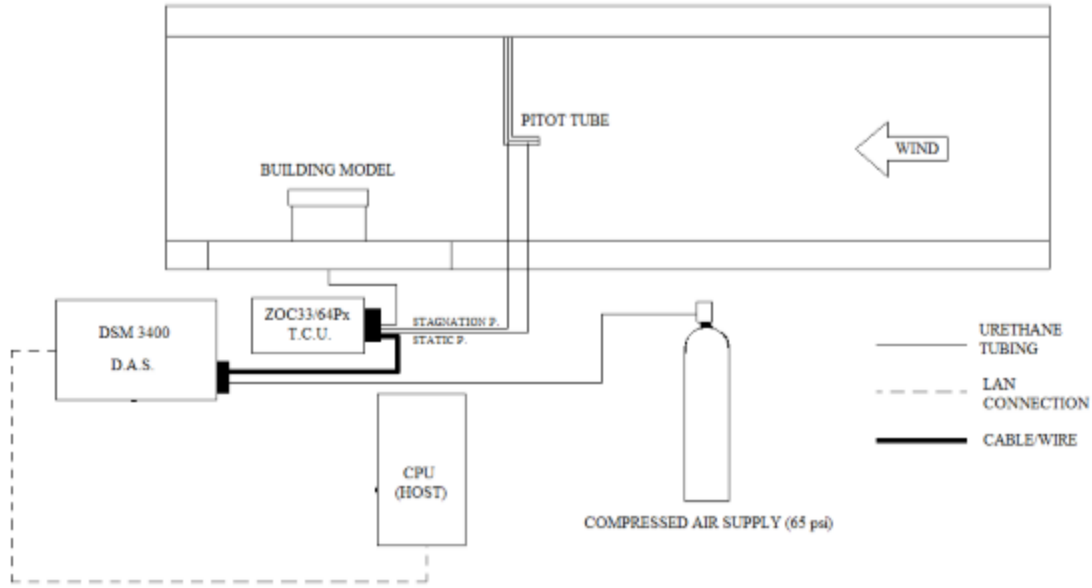
Figure 3.3 Sketch of the experimental setup at the boundary layer wind tunnel (Candelario 2012)

are defined and evaluated in this section to assess the validity of the experimentation.

The variation of the mean velocity($\overline{V_Z}$) as a function of elevation (Z) and the location of the gradient height (Z_G) after which the mean wind velocity is constant ($\overline{V}_G$) are instrumental for the modelling of atmospheric boundary layer. Figure 3.4 presents a sketch of boundary layer flow and above-mentioned parameters. The average and root mean square longitudinal velocities ($\overline{V_Z}$ and V_{rms}) were measured at different height at the centre of the wind tunnel test section without the model in place. The corresponding average velocities and longitudinal turbulence intensity ($\frac{V_{rms}}{\overline{V_Z}}$) are shown in Figure 3.5 as a function of Z/Z_g. The experimental values are compared with the theoretical values according to the power law equation:

$$\frac{\overline{V_Z}}{\overline{V_G}} = \left(\frac{Z}{Z_G}\right)^\alpha \qquad\qquad 3.1$$

where α is the power law exponent which depends on the type of exposure. It has been observed that a power law exponent of α = 0.15 provides the best agreement with the measured values, which conforms to full scale measurements of an open terrain exposure (Liu 1991). The experimental turbulence intensity is compared to the theoretical values as given by:

$$I_Z = C.\left(\frac{Z}{10}\right)^{-d} \qquad\qquad 3.2$$

where c and d are terrain-dependant coefficients (Zhou and Kareem 2002) taken as 0.15 and 0.11, respectively, for an open terrain exposure. In general, the experimental values obtained for the velocity and turbulence intensity profiles show a good agreement with the theoretical properties of an atmospheric flow at an open terrain exposure.
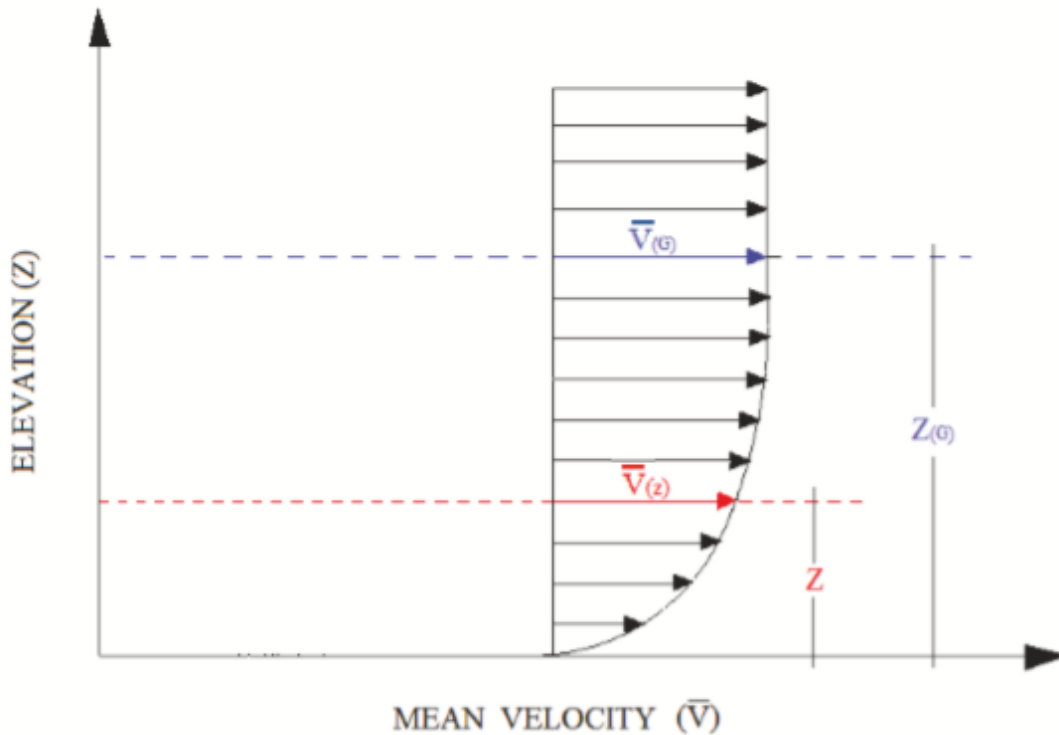
Figure 3.4 Representation of boundary layer flow and mentioned parameters (Candelario 2012)

Velocity fluctuations at a certain height inside the atmospheric boundary layer can be defined as a sequence of eddies being transported by the mean wind velocity in a periodic fluctuation with a circular frequency. The integral scales of turbulence measure the average size of these eddies. The length of an eddy can be measured in three dimensions for three different components of the fluctuating wind (longitudinal, transverse, and vertical). As a result, nine integral length scales of turbulence have been defined (Simiu and Scanlan 1996).
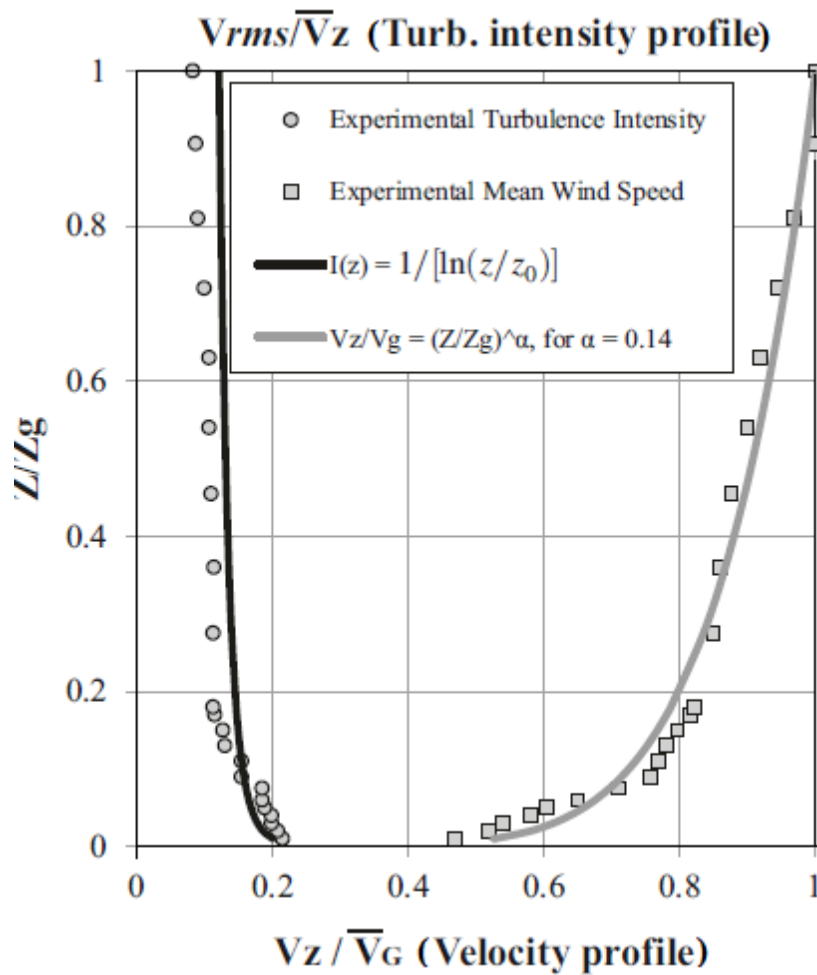
Figure 3.5 Wind velocity and terbulance intensity profile for open terrian exposer
(Candelario et al 2014)

For wind tunnel experimentation, it has been found that the most important to simulate amongst the nine integral scales of turbulence is the longitudinal size of the eddy in the longitudinal direction of the velocity fluctuations. Mathematically, the integral length scale of turbulence in the longitudinal direction is defined as:

$$L_v^x = \frac{V}{v} \int_0^\infty R_v(\tau) d\tau \qquad\qquad 3.3$$

where $R_v(\tau)$ is the autocovariance function of the fluctuation $v(x_1, t)$ which relates the similarity of the wind signal to itself at a certain time lag. An experimental value of 112m for L_v^x has been estimated at one sixth of the boundary layer depth for an open terrain exposure (Stathopoulos, 1984). In addition, the following empirical expression has been proposed (Counihan 1975) for estimation of length scale of turbulence in the longitudinal direction:

$$L_v^x = C.z^m \qquad\qquad 3.4$$

where z is the height in meters, and C and m , which are function of the roughness length z_0, can be determined from Figure 3.6. Evaluating the expression at an elevation of one sixth the gradient height and using the experimental roughness length z_0 = 0.01cm, an approximated value of L_v^x = 122m is obtained. It can be noted that both values obtained for the approximation of the integral length scale of turbulence in the longitudinal direction fall within the ranges of the experimental values measured for an open terrain exposure (Shiotani 1971).
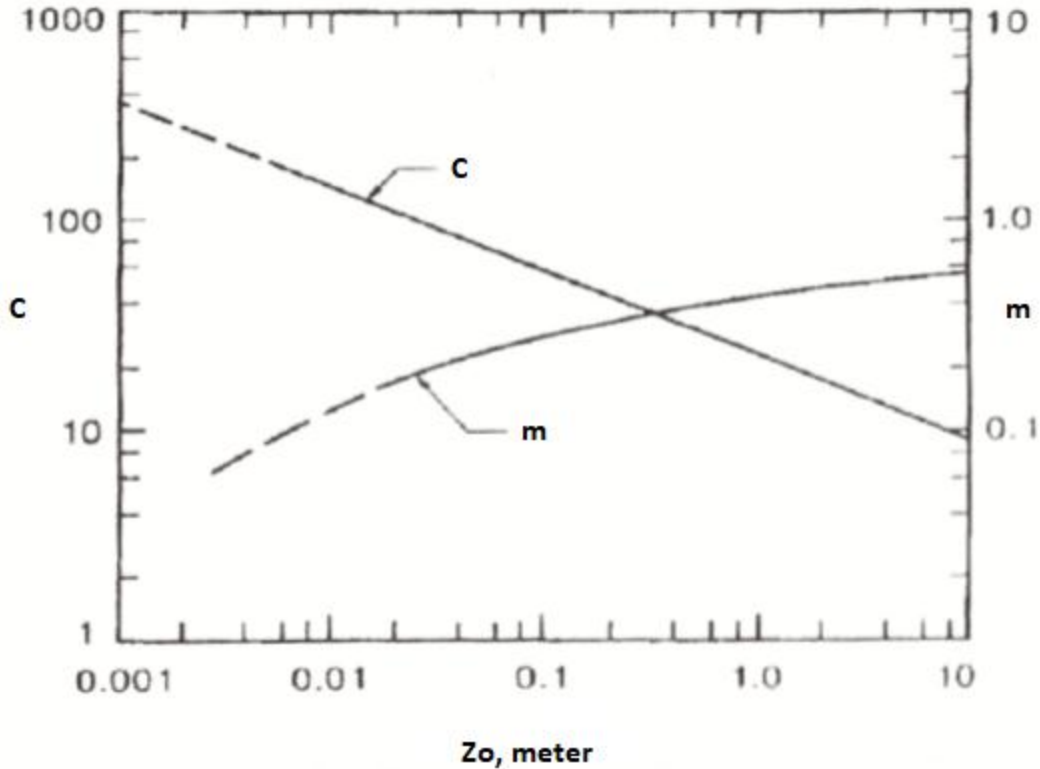
Figure 3.6 Variation of C and m with roughness length, after counihan 1975

It is well known that variations in velocity at a certain height can be defined as a sequence of eddies being transported by the mean wind velocity in a periodic fluctuation with a circular frequency. These turbulent fluctuations determine the total kinetic energy of the flow. If the fluctuations of the wind with respect to time are analyzed as signals, then the sequence can be decomposed in different frequencies. The signal can thus be represented in the frequency domain instead of the time domain. This is useful to describe the total amount of kinetic energy generated by the eddies. The mathematical definition for the spectrum of the wind at a given height z is:

$$\sigma^2 = \int_0^\infty S_z(n)\,dn \qquad\qquad 3.5$$

where σ^2 is the variance of the longitudinal wind speed, n is the frequency and $S_z(n)$ is the power spectral density of the longitudinal turbulence component at a given height z. Two

principal analytical and empirical spectral representations have been regarded to closely approximate the behavior of the atmospheric flow. The first is the analytical expression, known as Von Karman's equation:

$$\frac{n\,S(n)}{\sigma^2} = \frac{4\,n'}{(1+70.8\,n'^2)^{5/6}}$$

3.6

n' is defined as:

$$n' = \frac{nL_v^x}{\overline{V_Z}}$$

3.7

where L_v^x is:

$$L_v^x = \frac{25(Z-d)^{0.35}}{{Z_0}^{0.068}}$$

3.8

$\overline{V_Z}$ is mean wind speed at height Z, L_v^x is the length scale of turbulence in the longitudinal direction, d is the displacement length and Z_0 is the roughness length

The second one is known as Davenport's empirical expression defined as:

$$\frac{n\,S(n)}{V_*^2} = \frac{2}{3}\frac{n'^2}{(1+n'^2)^{4/3}}$$

3.9

$$\text{where } n' = \frac{n}{\overline{V_{10}}}$$

$\bar{V}_{10}$ is the mean wind speed at 10 m (32.8 ft) height. It must be noted that this expression does not take into consideration the variation of the spectrum with respect to height. The spectra of longitudinal velocity fluctuations have been measured at the BLWT at the Building Aerodynamics Laboratory of Concordia University at a height of one sixth of the boundary layer height, for an open terrain exposure (Stathopoulos, 1984). Figure 3.7 shows the comparison of the experimental spectrum compared to the curves obtained from Von Karman's and Davenport's equations. It can be seen that for lower wave numbers, Von Karman's equation seems to coincide better with the experimental data. For the intermediate wave numbers, where the highest energy in the turbulence occurs, Davenport's equation provides a better fit. In general, there is a good agreement between the experimental and theoretical values.
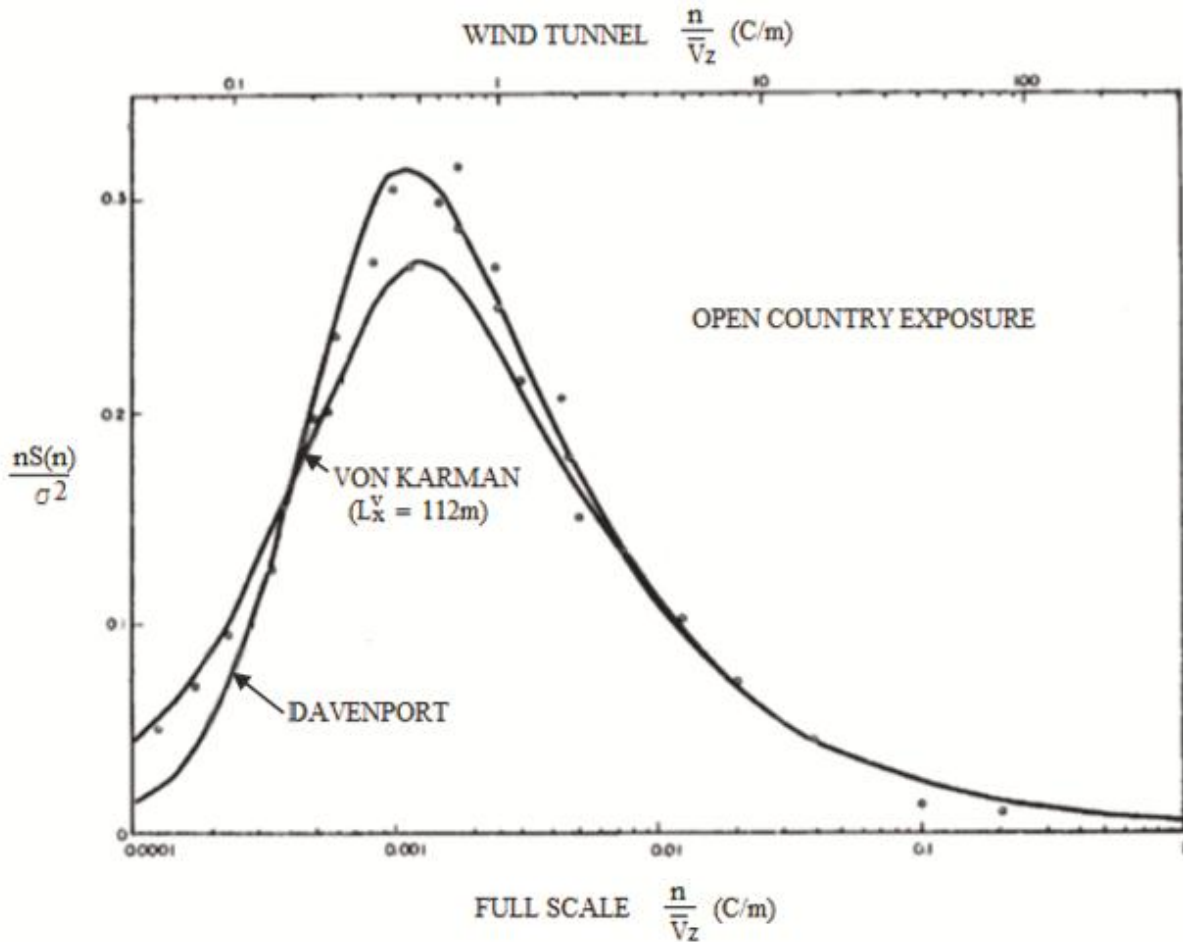
Figure 3.7 Spectra of longitudinal terbulance component at Z/Zg = 1/6, after Stathopoulos (1985)

3.3 Concept of pressure coefficient and related formula

The magnitude of the forces exerted on a structure exposed to wind activity depends on factors related to either the characteristics of the building or the properties of the wind. The effect that the geometry of the building has on the pressures is extremely important of most boundary layer wind tunnel experimentation for codification purposes. The properties of the wind that have an impact on the pressures, most importantly the wind speed, can vary significantly for different geographic location, different terrain exposures and different wind directions. Pressure coefficients are thus a convenient way to express relative pressures, only as a function of the

structure's geometry. In this section, the fundamental definition of a pressure coefficient is provided, and the specific pressure coefficients used in this study are defined.

3.3.1 Concept of pressure coefficient

The relation between the pressure, p, and velocity, V, in atmospheric and wind tunnel flows is widely governed by Bernoulli's equation.

$$p + \frac{1}{2}\rho V^2 = constant \tag{3.10}$$

which remains constant along the same streamline. V represents the velocity on the streamline outside the boundary layer that formed on the body surface where the Bernoulli's equation is only valid. In order to calculate the local pressure, the atmospheric pressure (Po) will be used as a reference pressure.

$$p + \frac{1}{2}\rho V^2 = p_0 + \frac{1}{2}\rho V_G{}^2 \tag{3.11}$$

where V_G is the free stream flow velocity

The above equation can be rearranged as:

$$p - p_0 = \frac{1}{2}\rho(V_G{}^2 - V^2) \tag{3.12}$$

The pressure coefficient is generally expressed as:

$$C_p = \frac{p - p_0}{\frac{1}{2}\rho V_G{}^2} \tag{3.13}$$

where

$\frac{1}{2}\rho V_G{}^2 =$ dynamic pressure $= q$

ρ= air density.

Also, it can be transformed as:

$$C_p = 1 - \left(\frac{V}{V_G}\right)^2 \qquad\qquad 3.14$$

In wind tunnel tests, the velocity (V_G) is measured usually by a Pitot tube. This velocity is zero at the stagnation point. According to equation 3.14 the mean pressure coefficient will be the maximum at the stagnation point and equal to +1. At the region around the point of the interaction, wind will be accelerated $V > V_G$ and therefore C_p values will be negative with no limit.

Peak, mean and RMS pressure coefficients are defined as:

C_p (peak pressure coefficient, positive or negative)= $\frac{P_{peak} - P_0}{q}$

C_p (mean pressure coefficient, positive or negative)= $\frac{P_{mean} - P_0}{q}$

C_p (root mean square, rms)= $\frac{P_{rms} - P_0}{q}$

If the pressure coefficient at a specific location along the body of a structure is known, then the corresponding force can be easily obtained by multiplying the pressure coefficient by the design dynamic pressure q and the corresponding tributary area A:

$$F = C_p . q . A \qquad\qquad 3.15$$

3.3.2 Pressure coefficients applied to this study

In this study, the time history of the wind loading on the attached canopy has been received by the pressure taps on both upper and lower surface of the canopy and then transformed into pressure coefficient using the following expression

$$C_p = \frac{Pi - Po}{q_{mrh}}$$
3.16

where C_p is the pressure coefficient on that pressure tap, P_i is the instantaneous pressure at that pressure tap, P_o is the static pressure and q_{mrh} is the dynamic pressure at mean roof height converted from q_{pitot} by use of the power law as follows:

$$q_{mrh} = \left(\left(\frac{Z_{mrh}}{Z_g}\right)^{0.15}\right)^2$$
3.17

Using theses two equations, we can calculate the instantaneous pressure coefficient for upper and lower surfaces. Since the attached canopy is generally a thin element exposed to wind pressures on both upper and lower surfaces, it is essential to consider the pressures acting simultaneously on each plane. This is done by using net pressure coefficients, as defined in the following equation:

$$C_{p,net} = \frac{P_{i,upper} - P_{i,lower}}{q_{mrh}}$$
3.18

where $P_{i,upper}$ and $P_{i,lower}$ are measured at top and bottom components, respectively, of a pressure tap pair, as illustrated in Figure 3.8. It must be noted that the negative sign represents a pressure directed away from the surface (suction) and a positive sign represents a pressure directed towards a surface. If this convention is maintained when computing net loads in accordance with

Eq. (3.25) a negative value for a $C_{p,net}$ will result in a net uplifting load, where a positive value will result in a net downwards loading.

Throughout this study peak and mean pressure coefficients may be identified as either local or area averaged. A local peak refers to the critical value experienced at a single pressure tap (or pressure tap pair in the case of net local pressure coefficient). An area-averaged pressure

coefficient refers

to the peak value that the entire surface experiences and is determined by the average of every pressure tap (or pressure tap pair) simultaneously. Additionally, local and area-averaged peak and mean pressure coefficients may be referred to as either minimum (maximum suction) or maximum (maximum pressure).

Additionally, all kinds of pressure coefficients presented in this thesis are referred to wind speed averaged over 1 hour in full scale (equivalent for 27 second wind in the wind tunnel). Major building codes and standards provide pressure coefficients that conform to different averaging periods, most commonly: 3-seconds gust, 10-minutes, and 1 hour. The relationship between the velocities and the averaging period has led to numerous studies and debates, however, the Durst gust duration curve (Durst, 1960) presented in Figure 3.8 is widely regarded as a useful tool to estimate the relationship between velocities corresponding to different averaging periods ($\frac{V_t}{V_{3600s}}$).
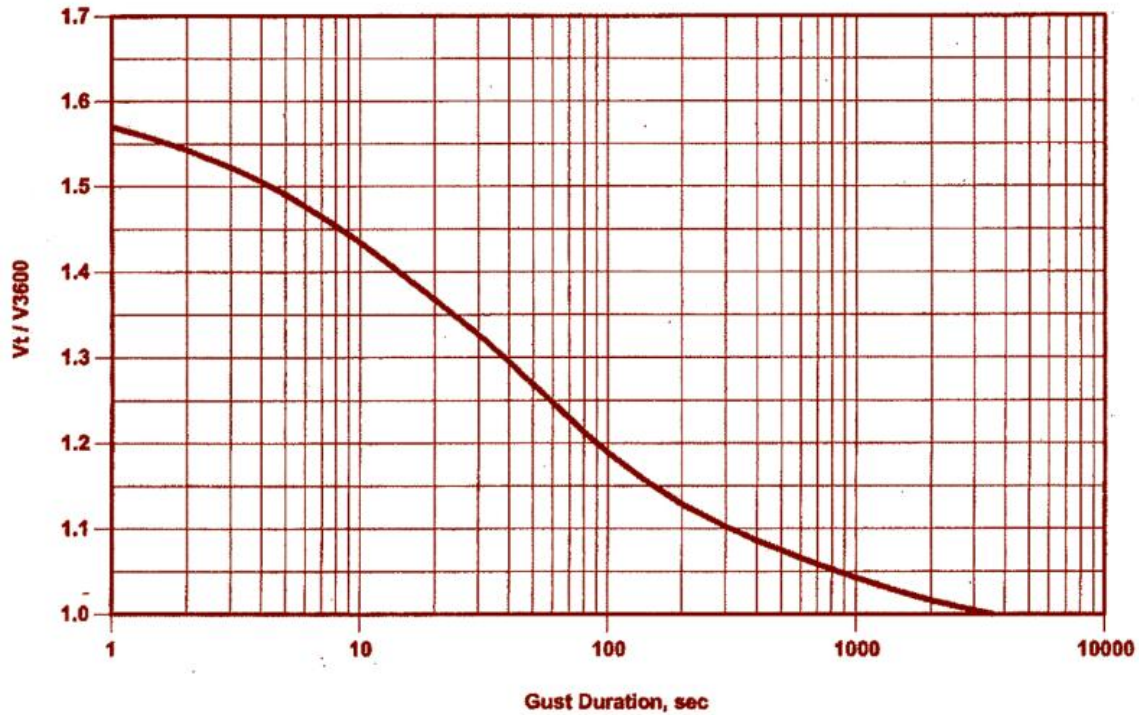
Figure 3.8 Gust duration curve, after Durst (1960)

3.4 Configurations of the model buildings and canopies

In total, three building heights were used. Equivalent real scale heights of the buildings were 7.15, 18.5 and 37 meters. Different canopy heights for each building were considered. Also, three different canopy widths i.e. 6.5, 2.7 and 1.5 meter were considered. The models were scaled as 1:100. The buildings had flat roofs and no extended portions. In total 24 configurations (Table 1) were tested. All the configurations were built with acrylic glass and they were attached to a metallic canopy model of the same geometric scale. For all configurations, the building dimension was 38 by 23.5 meters. Table 3.1 presents the details of the configurations. In all configurations, the canopy length was 36.5 meters and canopy edge to the building edge distance was 0.75 meters. Canopy model was made out of thin sandwiched metallic plates. Primarily, the

canopy had a width of 6.5 meters. But it could be pushed deeper to have canopy widths of 2.7 and 1.5 meters. Pressure taps were
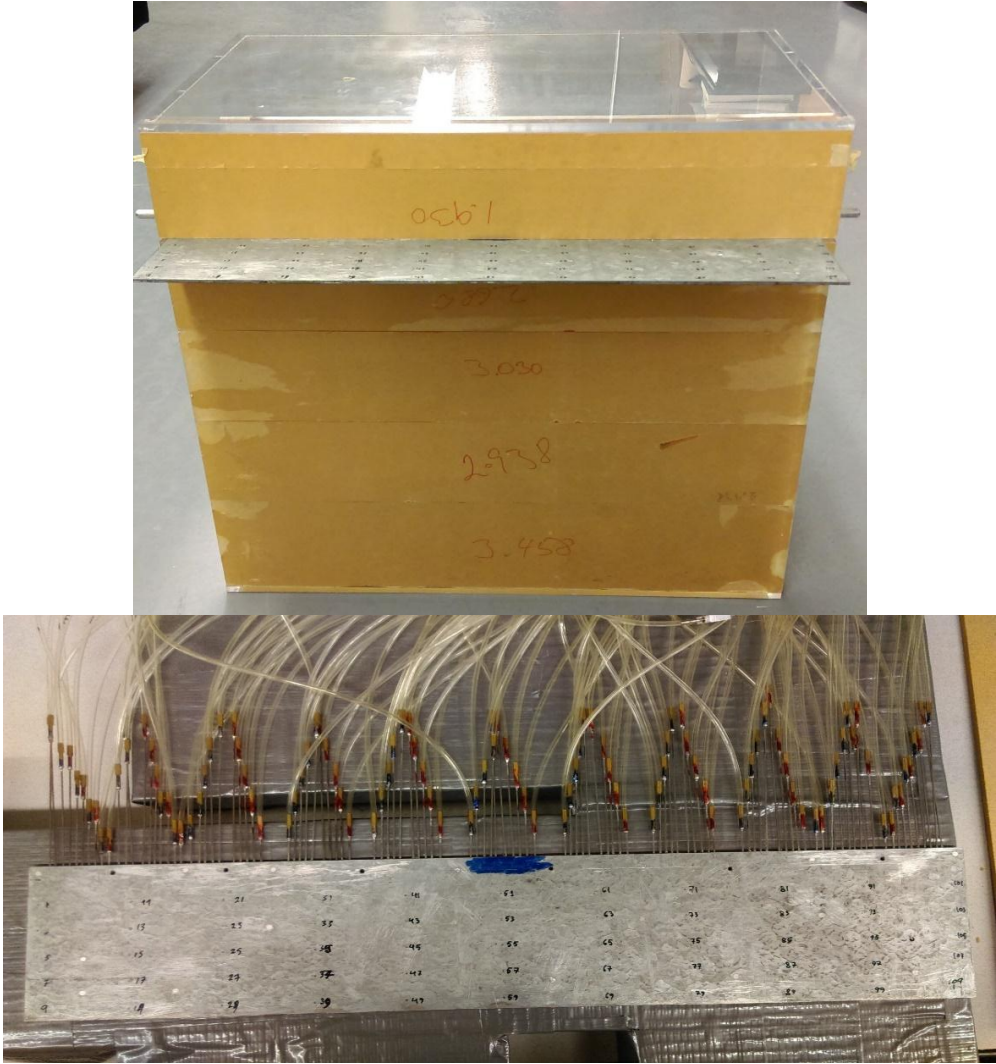
Figure 3.9 The model building and instrumented canopy

placed at both upper and lower surfaces of the canopy at almost the same locations to form pressure tap pairs that enable the determination of net pressure coefficients. Figure 3.8 shows real life picture of model building and instrumented canopy. Figure 3.9 presents a sketch with necessary details of the model canopy. The full width (6.5 m) canopy had total 55 pressure tap pairs, canopy width of 2.7 m had 22 pressure tap pairs and canopy width of 1.5 m had 11

pressure tap pairs (see Figure 3.10). Pressure taps were connected by urethane tubing to a pressure-sensitive scanner (ZOC33/64 Px-2003, Scanivalve Corp.), which is in turn connected to
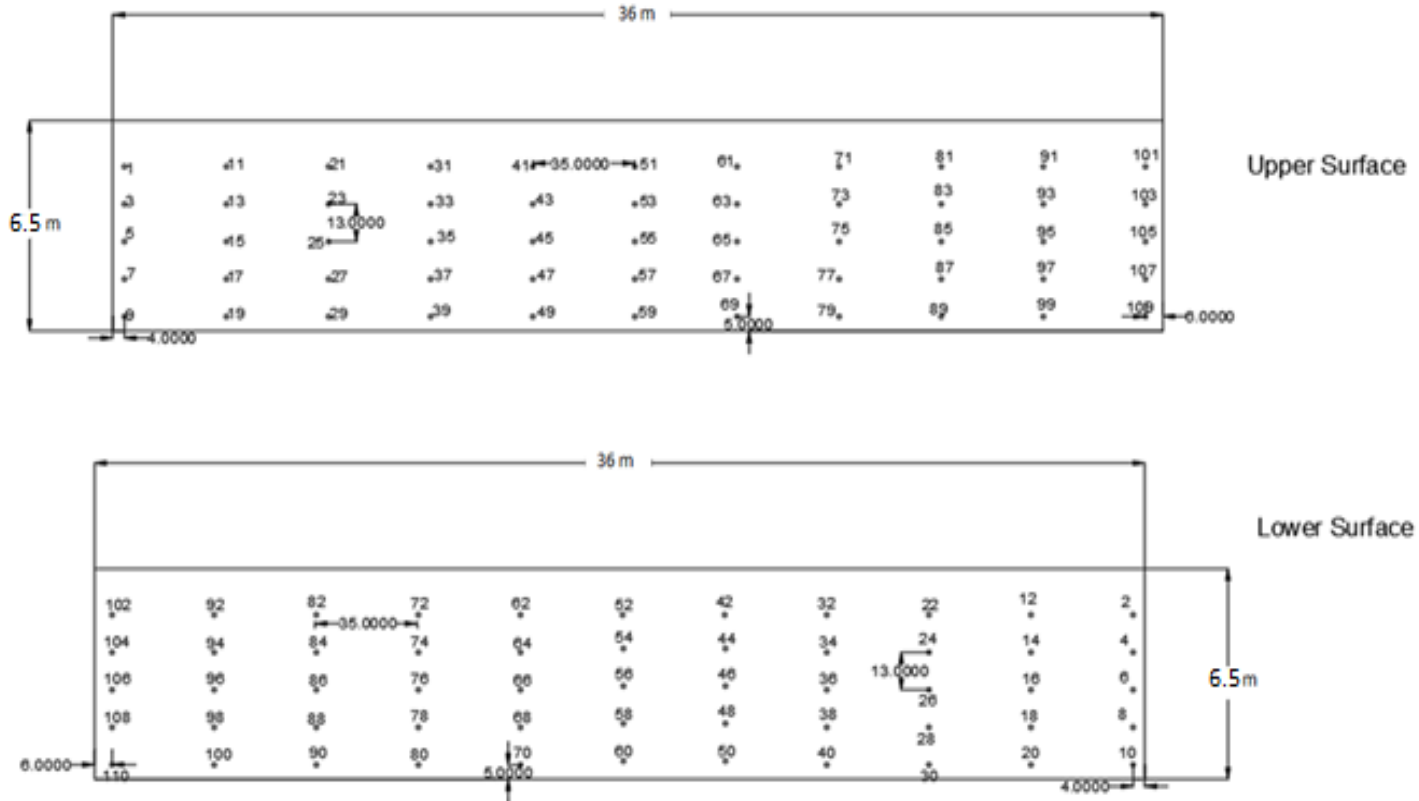
Figure 3.10 Details of model canopy (if not mentioned, dimensions are in milimeters)

the data acquisition system (DSM 3000, Scanivalve Corp.). A pitot tube was placed at the free flow above the boundary layer and was connected to the scanning system to measure the dynamic

and static pressure. The system was set to operate at a scanning frequency of 300 Hz generating 8,200 pressure readings.

In Figure 3.11, a sketch of the model is provided. Canopy length, canopy width, canopy height, building height and length of the parent wall is expressed by L_c, w_c, h_c, h and L, respectively.

36 m
C_L

6.5 m	°1	°6	°11	°16	°21	26	31°	°36	°41	°46	51°
	°2	°7	°12	°17	°22	27	32°	°37	°42	°47	52°
	°3	°8	°13	°18	°23	28	33°	°38	°43	°48	53°
	°4	°9	°14	°19	°24	29	34°	°39	°44	°49	54°
	°5	°10	°15	°20	°25	30	35°	°40	°45	°50	55°

36 m
C_L

| 2.7 m | °4 | °9 | °14 | °19 | °24 | 29 | 34° | °39 | °44 | °49 | 54° |
| | °5 | °10 | °15 | °20 | °25 | 30 | 35° | °40 | °45 | °50 | 55° |

36 m
C_L

| 1.5 m | °5 | °10 | °15 | °20 | °25 | 30 | 35° | °40 | °45 | °50 | 55° |
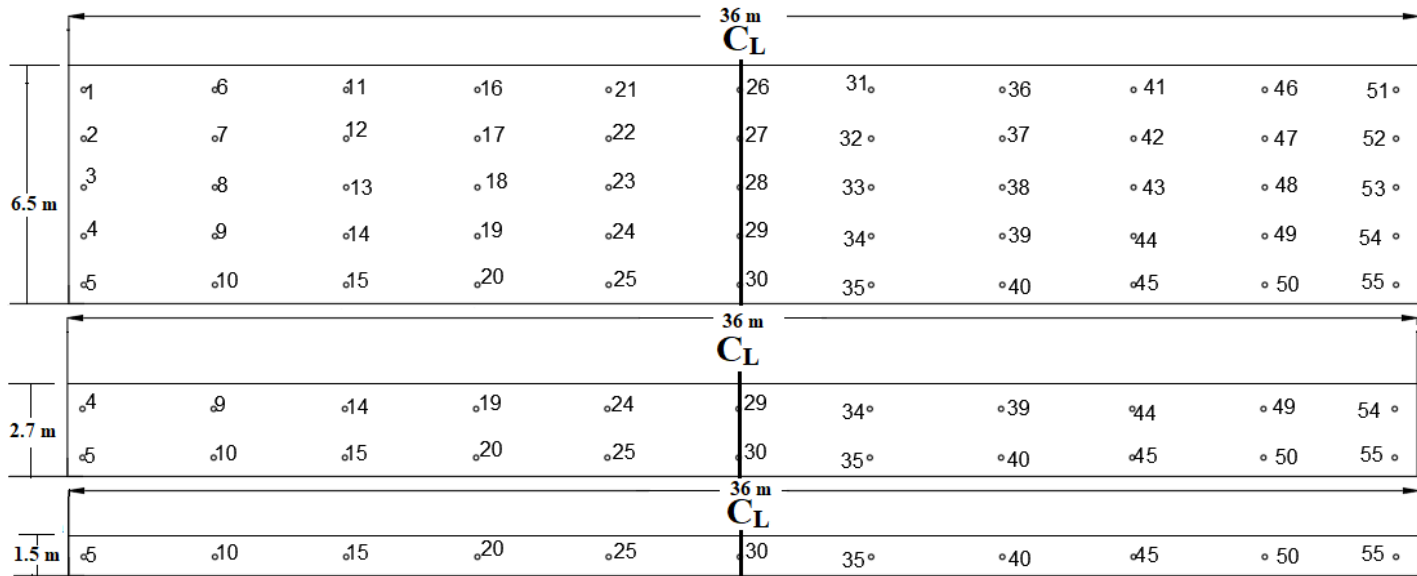
Figure 3.11 Different canopy widths with pressure taps
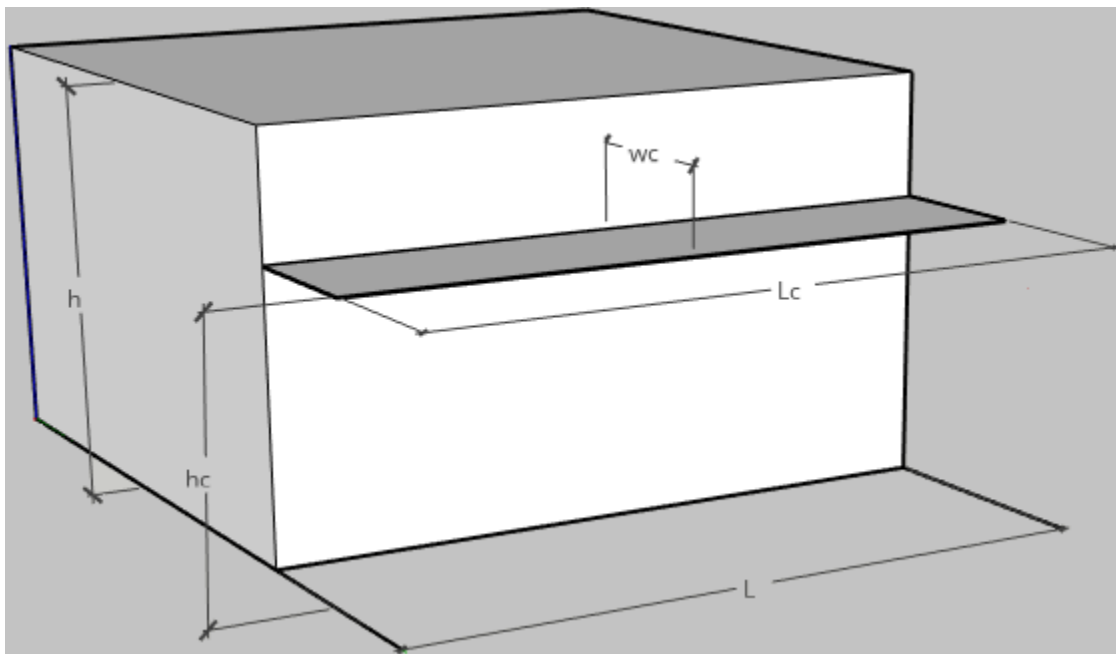
Figure 3.12 Sketch of the model with nomenclature of dimensions

43

Table 3.1 Number of configurations tested in the experiment

Building height, h	Canopy height, h_c	Canopy width, w_c	No. of configurations
7.15 m	3 m	6.5 m, 2.7 m, 1.5 m	3
	3.9 m	6.5 m	1
	6.45 m	6.5 m, 2.7 m, 1.5 m	3
18.5 m	3.9 m	6.5 m	1
	6.8 m	6.5 m	1
	7.8 m	6.5 m	1
	10.5 m	6.5 m	1
	17.9 m	6.5 m	1
37 m	3.9 m	6.5 m	1
	6.4 m	6.5 m, 2.7 m, 1.5 m	3
	15 m	6.5 m	1
	21.6 m	6.5 m, 2.7 m, 1.5 m	3
	28.8 m	6.5 m	1
	36.4 m	6.5 m, 2.7 m, 1.5 m	3
			Total 24

Chapter 4   Pressure coefficients on upper and lower surfaces of attached canopies

4.1 General

Canopies are often constructed as a beam and joist system to which the sheathing elements are connected. Sheathing elements are commonly attached to the upper side of the joists. However, it is not uncommon to add an additional layer of sheathing underneath the joists as can be seen in Figure 4.1. When both sides of a sheathing element are unexposed to wind loads, the pressures acting independently on the upper and lower surfaces are essential for the design of the fasteners with the joists. Furthermore, cladding elements such as roof tiles and shingles commonly fixed to the sheathing are always exposed to wind loads in only one surface. The analyses and observations made on this section serve as the basis for their recommended design provisions.

Although the failure of these components will rarely result in the complete failure of the canopy, lose sheathing component and cladding elements may act as projectiles resulting in more significant damage to neighbouring buildings or to the parent building itself. There are many factors that can affect the wind induced pressure on canopies. These are building height, wind direction, canopy height and width, considered canopy area etc. Effects of these factors are discussed in different sections.

4.2 Effect of building height on wind induced pressure on canopies

Building height is an important geometrical parameter that can affect wind induced pressure on canopies. In this study, we had three different building heights having the same plan dimensions. This offers an opportunity to investigate the effect of building height on wind loading on

Figure 4.1 Canopies with sheathing attached to the lower surface of the beam and joist system (Candelario 2012)

canopy. For the three buildings with three different heights, i.e. 7 m. 18.5m, 37m, canopies were placed at different heights (Table 3.1). The mean and peak values of Cp for upper surface and lower surface against hc/h are shown in Figures 4.2 and 4.3, respectively. The considered canopy width in Figures 4.2 and 4.3 is 6.5 m. The effect of building height on wind loading on canopies having same width and hc/h can be observed from Figs. 4.2 and 4.3. Figure 4.2 shows that the mean negative C_p values at lower surface are not much affected by the building height. In fact, mean negative Cp values do not vary much when hc/h≤ 0.5, for both upper and lower surface. That means, if canopy is situated at or under the mid-height of the building, mean Cp values are

quite close to each other. Same observation was made in the case of peak C_p values. From Figure 4.3, it is observed that peak negative C_p values for both upper and lower surfaces of canopies are comparatively stabilized when hc/h ≤ 0.5. In fact, a large variation of Cp values, in case of hc/h> 0.5, is clear. Upper canopy surfaces experience the highest mean negative loading when the canopy is near the roof of the building, 0.9≤hc/h≤1. This can be easily observed in case of taller buildings (in this study, when building height, h=18.5 m and 37 m). In case of peak negative Cp values, the same phenomenon, except a small difference, was observed. For peak negative Cp values, upper surface experienced almost same pressure for both h=18.5 m and h=37 m, but in case of mean negative Cp values, upper surface experiences more suction for h=37 m. Upper surface's peak negative Cp value in case of h=37 m is 67% more than that of for h=7 m, which indicates building height plays an important role in case of peak negative pressure for upper surface of canopy. The lower surface experienced almost constant mean and peak negative C_p values regardless of building height or h_c/h ratio. For all building heights, upper surface of canopy experienced little positive pressure when canopy was close to the roof. This was true for both mean and peak positive pressure. Upper surface experienced high positive pressure when the canopy was below the mid height of the building. Lower surface of canopy experienced highest positive pressure
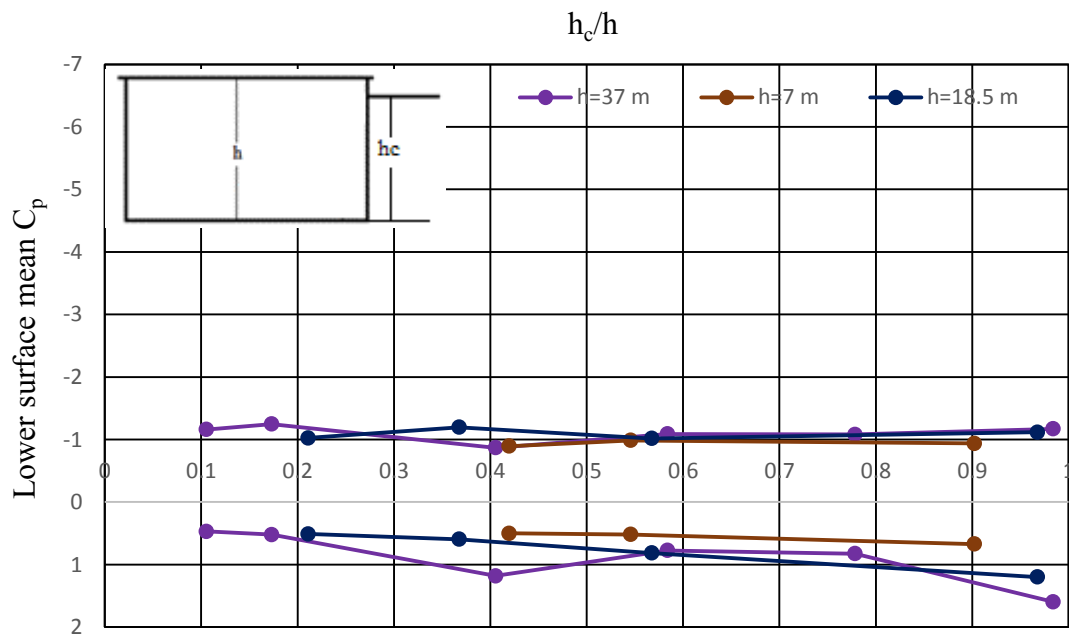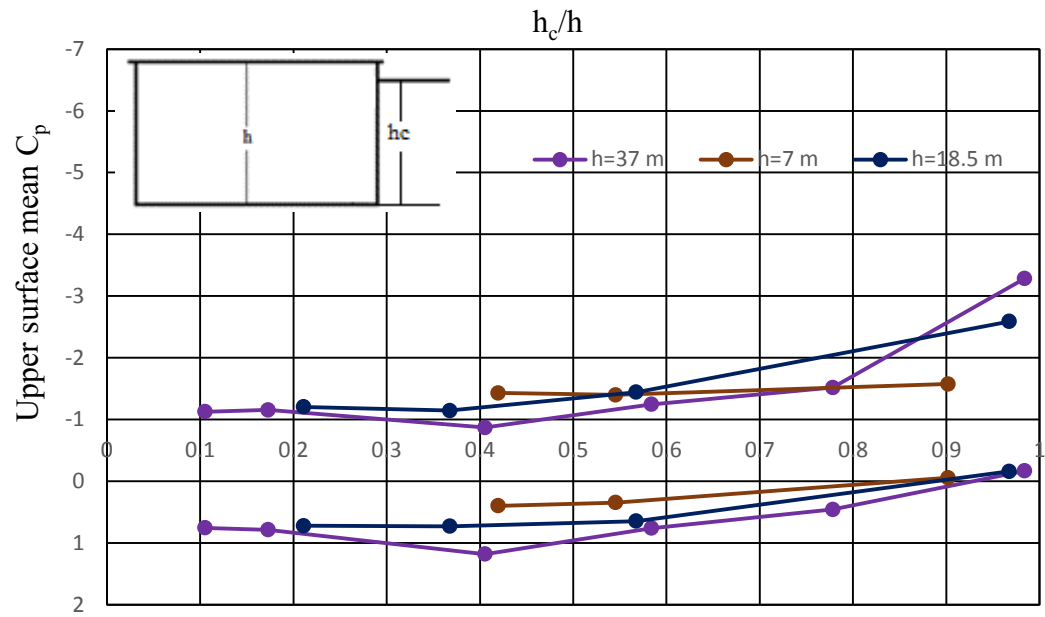
Figure 4.2 Mean Cp values for upper and lower surface with respect to hc/h for different building height
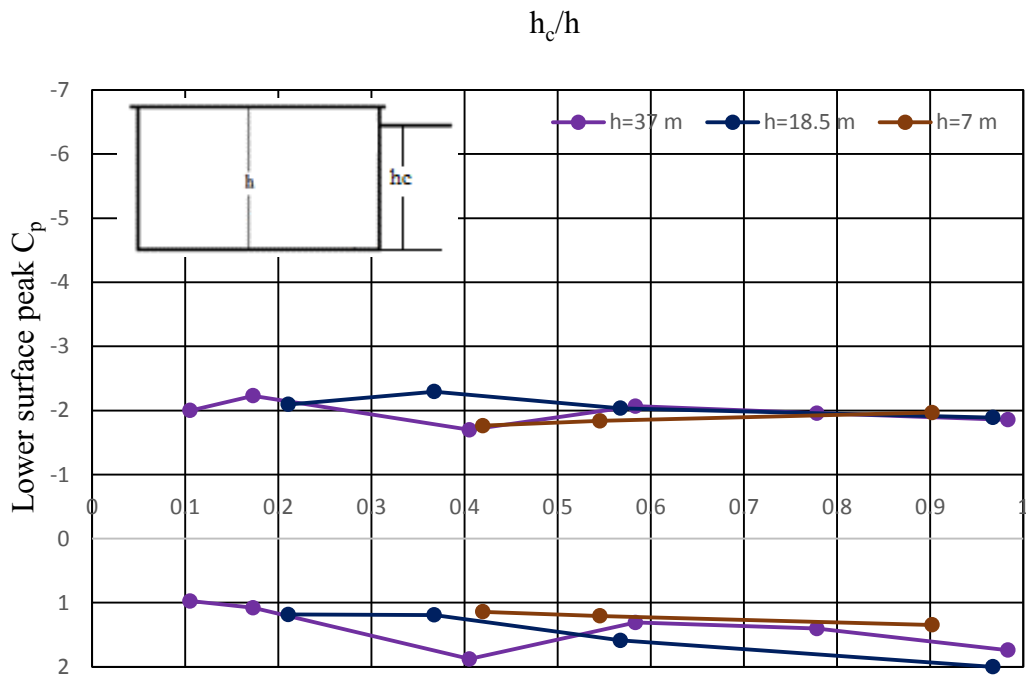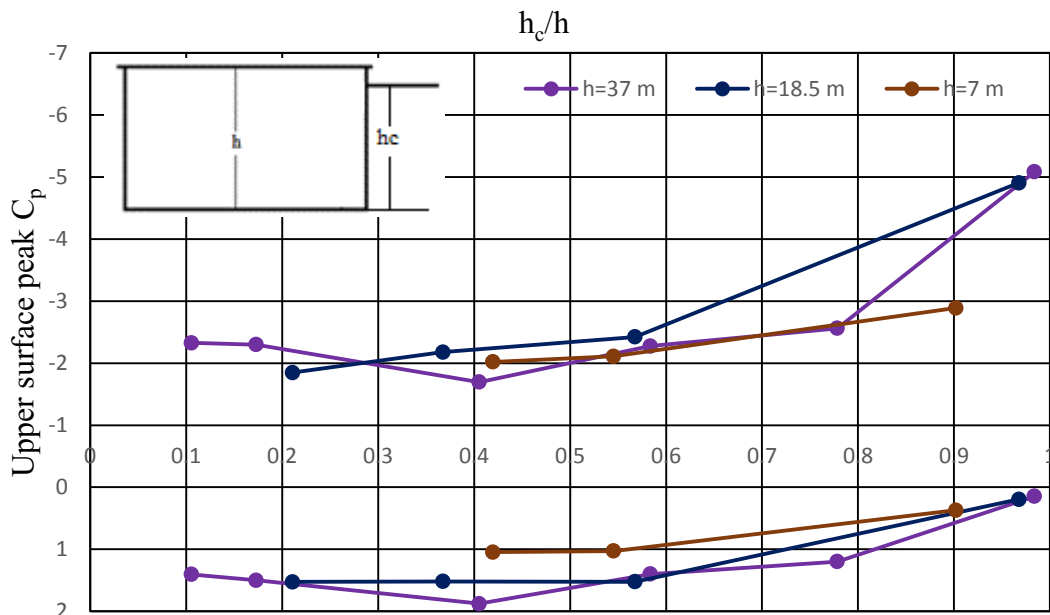
Figure 4.3 Peak Cp values for upper and lower surface with respect to hc/h for different building height

when the canopy was near the roof of the building for all building heights. For a certain value of h_c/h, canopies attached to taller buildings have higher positive mean and peak C_p values than canopies attached to low-rise buildings.

4.3 Effect of wind direction on wind induced pressure on canopies

Wind direction plays an important role in wind loading on canopy. Peak negative and positive pressure coefficients depend on the wind angle of attack. The wind angle for peak positive and peak negative C_p are different. Wind direction for peak positive and negative C_p also depends on canopy's vertical position (close to the roof or close to the ground or at mid height). Figures 4.4-4.6 show peak positive and negative C_p values in the upper and lower surfaces of canopies of three different widths, for three different hc/h, when h=37 meters.

Figure 4.4 represents the case where the canopy is at the top of the parent wall. The positive pressure on upper surface was found almost independent of wind direction. From Fig. 4.4, we do not find that many variations in case of positive pressure on upper surface. In case of peak negative pressure at upper surface, there is a lot of variation with respect to wind direction. From 0° to 60° wind direction, the absolute value of peak negative C_p keeps increasing, then, it keeps decreasing up to 120°. After 120°, the peak negative C_p becomes almost constant.

In case of peak positive pressure on lower surface, it remains constant for wind direction 0° to 60°. The highest positive pressure on lower surface occurs in this range. After 60°, the positive pressure decreases and it becomes constant again after 120°. The trend is a little different for peak negative pressure on lower surface. From 0° to 60° wind angle, the suction is almost constant. It keeps increasing after 60° and reaches the highest value at 90° wind direction.
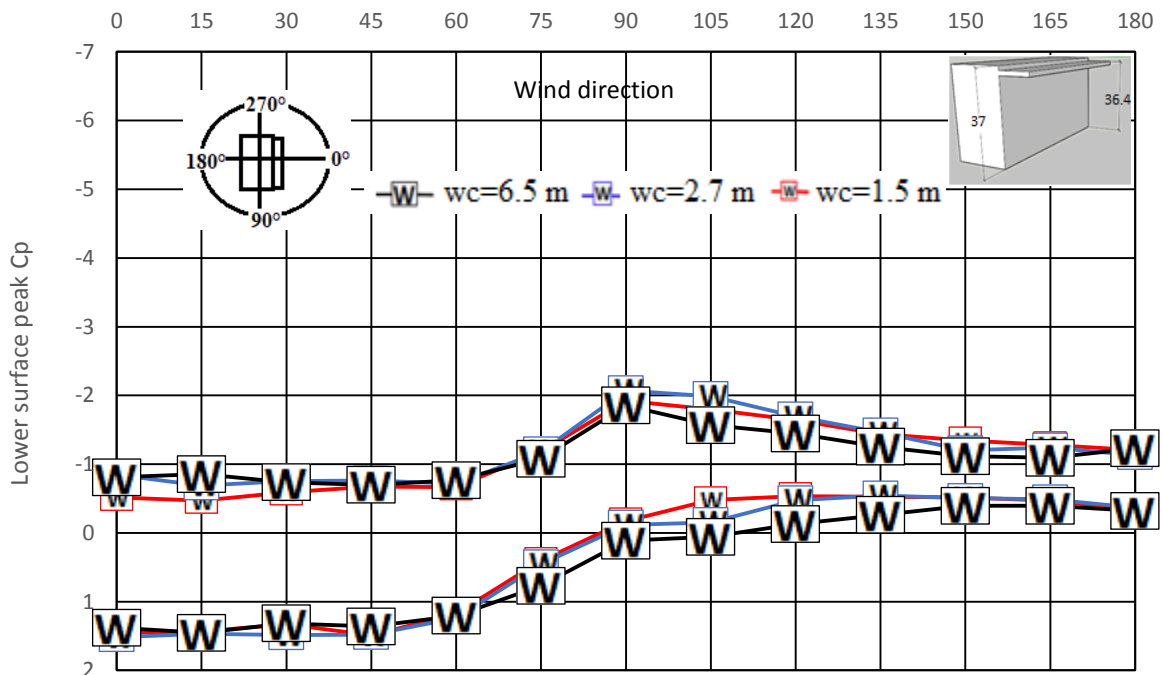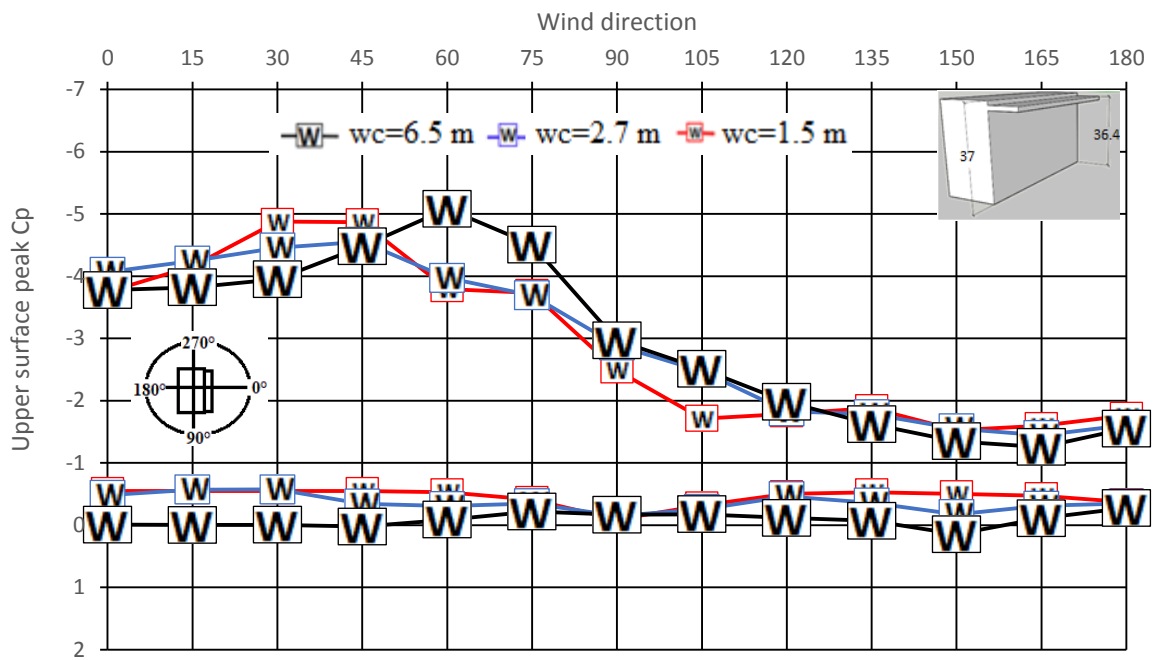
Figure 4.4 Upper and lower surface peak Cp values against wind direction for hc/h=0.98
(h=37 m)

Figure 4.5 represents the scenario when canopy is situated at the mid height (hc/h=0.56) of the parent wall. Suction on the upper surface remains constant from 0° to 60°, after that, the suction increases and reaches its highest value (absolute) at 90° wind direction. After that, the suction on the upper surface decreases. The highest peak positive pressure on the upper surface may occur between 0° and 45° wind direction. After this angle, positive pressure keeps decreasing.

The above-mentioned observation is also applicable for peak positive and negative pressure on the lower surface for this canopy position.

In Figure 4.6, the peak negative and positive C_p values for the upper and lower surfaces have been plotted against wind direction for canopy situated close to the ground (hc/h=0.18). Same observation is reported for both canopy at mid-height (hc/h=0.56) and canopy near to the ground (hc/h=0.18).

Figure 4.7 and Figure 4.8 show the effect of wind direction for different hc/h for a low-rise building (h =7 meters). Despite different building height, we can see the same tendency for both buildings against wind direction.

The observations indicate that lower surfaces experience the highest peak positive pressure at 0° or 15° wind angle and highest peak suction at 90° wind direction. This statement is true for the upper surface except when the canopy is near the roof.
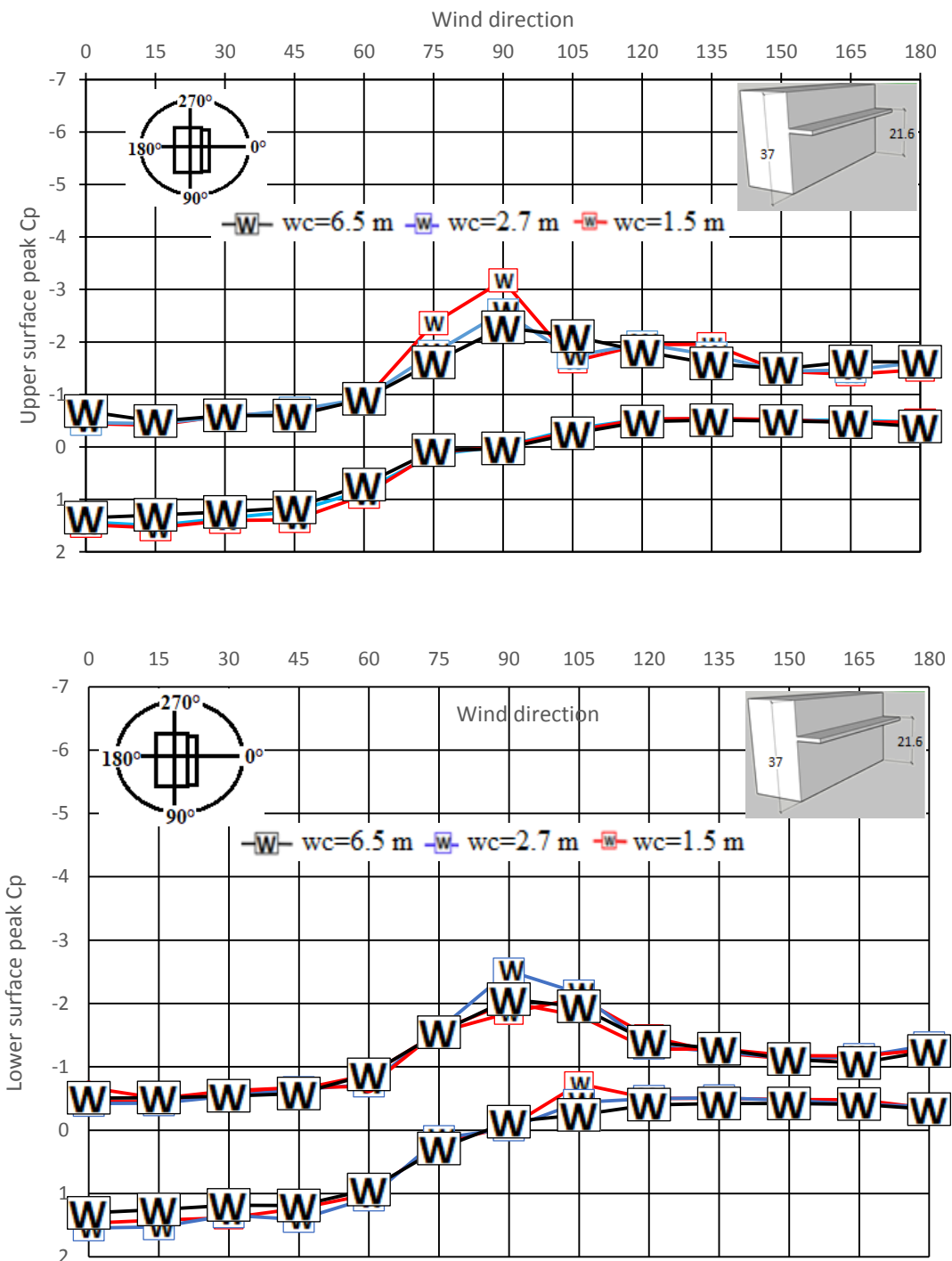
Figure 4.5 Upper and lower surface peak Cp values against wind direction for hc/h=0.56
(h=37 m)
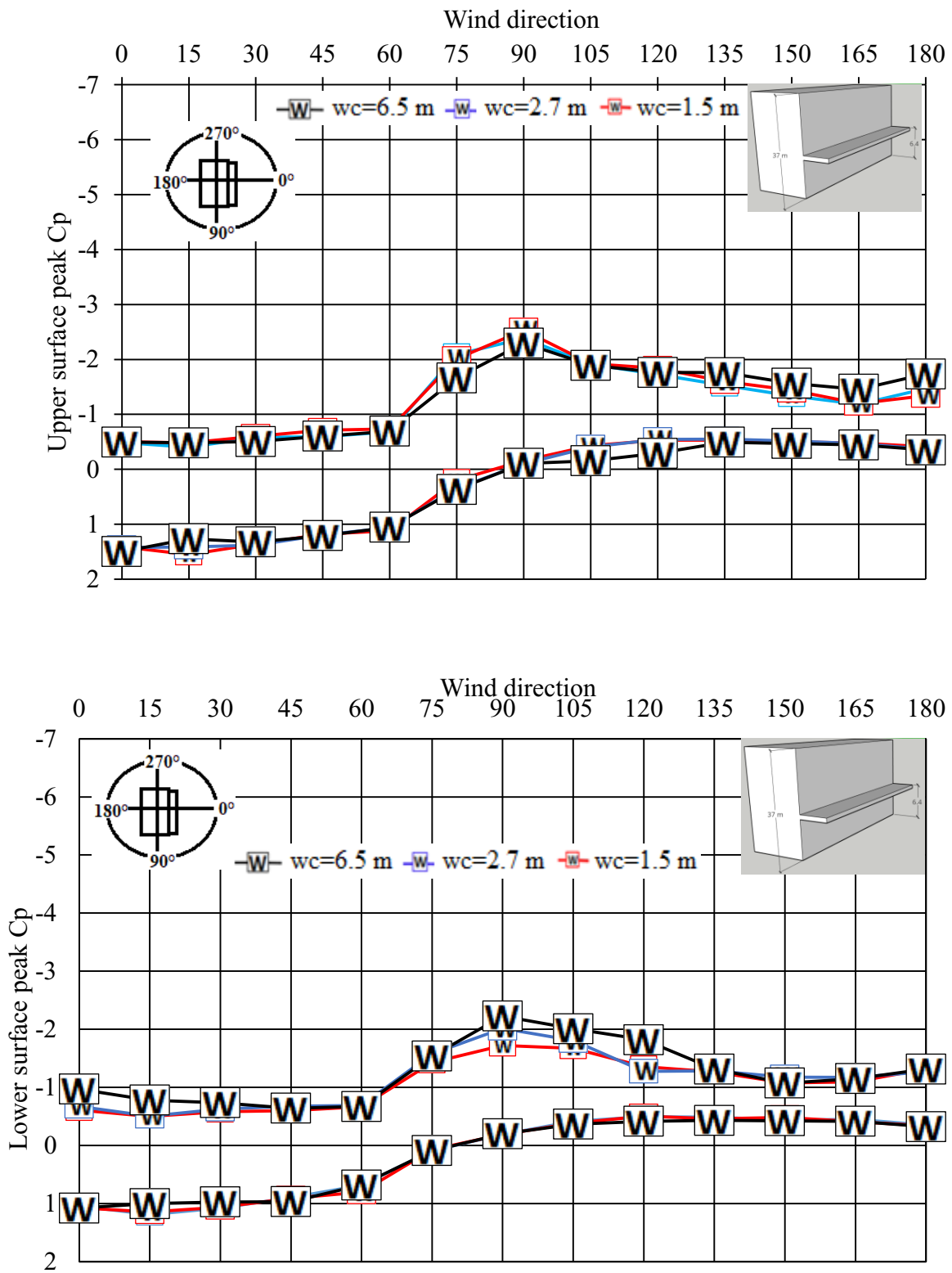
Figure 4.6 Upper and lower surface peak Cp values against wind direction for hc/h=0.18 (h=37 m)
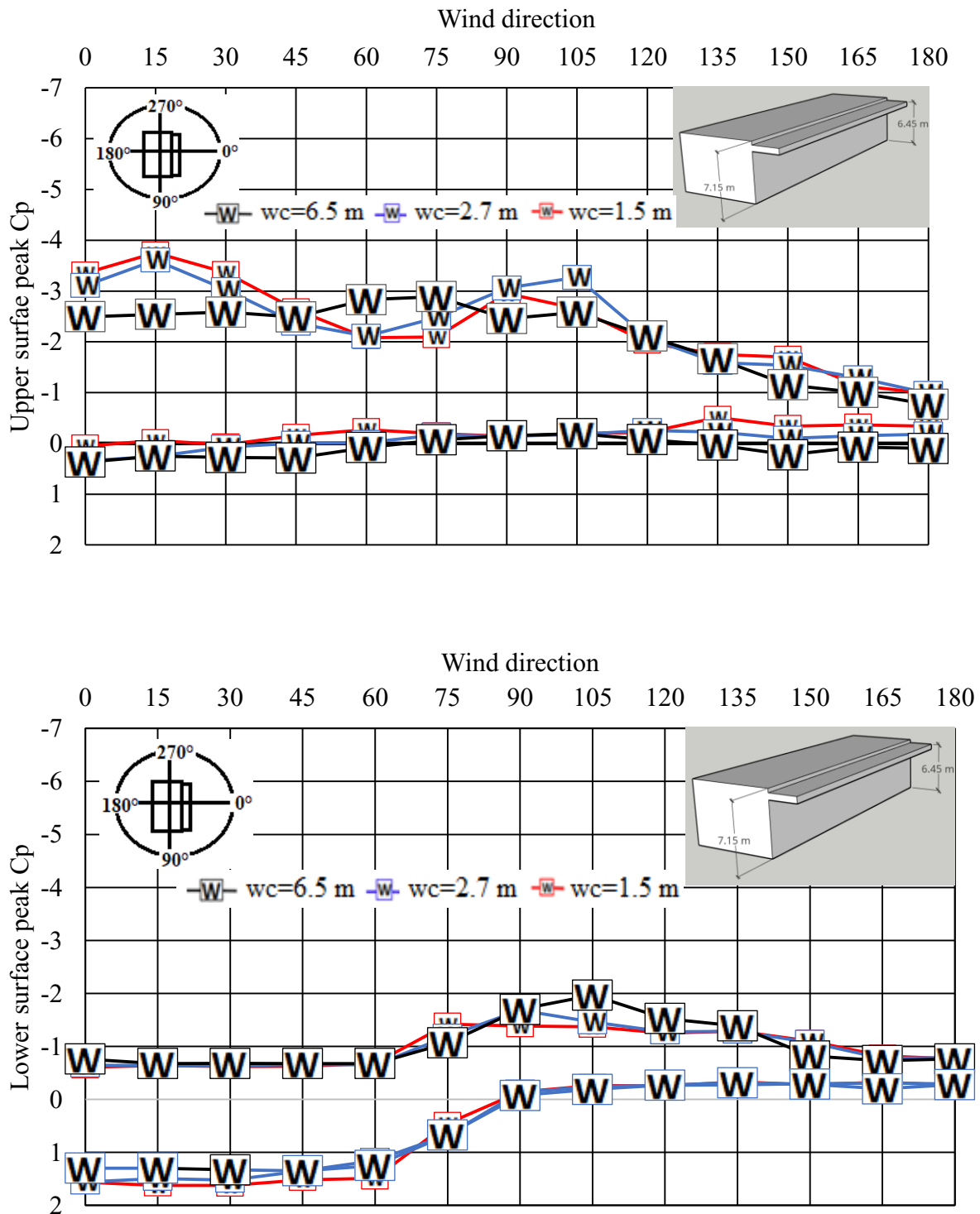
Figure 4.7 Upper and lower surface peak Cp values against wind direction for hc/h=0.9 (h=7 m)
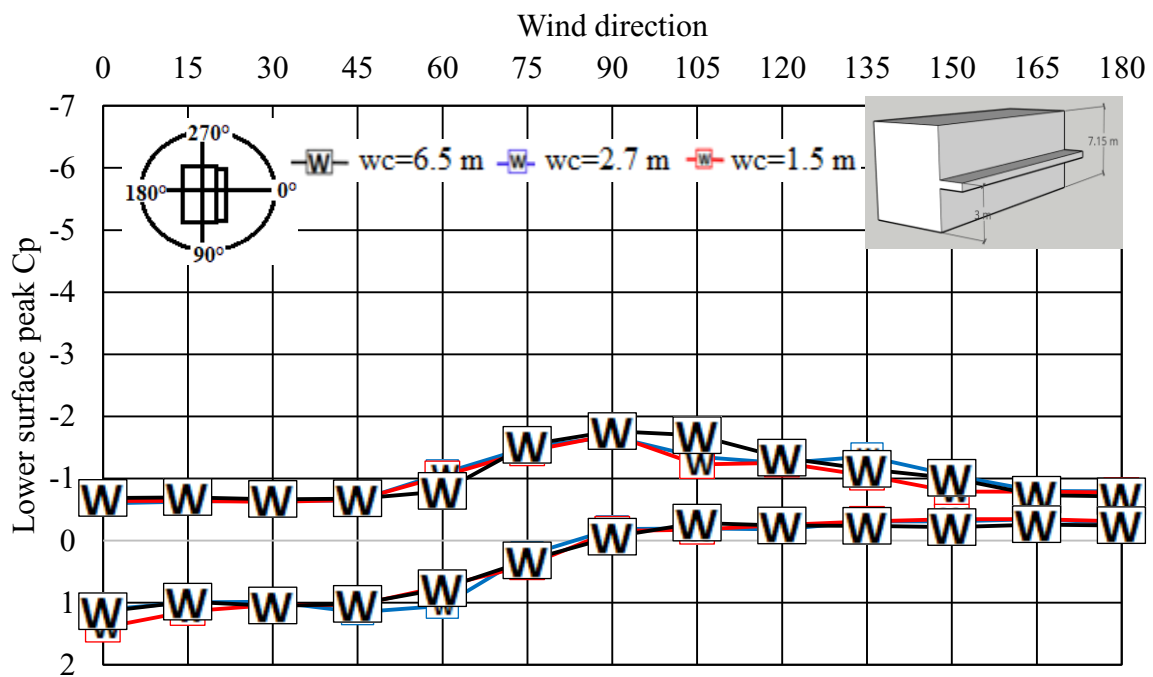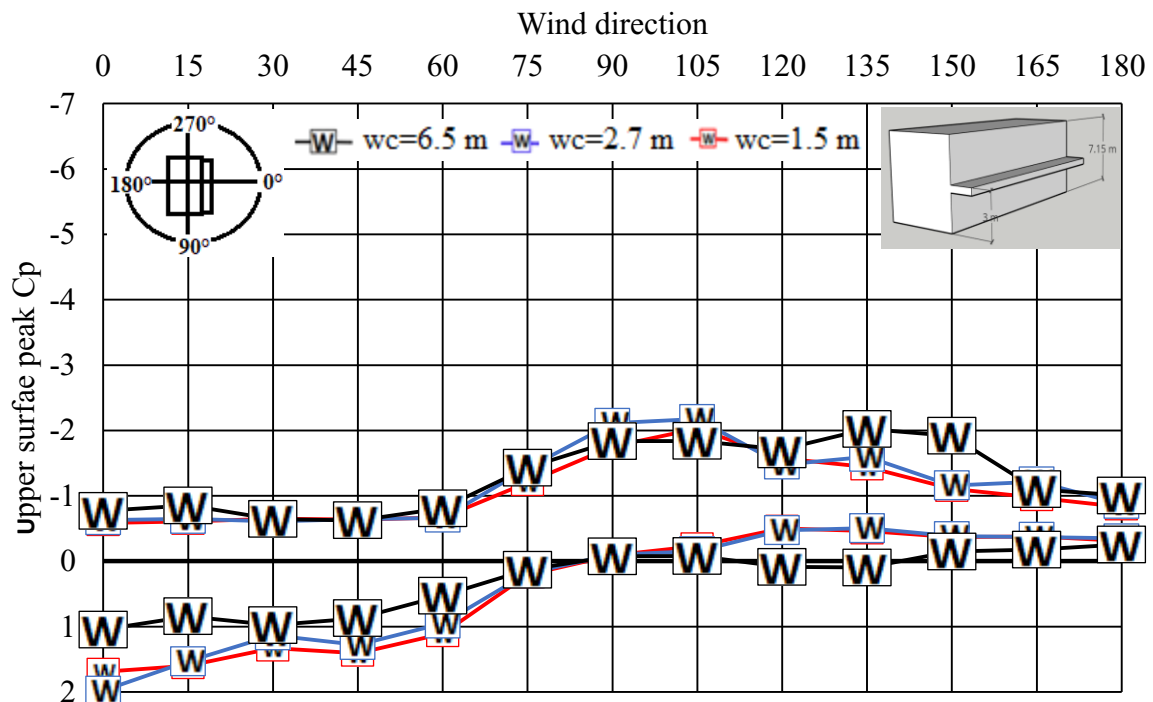
Figure 4.8 Upper and lower surface peak Cp values against wind direction for hc/h=0.5 (h=7 m)

4.4 Contours of wind loads acting on canopy surfaces

Contours have been plotted for mean and peak critical C_p values on upper and lower surfaces for h=37m and for peak critical C_p values on upper and lower surfaces for h=7 m. Figures 4.9 - 4.14 present these contours. All these contours are for the critical peak positive and negative C_p values, which means they do not represent any certain wind direction. They are the highest values (absolute values in case of negative C_p) regardless of the wind directions. Also, because of the symmetry, only half of the canopy is presented.
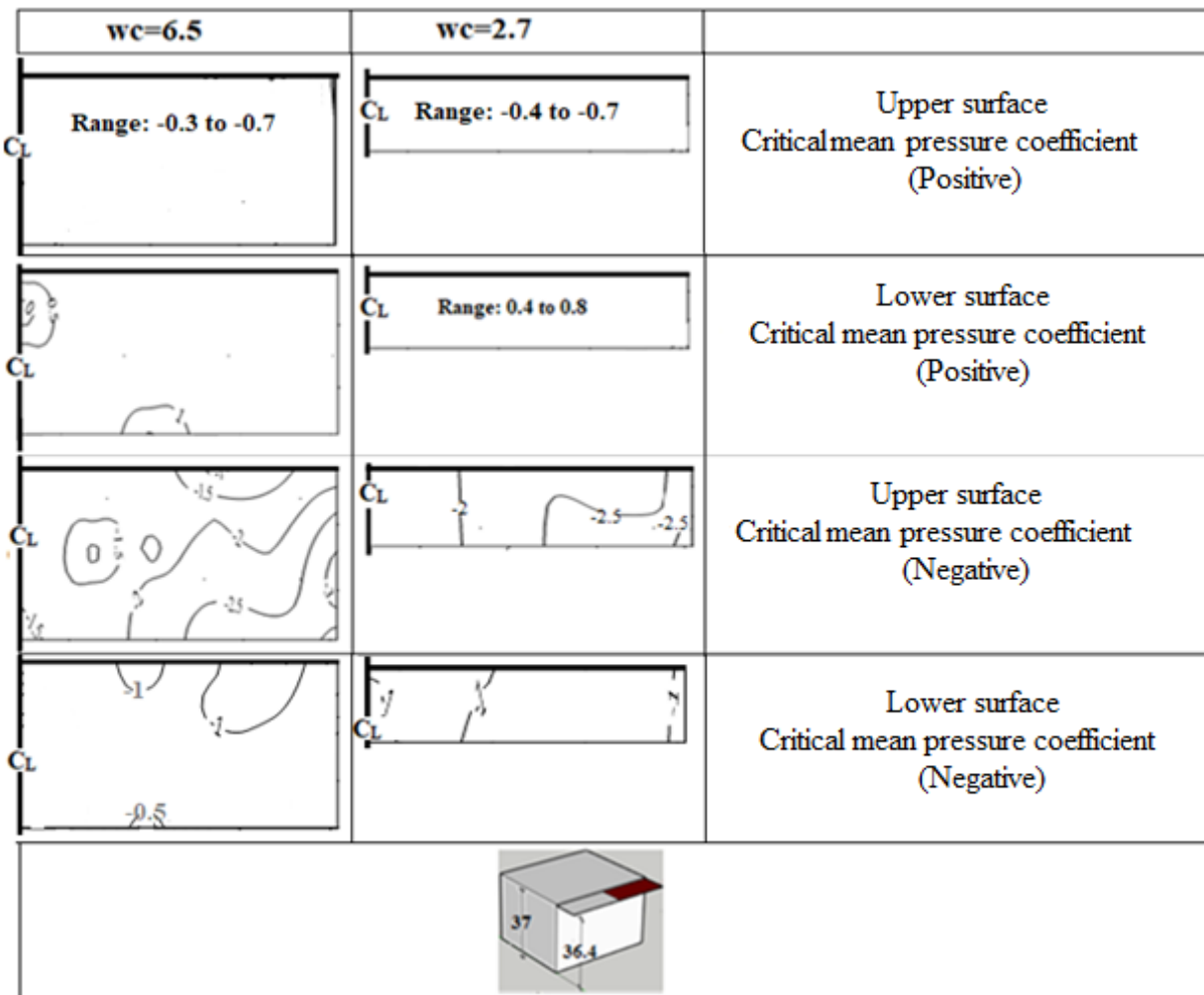
Figure 4.9 Contour plots of critical mean loading on both surfaces of canopy for different widths for hc/h=0.98 (h=37 m)

wc=6.5	wc=2.7	
		Upper surface Critical mean pressure coefficient (Positive)
		Lower surface Critical mean pressure coefficient (Positive)
		Upper surface Critical mean pressure coefficient (Negative)
		Lower surface Critical mean pressure coefficient (Negative)

Figure 4.10 Contour plots of critical mean loading on both surfaces of canopy for different widths for hc/h=0.18 (h=37 m)

Figures 4.11 and 4.13 present the contours where the canopy is located at the top. The critical peak positive C_p values on the upper surface in both figures are not that much significant. Focusing on the peak positive C_p values on lower surface, it is observed that the highest value is around 1.5. In Figure 4.11, the values seem to decrease near the center line of the canopy. In case of w=6.5m, highest value is at the opposite edge of the parent wall and in case of w=2.7 m, highest value is near the side edge. This is applicable for Figure 4.13 as well. Concentrating on the peak negative C_p values on upper surface, it is clear that the corners experience the most intense suctions. This is also true for the peak negative C_p on lower surface.

wc=6.5 m	wc=2.7 m	
Range: -0.3 to 0.1	C_L Range: -0.4 to -0.1	Upper Surface Critical Peak Positive Pressure Coefficient, Cp
0.5 1 C_L 1.5	C_L 1	Lower Surface Critical Peak Positive Pressure Coefficient, Cp
-2.3 -2.5 -1.5 -2 -2.5 -1.3 -2 C_L -3.5 -3.5 -3.5 -4	C_L -3.5 -3 -3.5 -3.5 -4 -4.5	Upper Surface Critical Peak Negative Pressure Coefficient, Cp
-1.5 C_L	C_L	Lower Surface Critical Peak Negative Pressure Coefficient, Cp
37 36.4		

Figure 4.11 Contour plots of critical peak loading on both surfaces of canopy for different widths for hc/h=0.98(h=37m)

One noticeable phenomenon is that contours on the lower surface are parallel to the side edge and on the upper surface, they are a little corner oriented. Figures 4.12 and 4.14 represent the contours where canopy is located under or near the mid height of the buildings. In Figure 4.12, canopy, which is attached to a tall building (h=37 m), is close to the ground and in Figure 4.14, canopy is attached to a low-rise building (h=7 m) and is located near the mid height. In Figure

4.12, C_p values are increasing near the center line and the edge is not feeling the highest pressure in case of peak positive pressure on the upper surface.
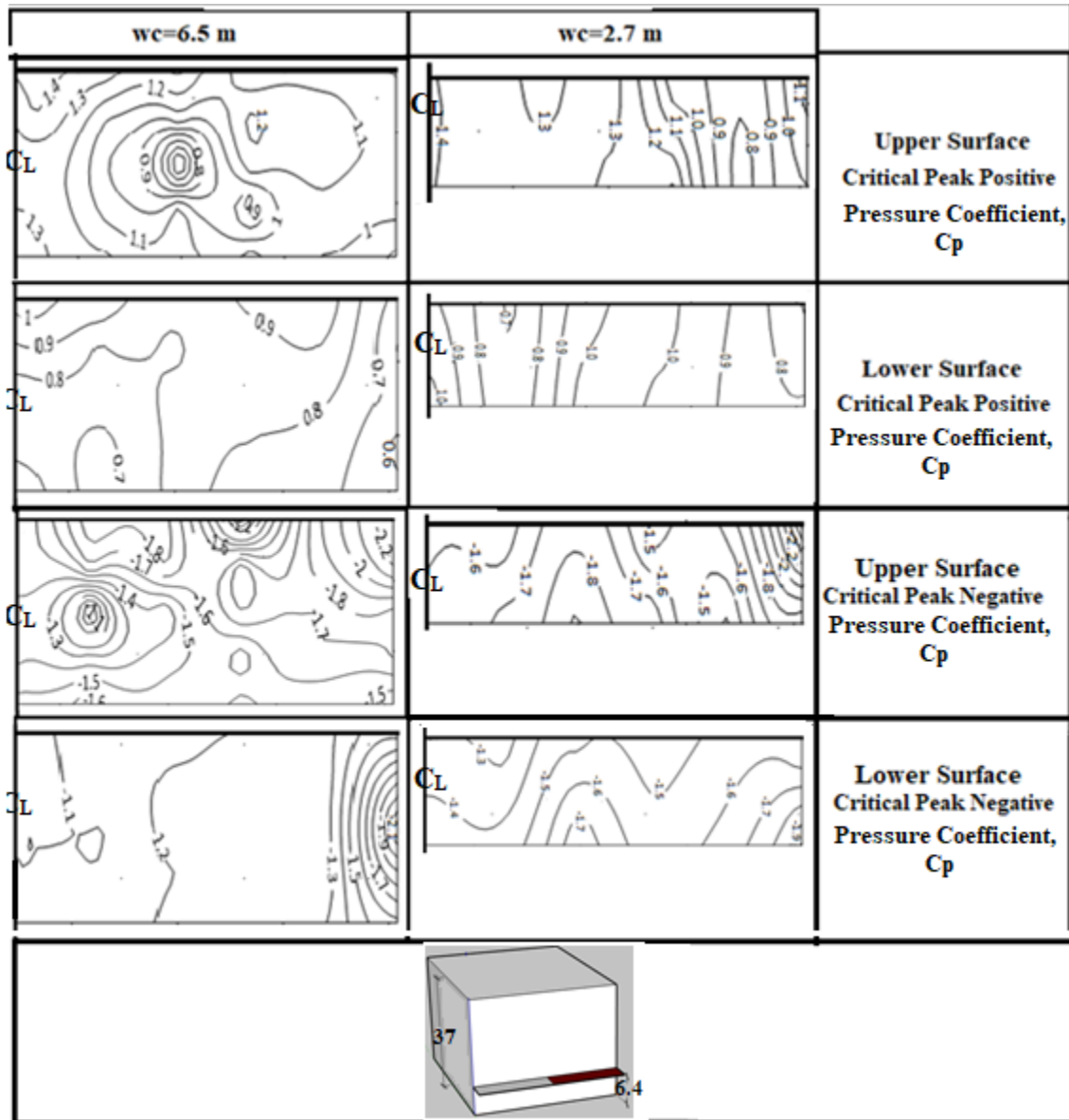
Figure 4.12 Contour plots of critical peak loading on both surfaces of canopy for different widths for hc/h=0.18(h=37m)

wc=6.5 m	wc=2.7 m	
C_L	C_L	Upper surface Critical Peak positive pressure coefficient, Cp
C_L	C_L	Lower surface critical peak positive pressure coefficient, Cp
C_L	C_L	Upper surface critical peak negative pressure coefficient, Cp
C_L	C_L	Lower surface critical peak negative pressure coefficient, Cp

7.15 m   6.45 m
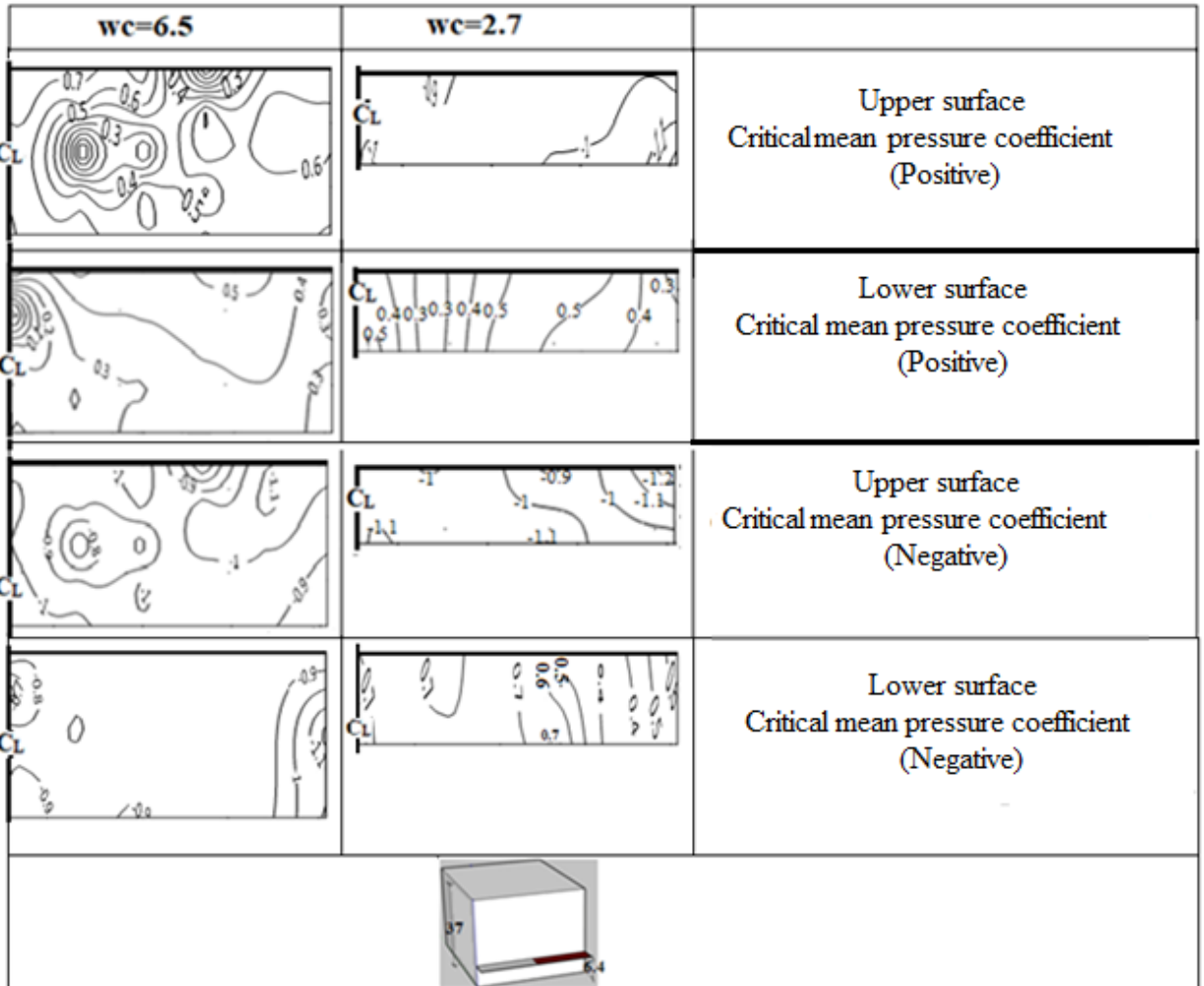
Figure 4.13 Contour plots of critical peak loading on both surface of canopy for different widths for hc/h=0.9(h=7m)

In Figure 4.14, the prominent pressure is exerted on the region which is middle of the edge and center line in case of positive loading on the upper surface. So, for both low-rise and taller buildings, the maximum peak positive pressure on the upper surface is not on the side edges. In case of peak positive pressure on lower surfaces, this trend is more clearly visible.

For peak negative C_p values on the upper surface, it is clear that the corners close to the parent wall take the highest suction (Figure 4.12 and 4.14). In case of lower surface, the side edges face the highest suction.

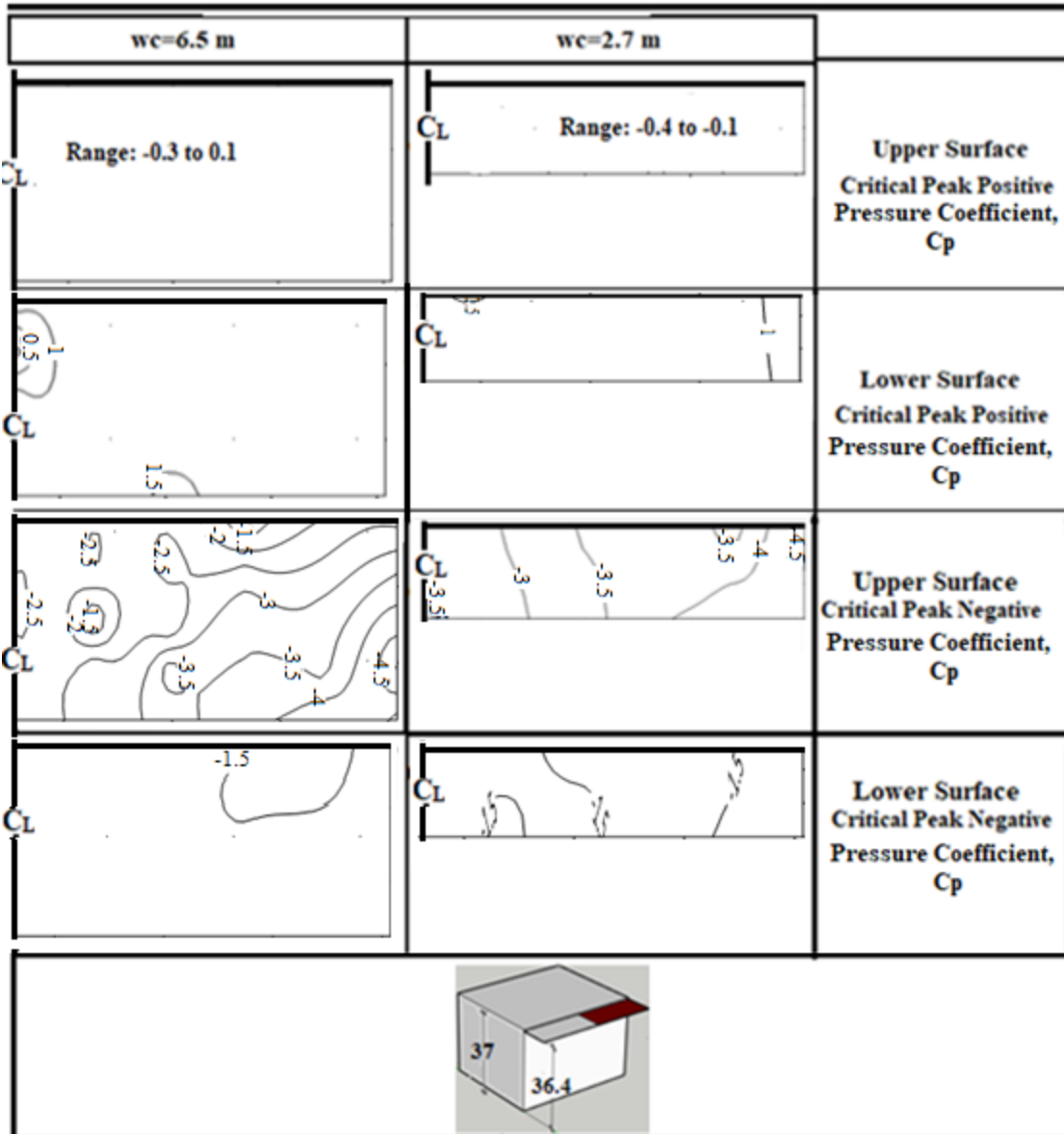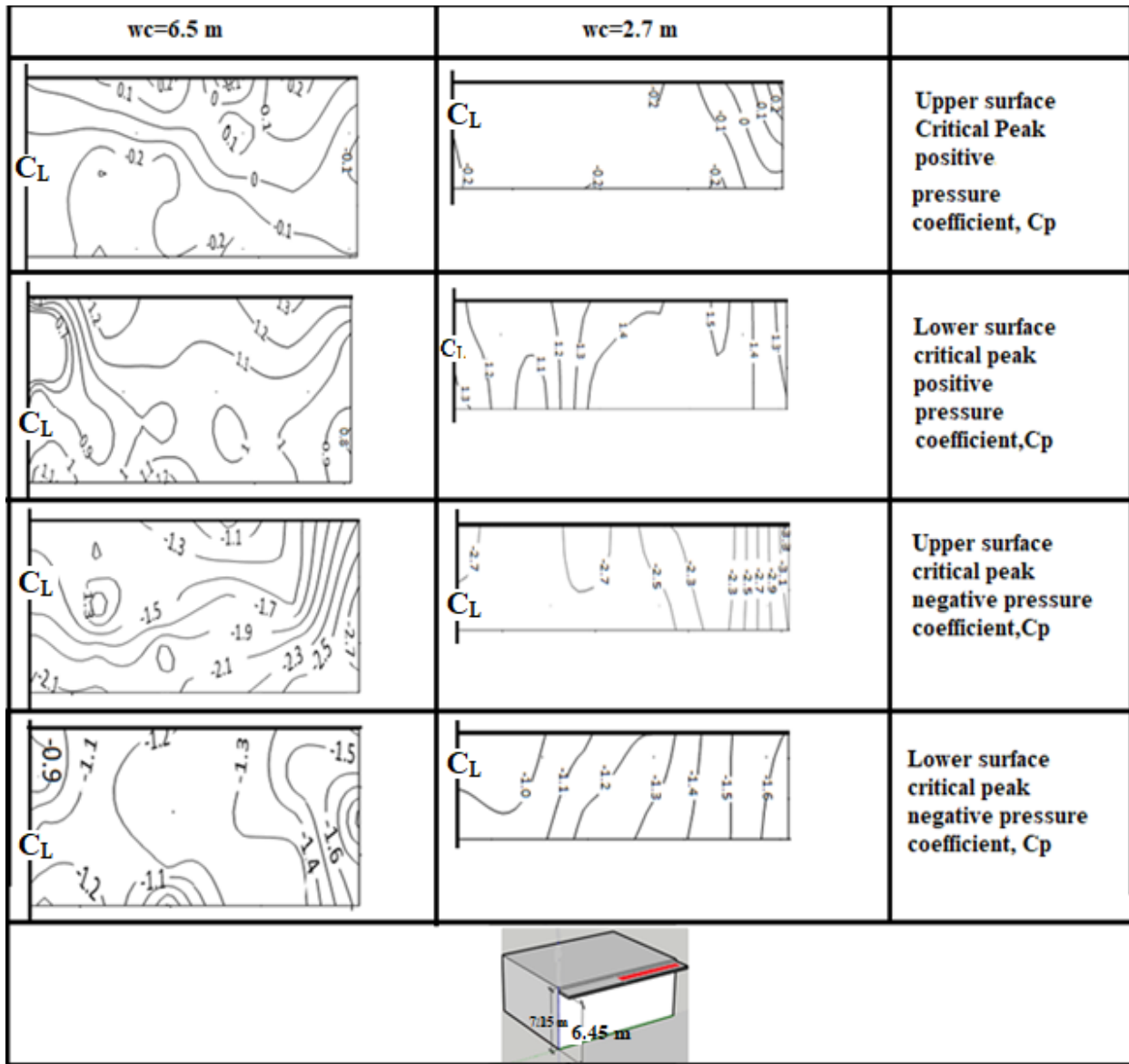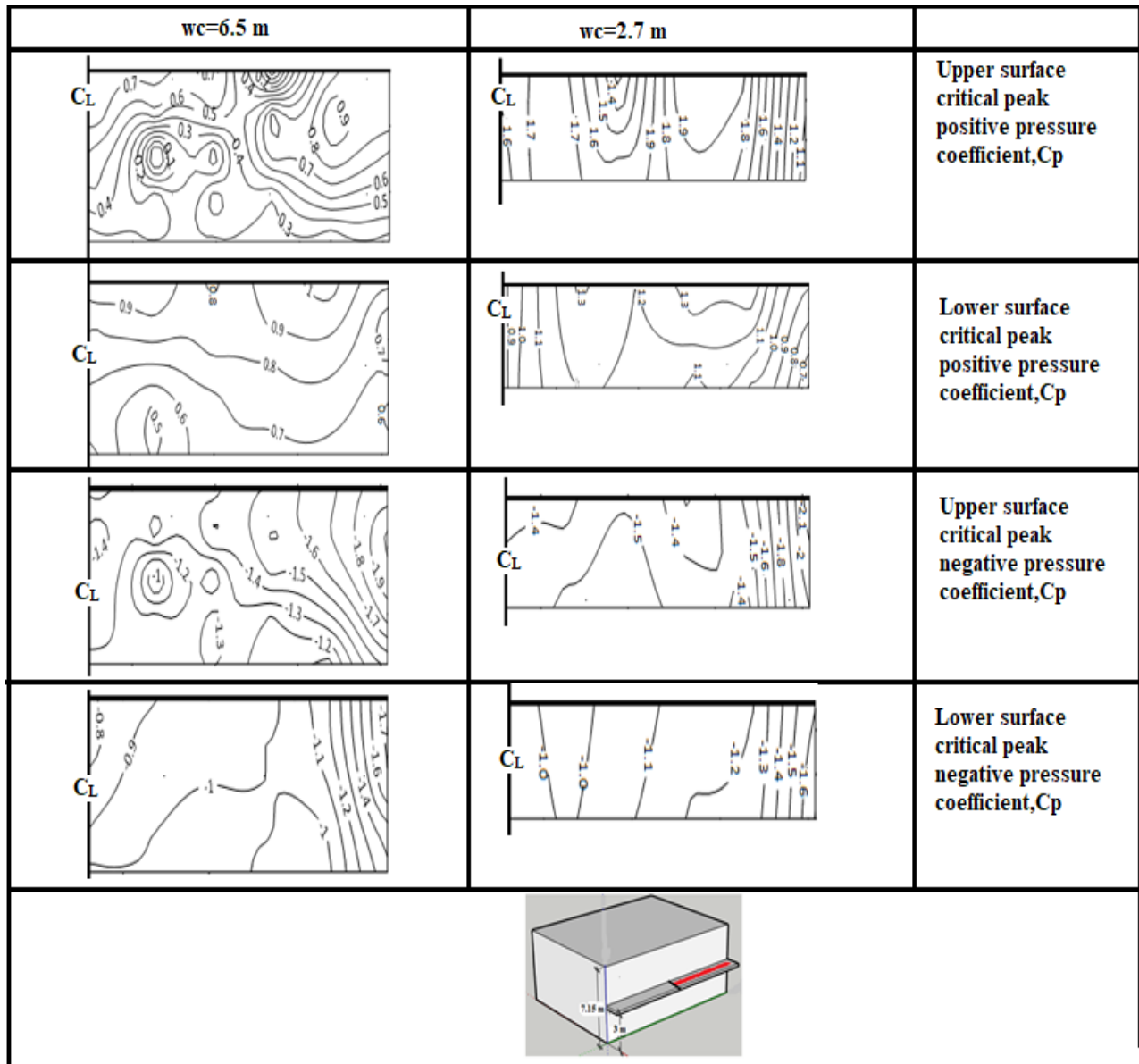| wc=6.5 m	wc=2.7 m	
		Upper surface critical peak positive pressure coefficient,Cp
		Lower surface critical peak positive pressure coefficient,Cp
		Upper surface critical peak negative pressure coefficient,Cp
		Lower surface critical peak negative pressure coefficient,Cp

Figure 4.14 Contour plots of critical peak loading on both surface of canopy for different widths for hc/h=0.46(h=7m)

So, in all cases, the negative pressure mainly affects the edges or corner areas. In case of positive pressure, the location of maximum pressure depends on canopy's vertical position. When the canopy is near the roof, the side and front edges of the canopy are most vulnerable due to positive pressure. In other cases, the areas near center line or near to the edge are most vulnerable.

4.5 Effect of h_c/h and canopy width on wind induced pressure on canopies

The relevant vertical position of canopy with respect to the roof height (expressed as h_c/h) is a particularly important parameter for studying wind loading on attached canopies. Positive or negative pressure on upper and lower surface of attached canopy vary significantly with h_c/h ratio. To verify the effect of canopy width, three different canopy widths were tested in this study. Figures 4.15-4.17 show the effect of h_c/h and canopy width on wind loading on canopies attached to buildings of different heights.

In Figure 4.15, tall building with h=37 m has been considered. It is clear that the upper surface experiences the highest peak positive pressure when h_c/h $\leq$ 0.5 and the value is almost constant up to this range of h_c/h. Peak positive pressure on upper surface quickly decreases when h_c/h exceeds 0.5. It is also observed that width of canopy does not affect peak pressure coefficient on the upper surface of the canopy attached to a tall building (h=37 m)

The trend for peak negative pressure on upper surface is opposite. With increase in h_c/h ratio, peak negative pressure (suction) is also increasing on upper surface. An interesting observation is, when h_c/h$\leq$ 0.5, the peak negative Cp values are almost constant and do not depend on canopy

width, except for canopy with 2.7 meters which experienced more suction than other widths when h_c/h =0.5. When h_c/h exceeds 0.5, there is quick increase in suction on upper surface and the
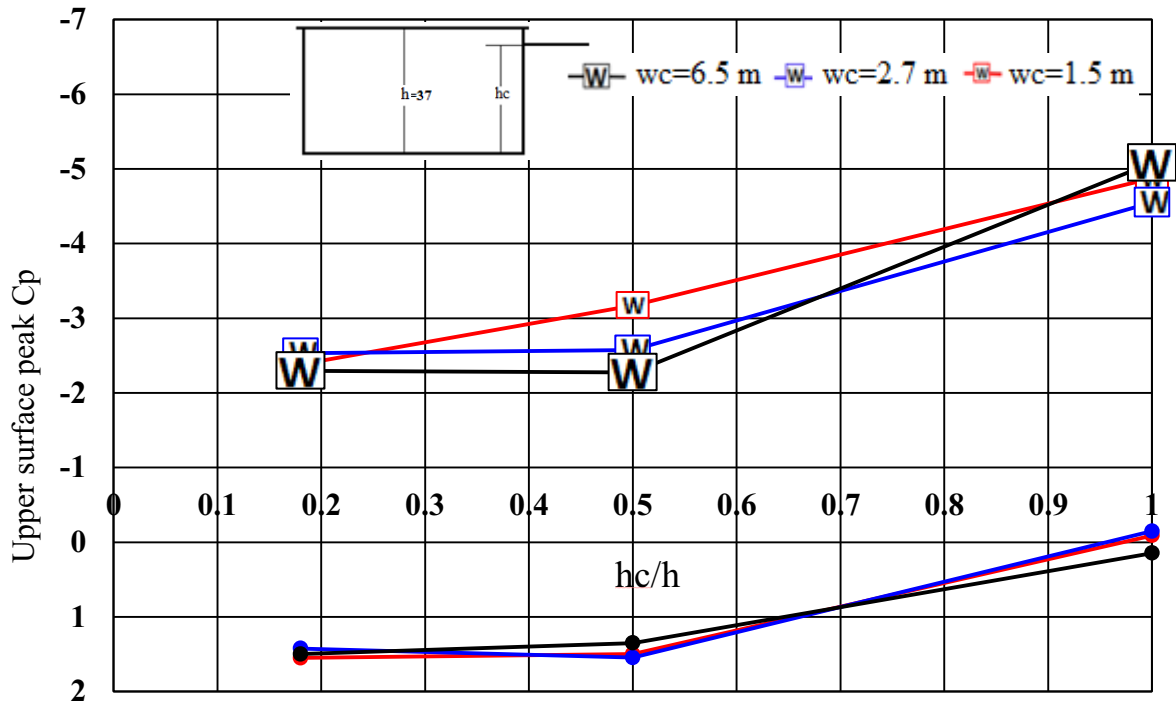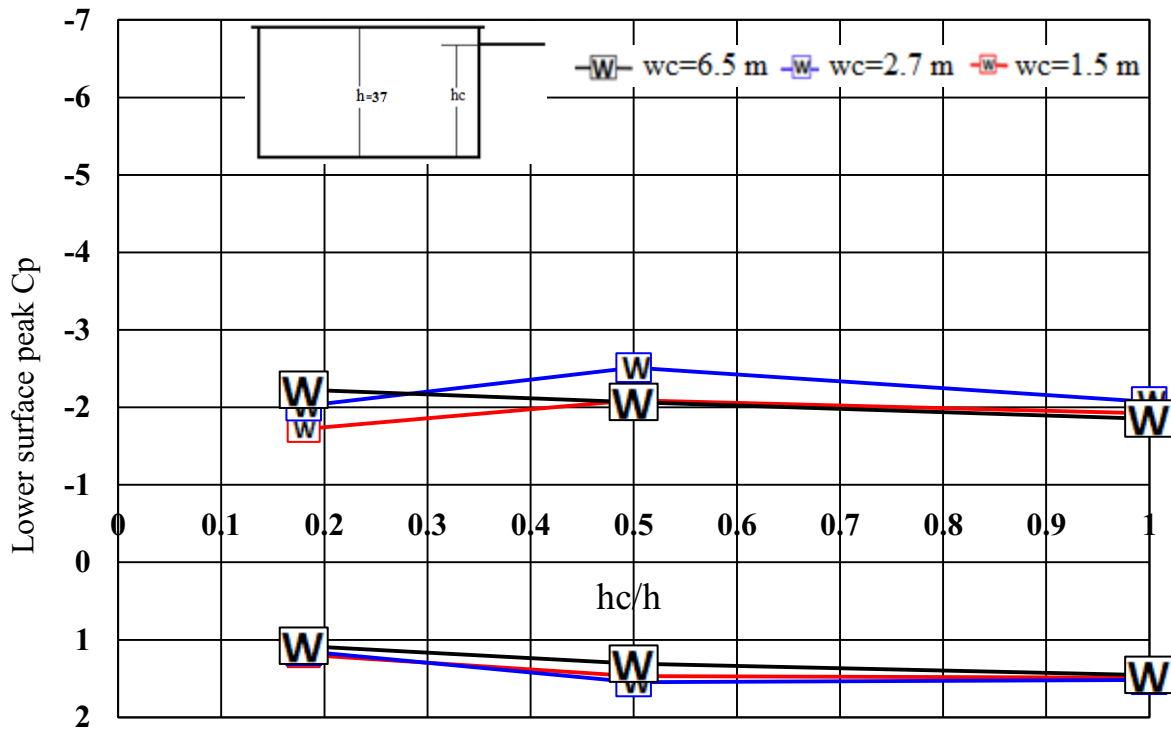
Figure 4.15 Peak Cp values on upper and lower surface with respect to canopy width and h_c/h for h=37 m

highest suction occurs when h_c/h is close to unity. The increase in suction is almost two times.

As shown in Figure 4.16, the highest value of peak negative pressure coefficient (absolute value) on the upper surface is not width dependent.

Figure 4.15 also shows that peak positive pressure on the lower surface attains its highest value when h_c/h is close to unity. In fact, from h_c/h=0.5, the peak positive pressure on the lower surface is almost constant. Peak positive pressure on the lower surface decreases when h_c/h< 0.5 with the highest Cp value is almost 1.5 times higher than the lowest value. Peak negative pressure coefficients on lower surface do not vary that much with respect to h_c/h, for canopy with w=1.5 m and w=6.5 m. Canopy with width 2.7 m undergoes a little variation as its lowest peak negative pressure coefficient (absolute value) is -2 when h_c/h=0.18 and h_c/h=1 and highest peak negative pressure coefficient (absolute value) is when h_c/h=0.5. So overall, lower surface of canopies

attached to tall building do not experience many variations in terms of both peak positive and negative Cp values with respect to h_c/h. Thus, we can say that width is not an important factor for wind loading on upper and lower surface of canopy attached to tall building (h=37 m) and pressure variation with respect to h_c/h is more significant for upper surface of the canopy.

In Figure 4.16, when the building height is 18.5 m, the same observations are applicable. Experimental results for only one canopy width, 6.5 m, for this building height is available.

For low-rise building, as shown in Figure 4.17, similar observations are true. One noticeable observation for low-rise building is that the canopy width plays a role in case of highest peak positive and negative (absolute value) pressure coefficients. When canopy is close to the building roof, peak negative pressure on the upper surface increases with decreased canopy width. Thus, for canopy width (w_c) of 1.5 m, 27% more peak negative pressure coefficient (absolute value) is observed than that for w_c of 6.5 m. In case of peak positive pressure coefficient, wider canopy (w=6.5 m) experience almost 80% less pressure than narrower canopies (w=2.7 m and 1.5 m)
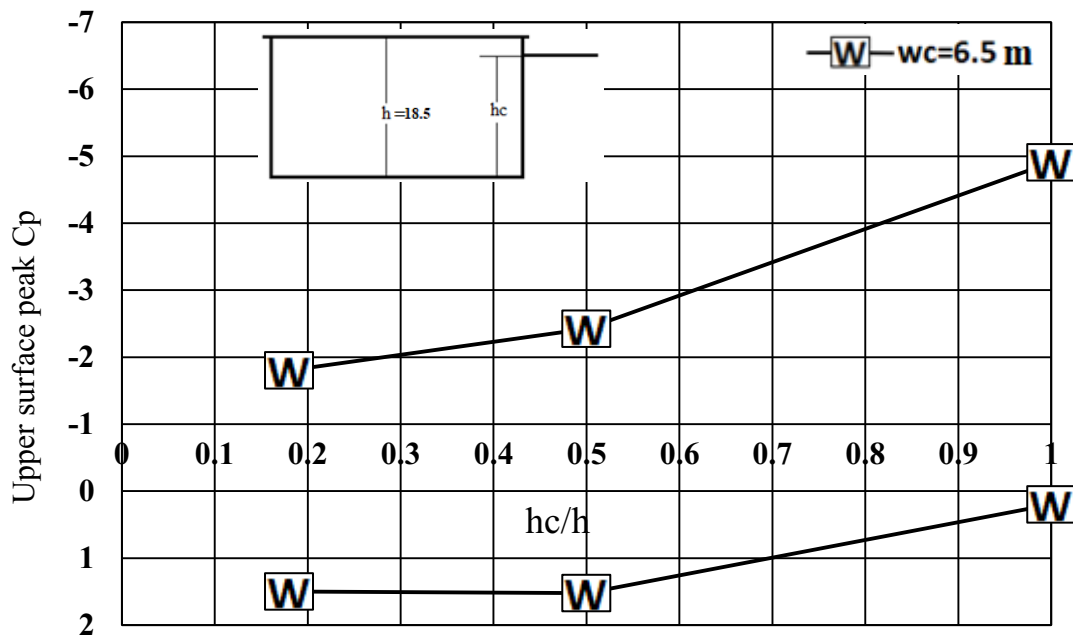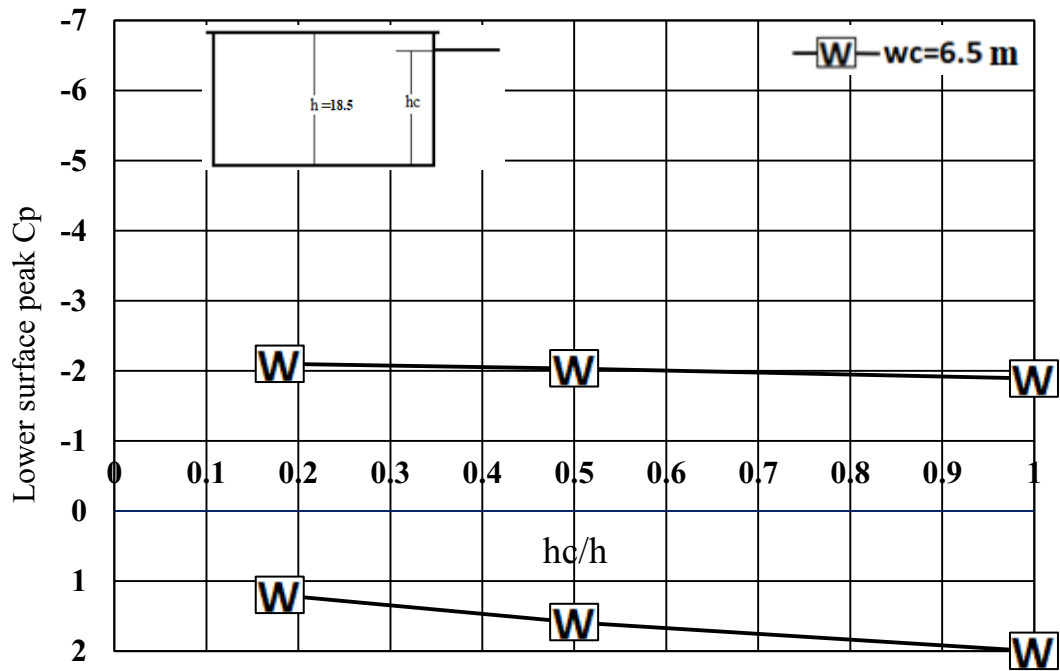
Figure 4.16 Peak Cp values on upper and lower surface with respect to canopy width and hc/h for h=18.5 m
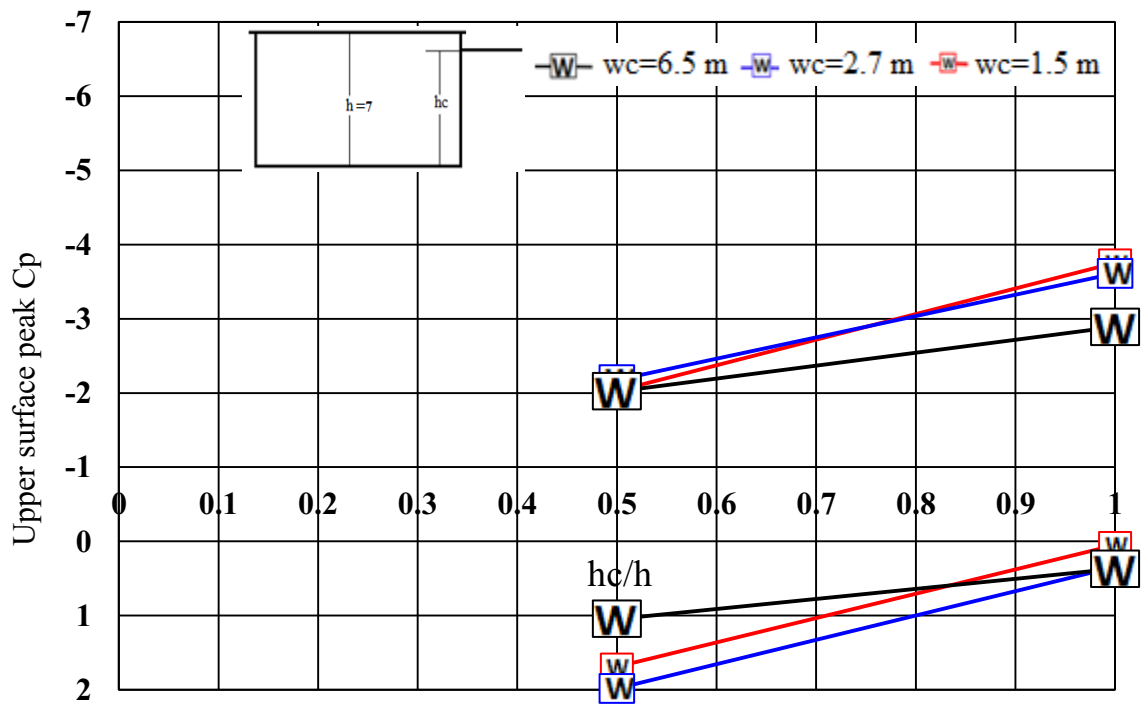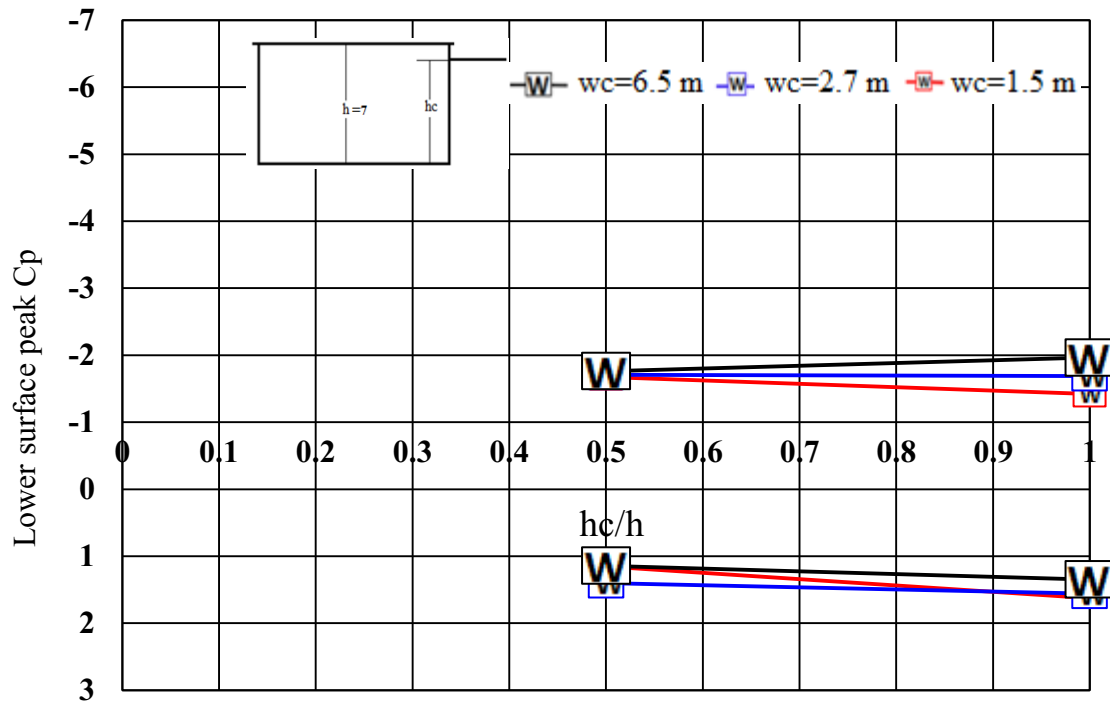
Figure 4.17 Peak Cp values on upper and lower surface with respect to canopy width and hc/h
for h=7 m

4.6 Effect of tributary area on wind induced pressure on canopies

In the previous sections, only local pressure coefficients i.e. C_p from one pressure tap was considered. In order to understand wind loading for large areas, the area average values for C_p need to be considered. The area-averaging effect on peak positive and negative C_p was determined by considering single or multiple sets of pressure taps and assigning them to their corresponding effective surface areas. The area average values of C_p are important for design recommendations. In general, while designing small areas (i.e. one nail) C_p from one pressure tap i.e. 1 ft^2 (0.1 m^2) is considered. For larger areas, area average C_p values over corresponding areas is considered.

Figures 4.18 - 4.20 present the area average peak C_p values for both upper and lower canopy surfaces for three different h_c/h values (canopy at the top, bottom and at the middle) for h=37 m.

Figure 4.18 shows that when the canopy is near the roof, the peak negative pressure for 1 ft^2 area is almost 150% more than that for 1000 ft^2 (92.9 m^2) area. In the case of lower surface, the difference between highest and lowest values for peak C_p (both positive and negative) is nearly double. The noticeable phenomenon for upper and lower surface is that Cp values are less dependent on canopy width.

In Figure 4.19, canopy is situated near the mid-height of the building. In case of peak negative C_p on upper surface, w=1.5 m experiences slightly more suction than other and on lower surface, w=2.7 m experiences slightly more suction than others. On upper surface, highest value of peak negative C_p is almost double than the lowest Cp value. For peak positive C_p, there is a 50% increase in C_p value due to reduction of considered area on both upper and lower surfaces.
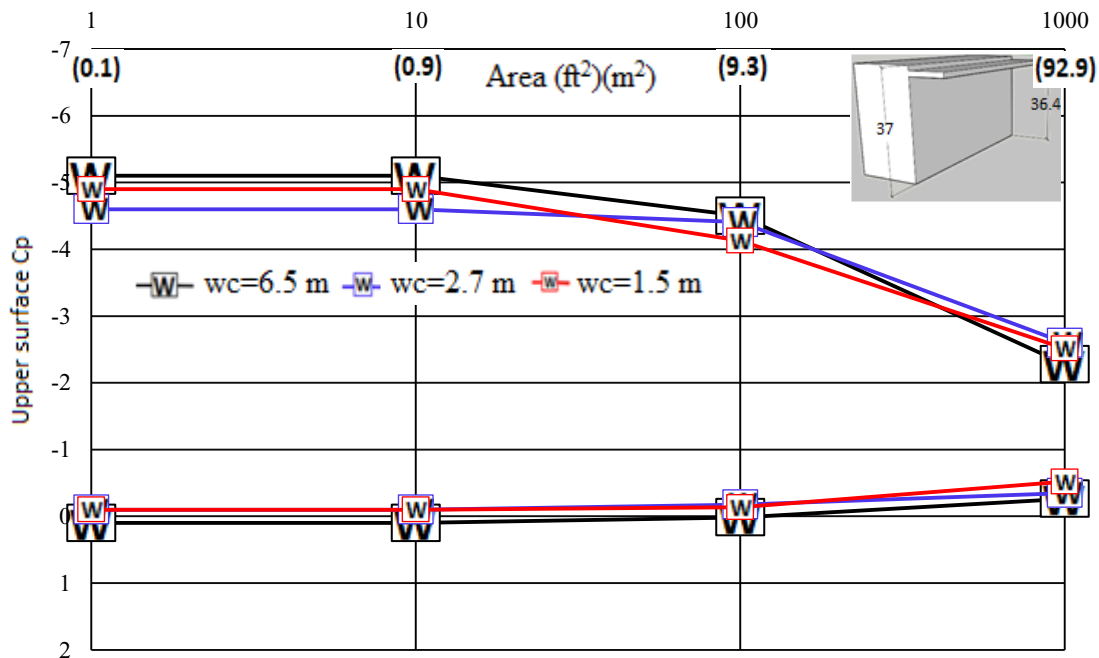
Figure 4.18 Peak Cp values as a function of effective area for hc/h=0.98, h=37 m
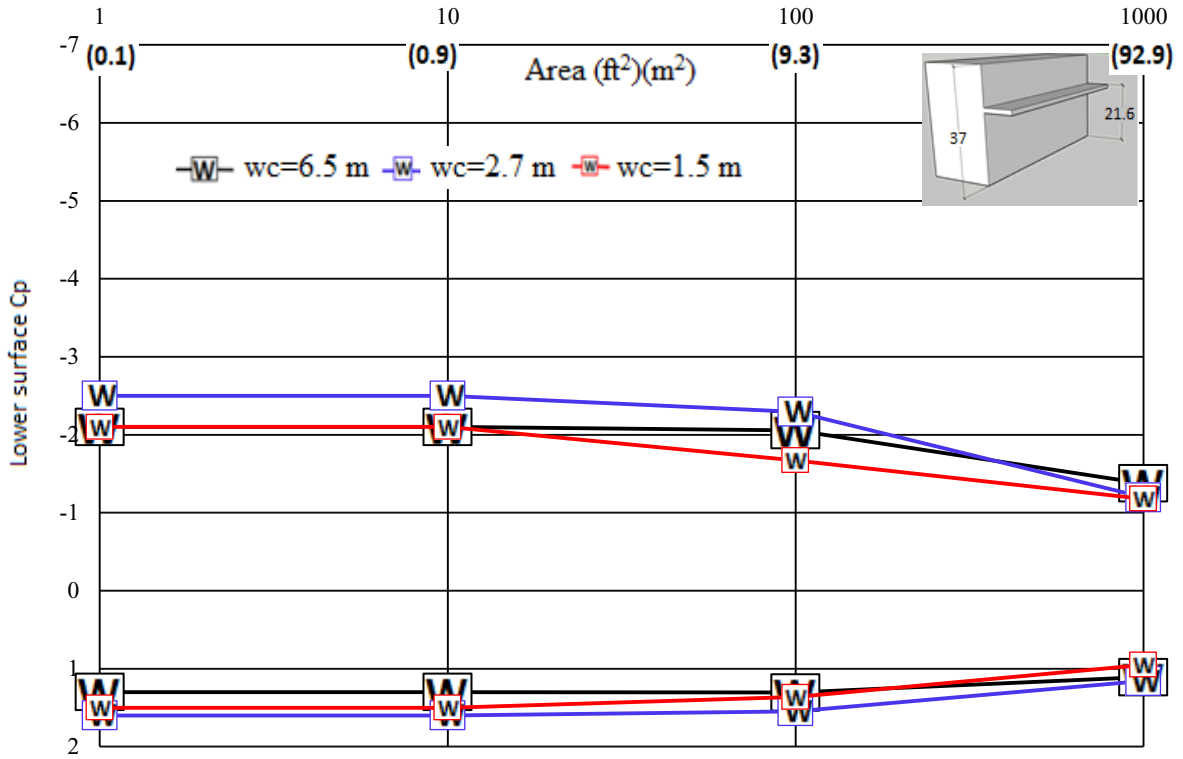
Figure 4.19 Peak Cp values as a function of effective area for hc/h=0.56, h=37m
Area (ft²)(m²)

Figure 4.20 Peak Cp values as a function of effective area for hc/h=0.18, h=37m

In Figure 4.20, the canopy is close to the ground. The variation between highest and lowest peak negative C_p values on the upper surface is more than double, which is also true for the lower surface. The variation in peak positive C_p value is around 50% due to the change in tributary area.

In general, the variation between highest and lowest value of peak positive and negative pressure due to change in tributary area is almost double. Although the upper canopy is observed to undergo more than 100% variation between the highest and the lowest value of peak negative C_p (absolute value), when the canopy is close to the roof or near the ground.

Figures 4.21 - 4.23 present area average peak C_p values for both upper and lower canopy surfaces for three different h_c/h values (canopy at the top, bottom and at the middle) for h=18.5 m. only one canopy width (w=6.5 m) is available for this building height.

Figure 4.21 demonstrate 100% rise in suction on the upper surface due to reduction of the considered area. The variation in peak positive C_p is negligible for the upper surface. Also, the variation for peak positive C_p and peak negative C_p due to change in tributary area is less on the lower surface.

In Figure 4.22, the canopy is close to the mid height of the building. In this position, the upper surface of the canopy is facing little change in peak negative C_p value with respect to the tributary area. This is also applicable in case of peak positive C_p on the upper surface. On the lower surface, the variation in peak negative and positive C_p due to considered area is close to double.
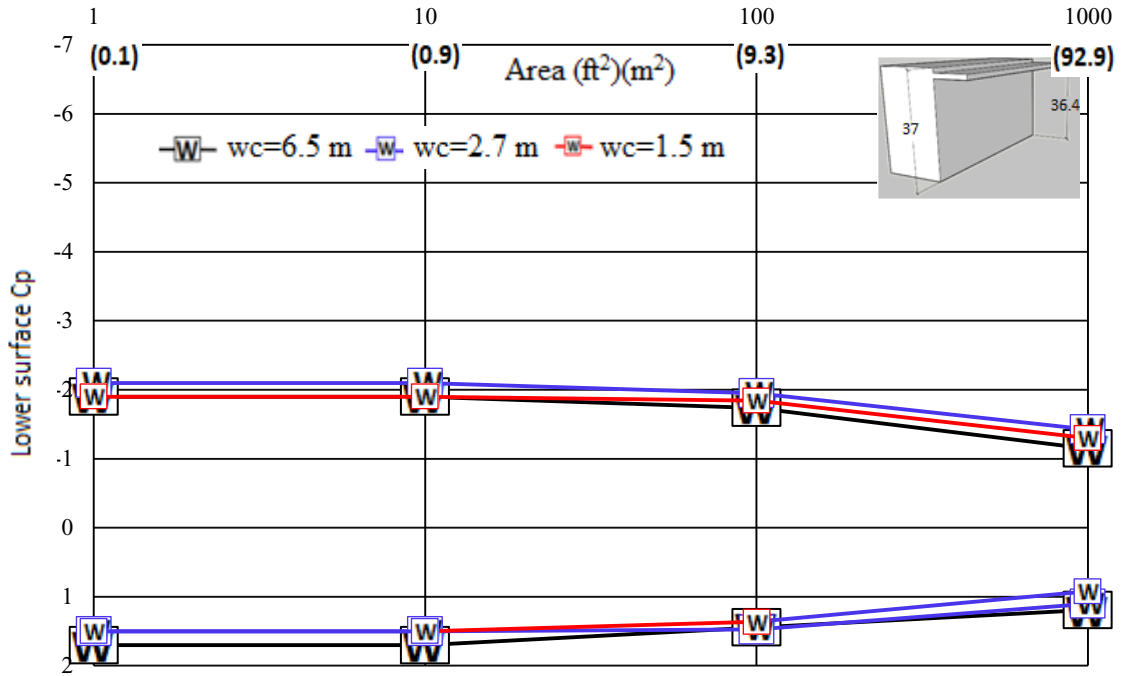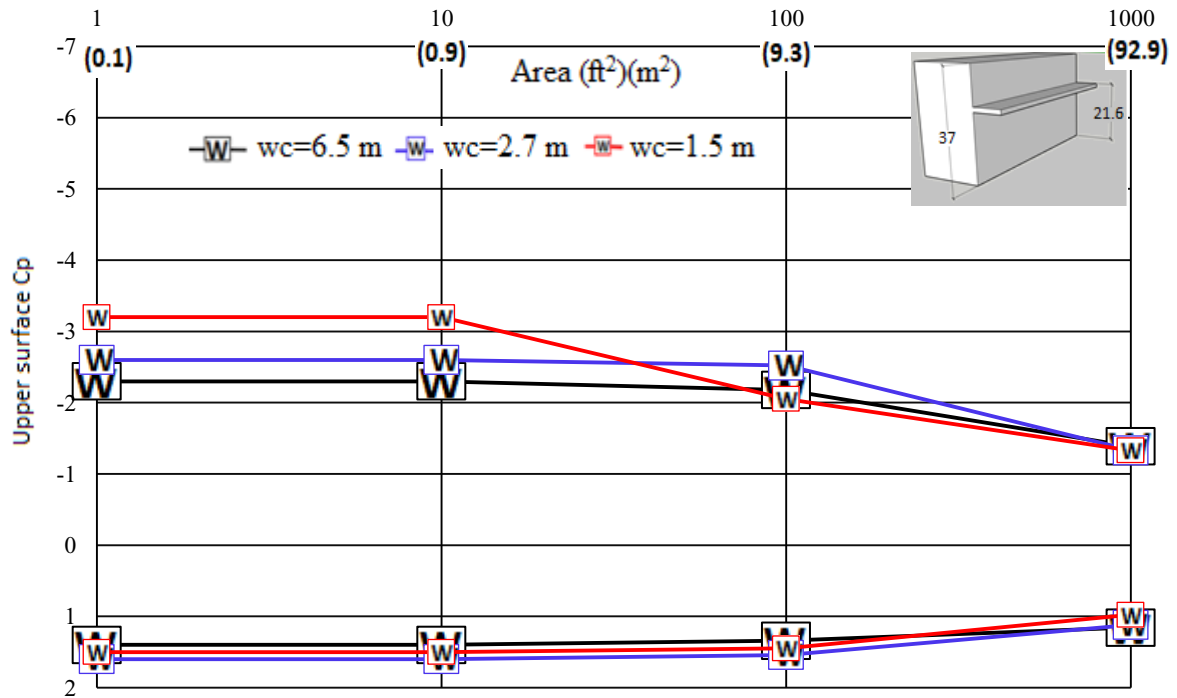
Figure 4.21 Peak Cp values as a function of effective area for hc/h=0.97, h=18.5 m

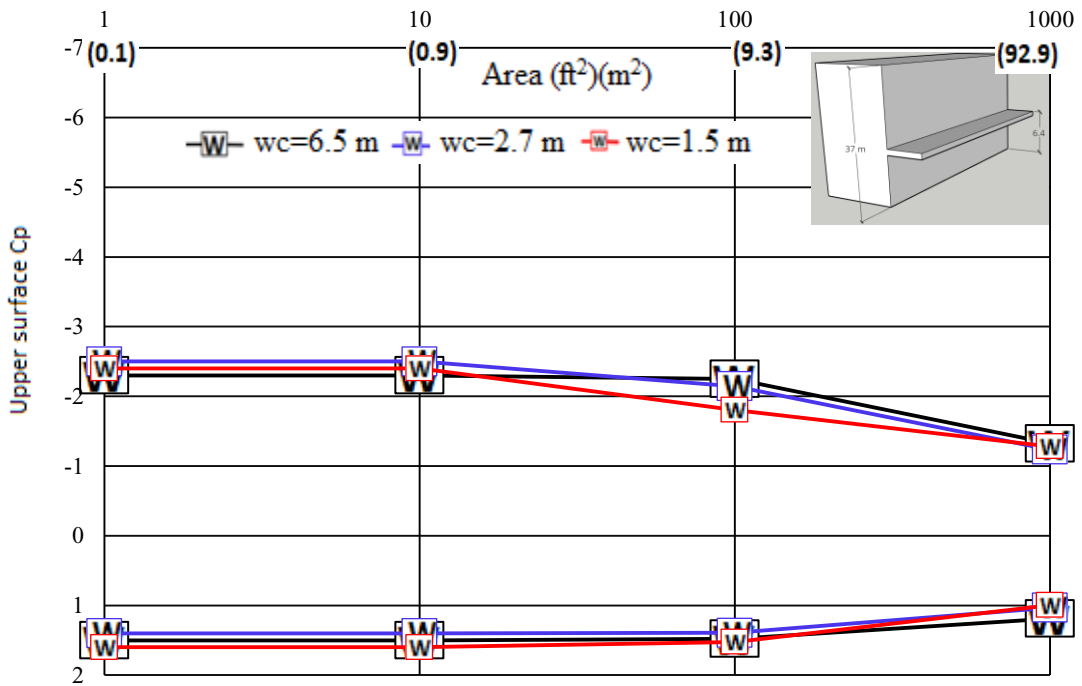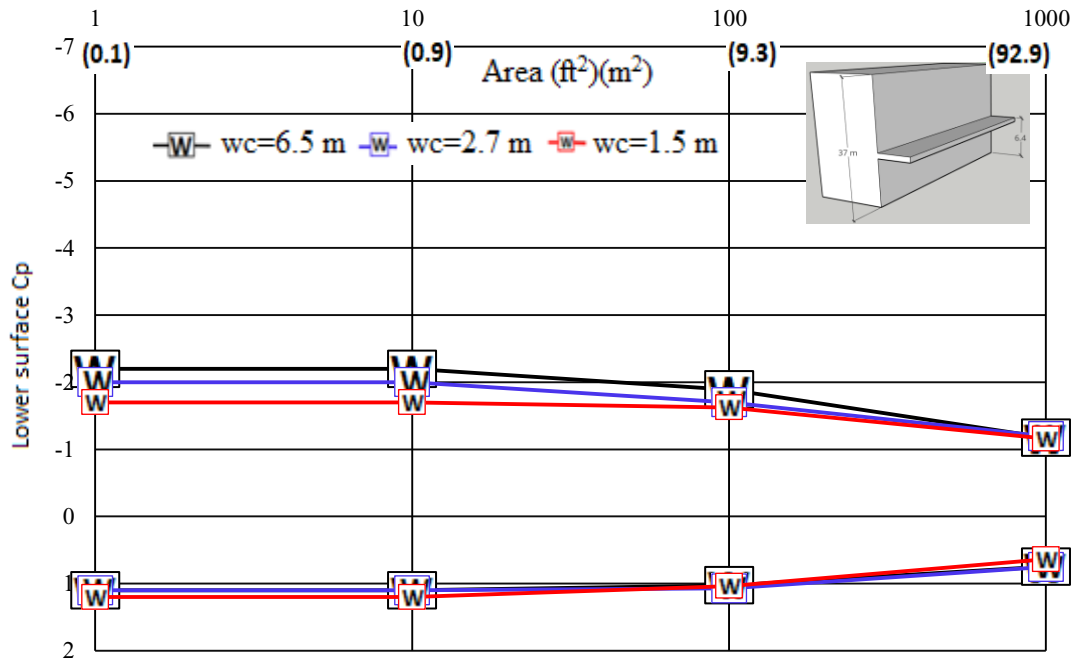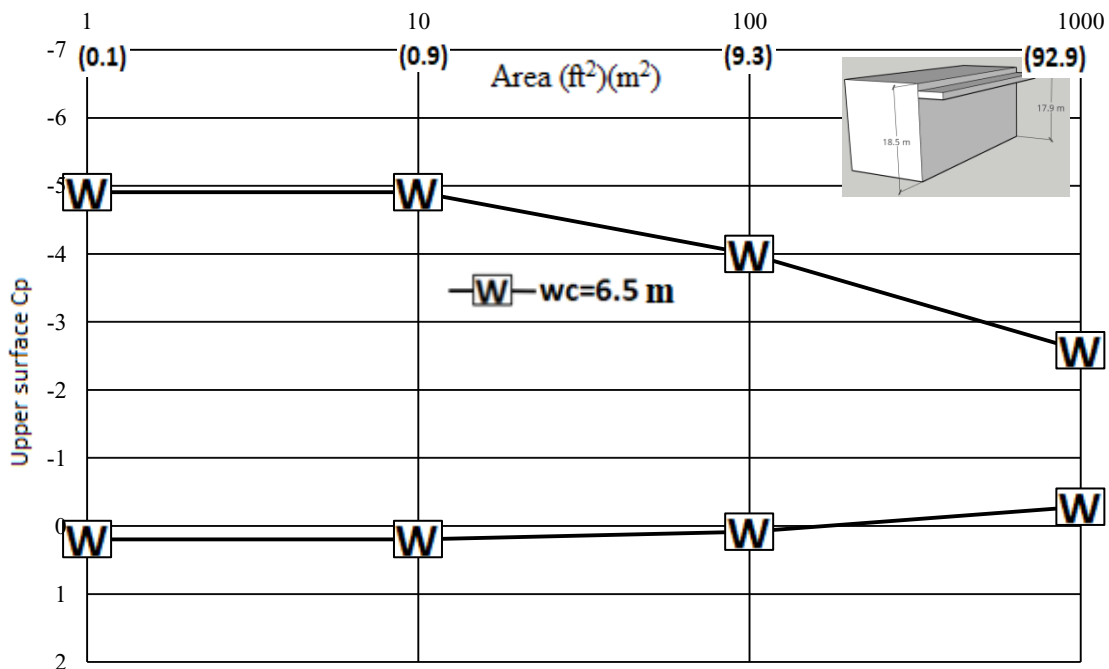Figure 4.22 Peak Cp values as a function of effective area for hc/h=0.57, h=18.5 m

Figure 4.23 Peak Cp values as a function of effective area for hc/h=0.21, h=18.5 m

76

In Figure 4.23, when the canopy is close to the ground, both the upper and lower surfaces have 100% reduction in peak negative C_p due to increase in the tributary area. The variation in peak positive C_p on both surfaces is less than 70%.

Figures 4.24 and 4.25 present the area average peak C_p values for both upper and lower canopy surfaces for three different h_c/h values (canopy at the top and at the middle) for h=7 m.

From Figure 4.24, it can be observed that the highest peak negative C_p (absolute value) values on the upper surface are 61% (for w=6.5 m), 40% (for w=2.7 m) and 39% (for w=1.5 m) higher than the lowest values for the corresponding width. The wider the canopy, greater the variation in case of peak negative C_p on the upper surface at a certain canopy position. This is also applicable for peak negative C_p on the lower surface.

In Figure 4.25, when the canopy is close to the mid height of the building, the variation for both peak positive and negative C_p on the upper surface is double between the highest and lowest values of C_p, which is roughly also applicable for the lower surface.

In general, the difference between highest and lowest value of peak C_p (both positive and negative) due to change in tributary area is roughly double.
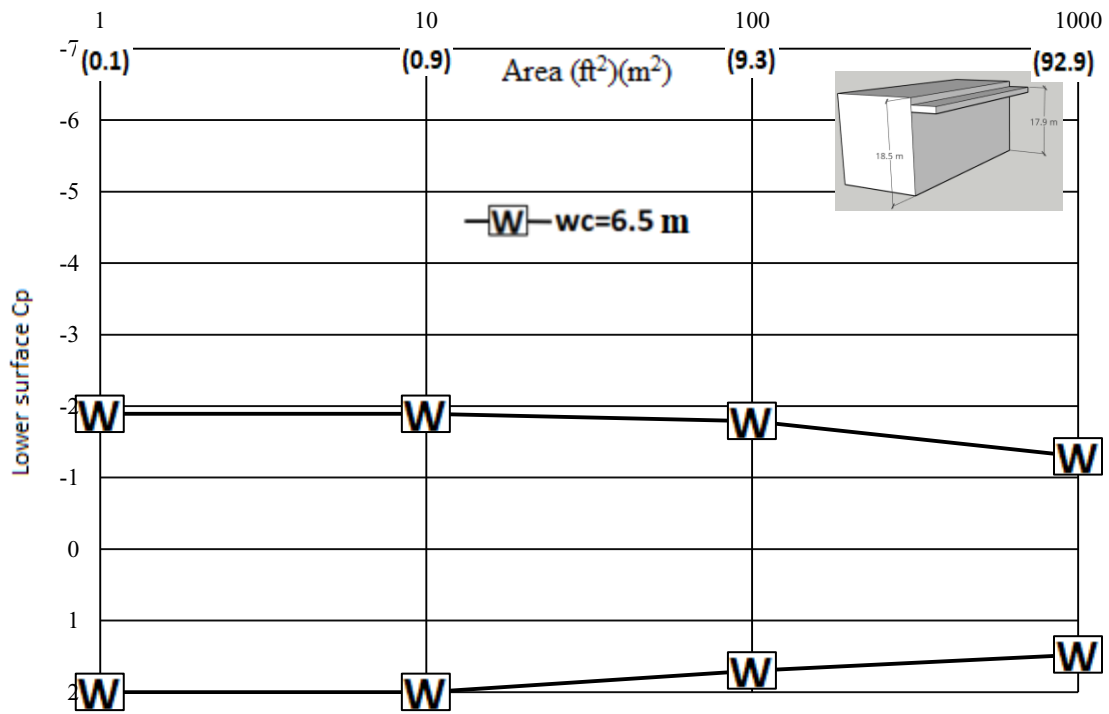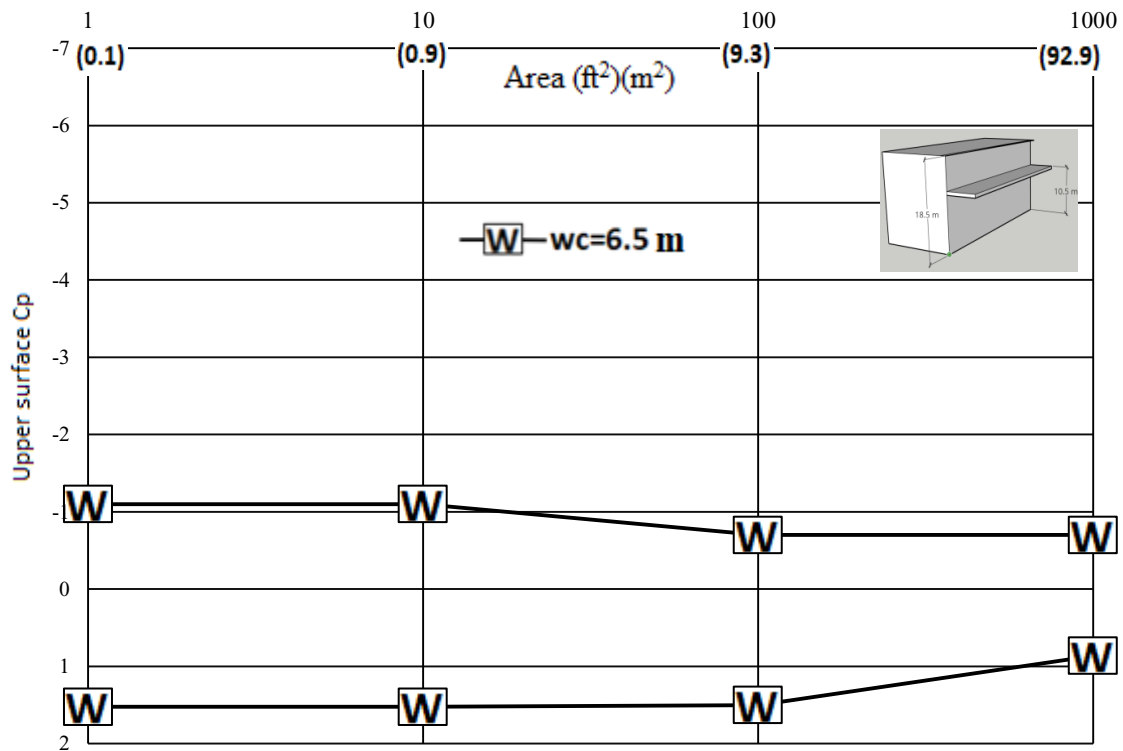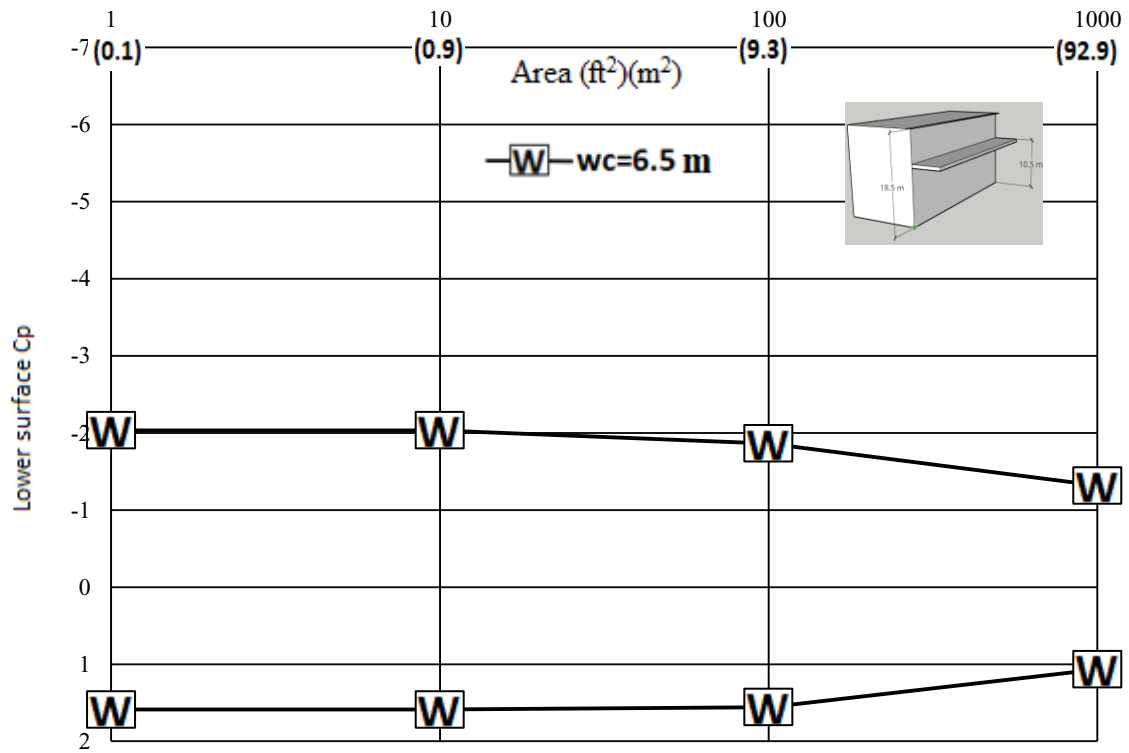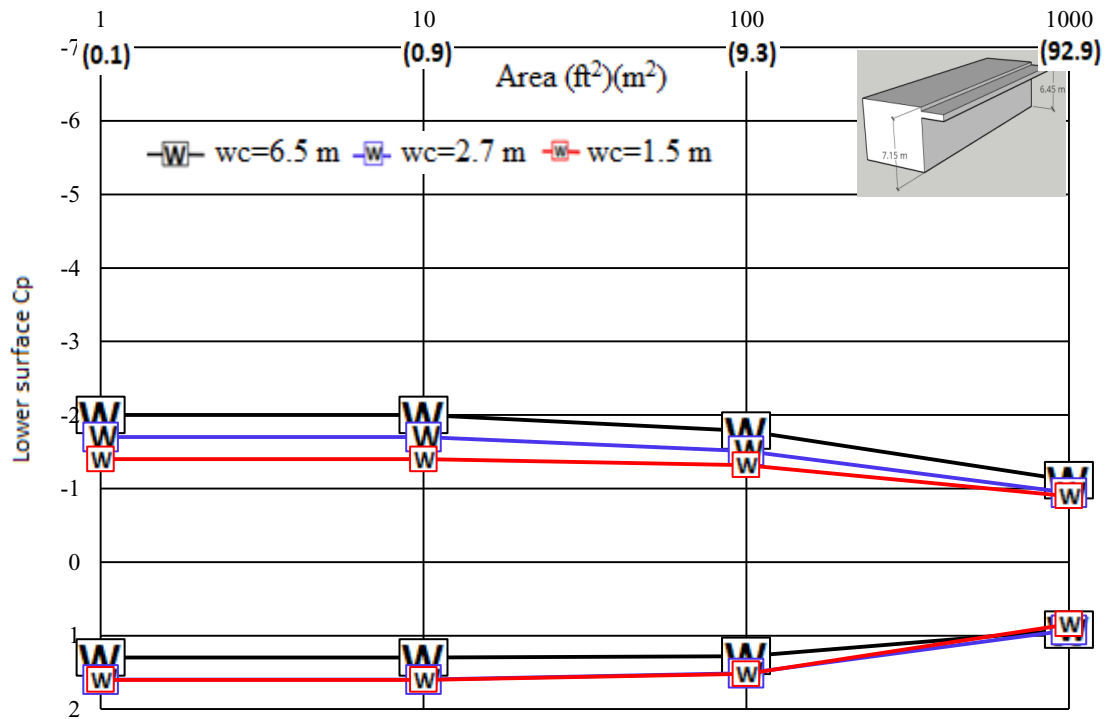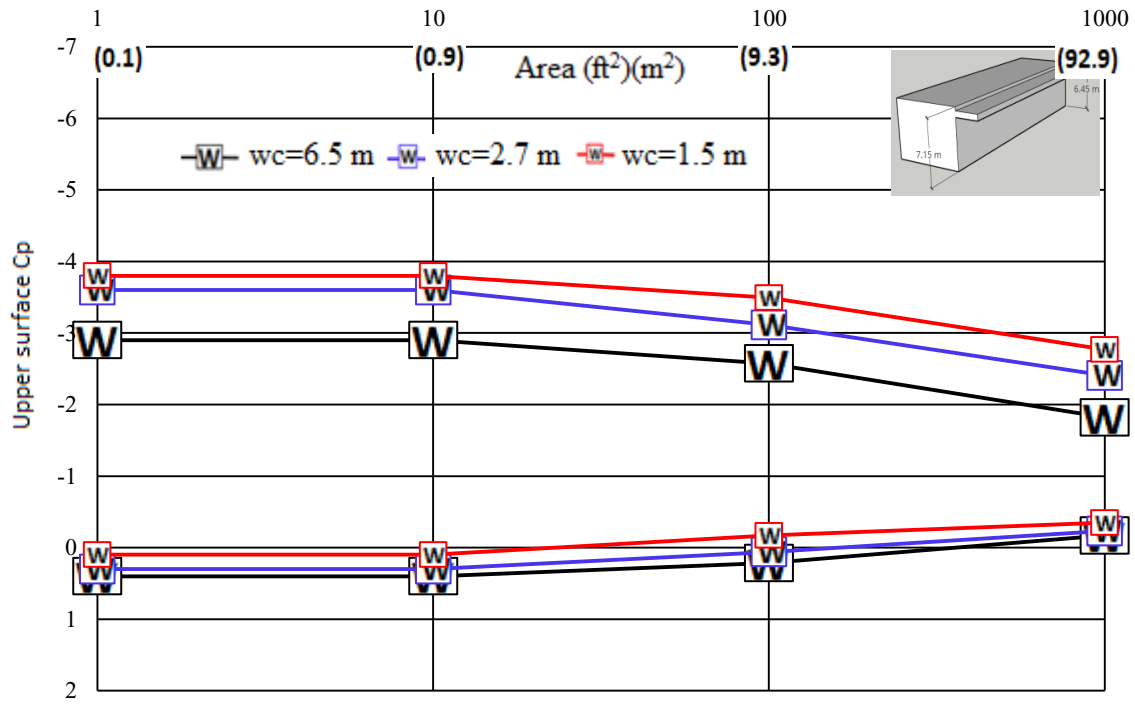
Figure 4.24 Peak Cp values as a function of effective area for hc/h=0.9, h=7 m

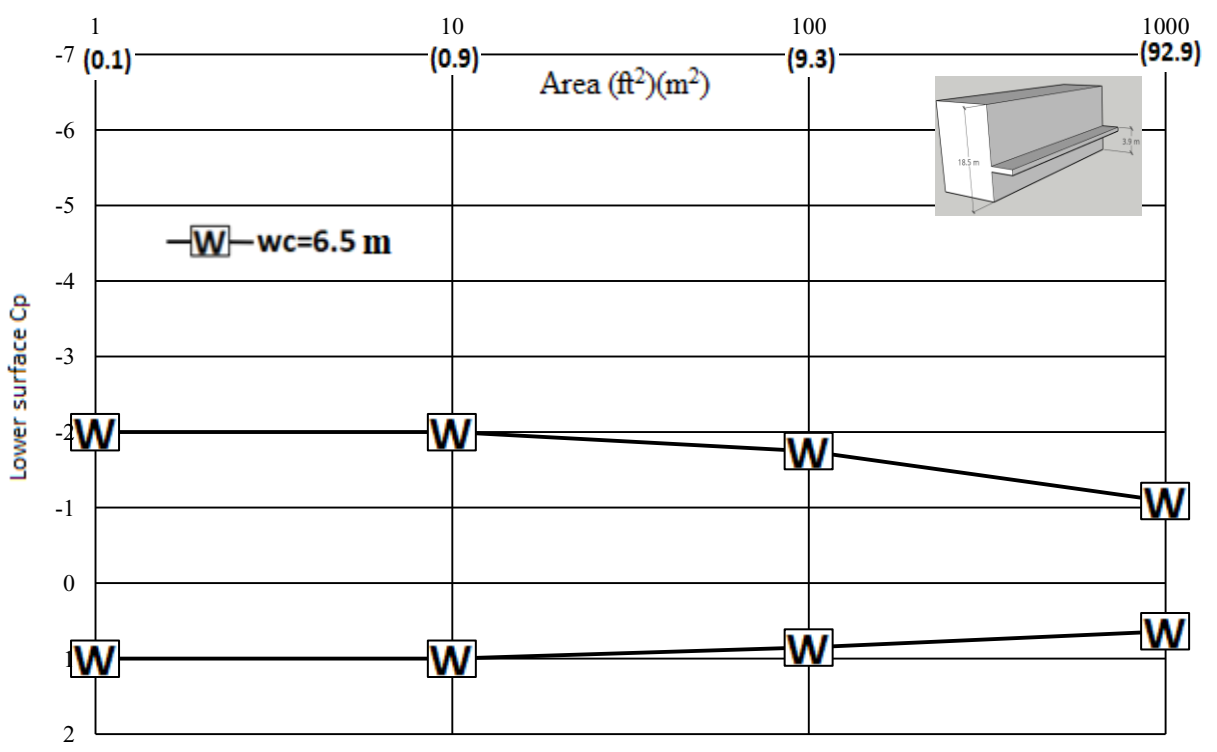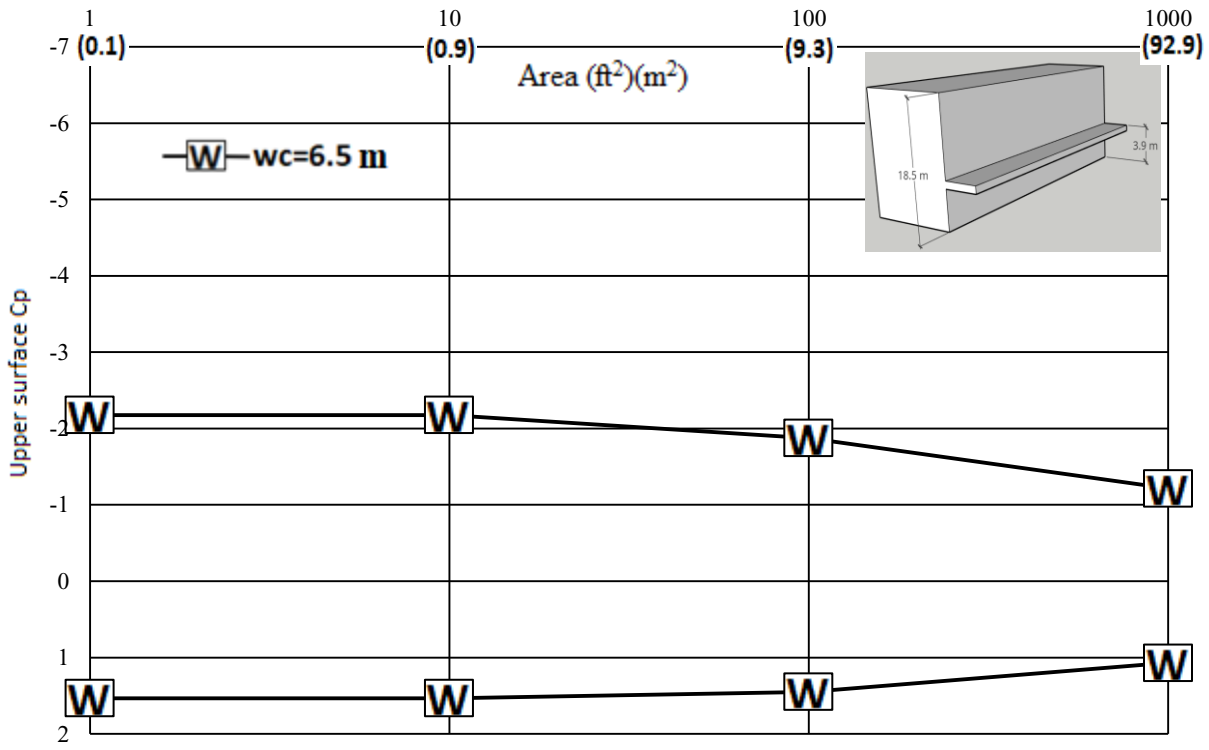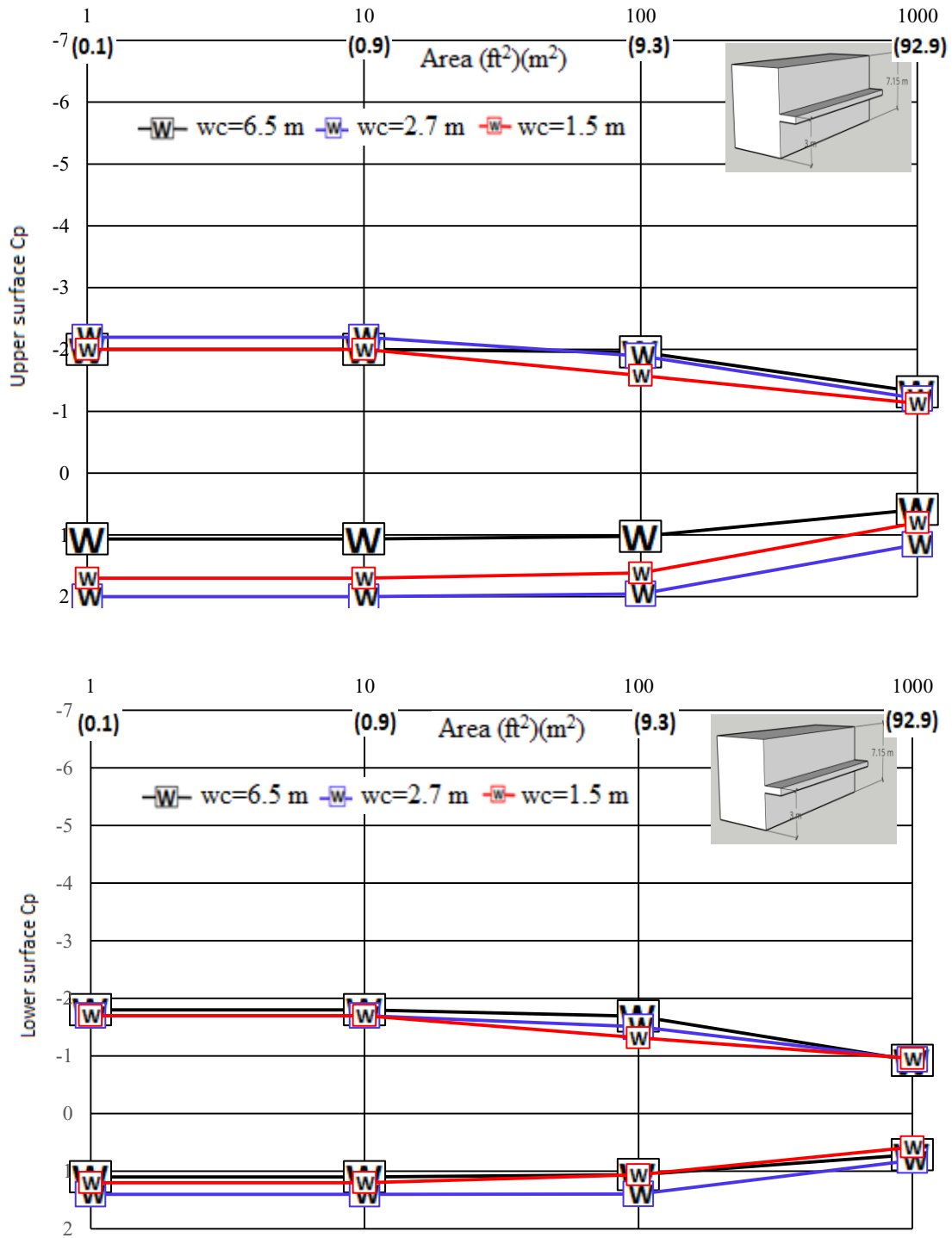Figure 4.25 Peak Cp values as a function of effective area for hc/h=0.43, h=7 m

Chapter 5   Net pressure coefficients resulting from wind loading on attached canopies

5.1 General:

Attached canopies are exposed to wind loads on both upper and lower surfaces simultaneously. Pressures applied to the sheathing elements are transferred to the main structural components of the canopy, namely the joists, header beam and the columns. This chapter focuses on the peak local and area-averaged net loads experienced by the canopy for different geometrical configurations. Figure 5.1 shows a sketch illustrating the principal components of a conventional canopy attached to a low-rise structure. The analysis and observations made on this section serve as the basis for the design of the labeled components for wind loading.
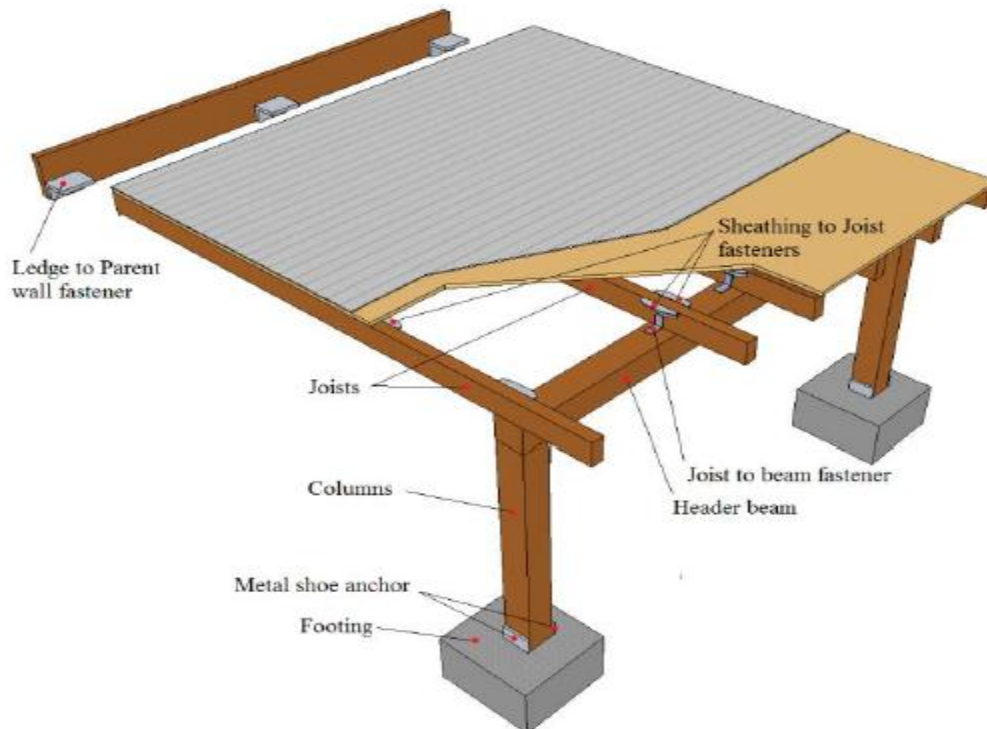
Figure 5.1 Schematic of a conventional canopy attached to a low rise building (not to scale) indicating the components affected by net wind loads(Candelario 2012)

5.2 Effect of building height on net mean and peak C_p values on canopies

Building height can affect wind induced pressure on canopies. For the three buildings with three different heights, i.e. 7 m. 18.5m, 37m, net mean and peak wind pressures on canopies were calculated. (The net mean and peak values of Cp against hc/h are shown in Figures 5.2 and 5.3, respectively. The canopy width for Figures 5.2 and 5.3 was 6.5 m. It is observed from Figures 5.2 that the net mean positive Cp values are not that much affected by the building height. Only, for h=7 meters, there is a small difference in the net mean positive Cp values with other building height, when hc/h is around 0.5. Canopies attached to low-rise building experience less net mean positive pressure than others when hc/h is around 0.5. This is also true in case of net peak positive Cp, as shown in Figure 5.3. Net mean negative Cp values do not vary much when hc/h≤ 0.5. That means if canopy is situated at or under the mid-height of the building, net mean negative Cp values are quite close to each other. The statement is also true in the case of net peak negative Cp values. From Figure 5.3 we can see that peak net negative Cp values for all building heights are close to each other when hc/h≤ 0.5. After hc/h> 0.5, there is a big difference between net negative Cp values for different building heights. For all building heights, canopies have experienced the highest net mean and peak negative loading when the canopy is near the roof of the building, 0.9≤hc/h≤1. The effect of building height is noticeable in this range of hc/h. In case of relatively taller buildings (h=18.5 m and 37 m), both net mean and peak negative Cp values are close. But canopies attached to lower buildings (h=7 m) may experience 50% of the suction experienced by canopies attached to taller buildings.
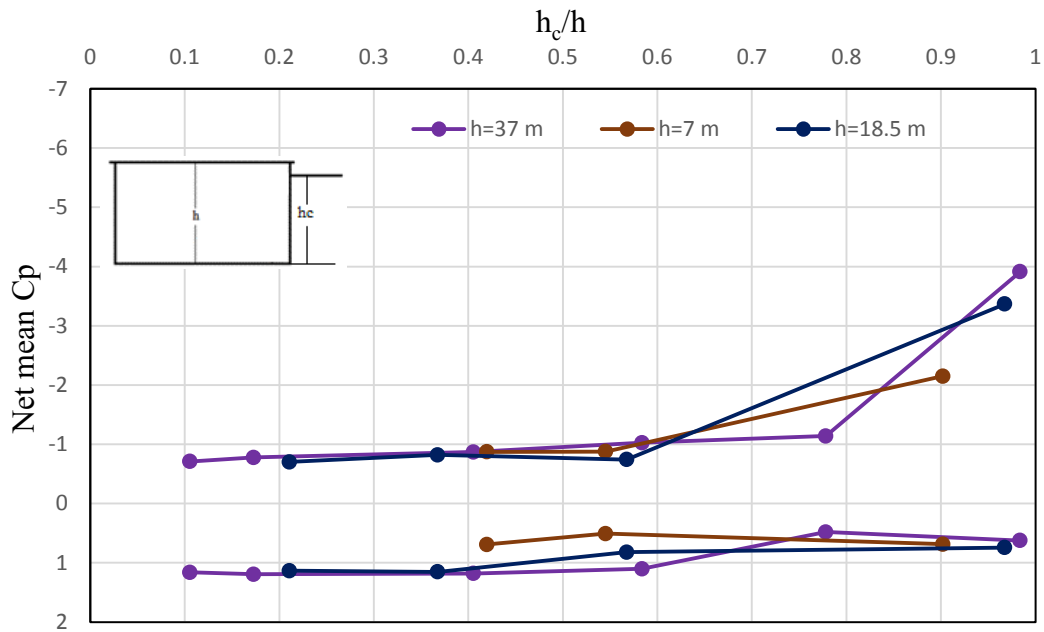
Figure 5.2 Net mean Cp values with respect to hc/h for different building height
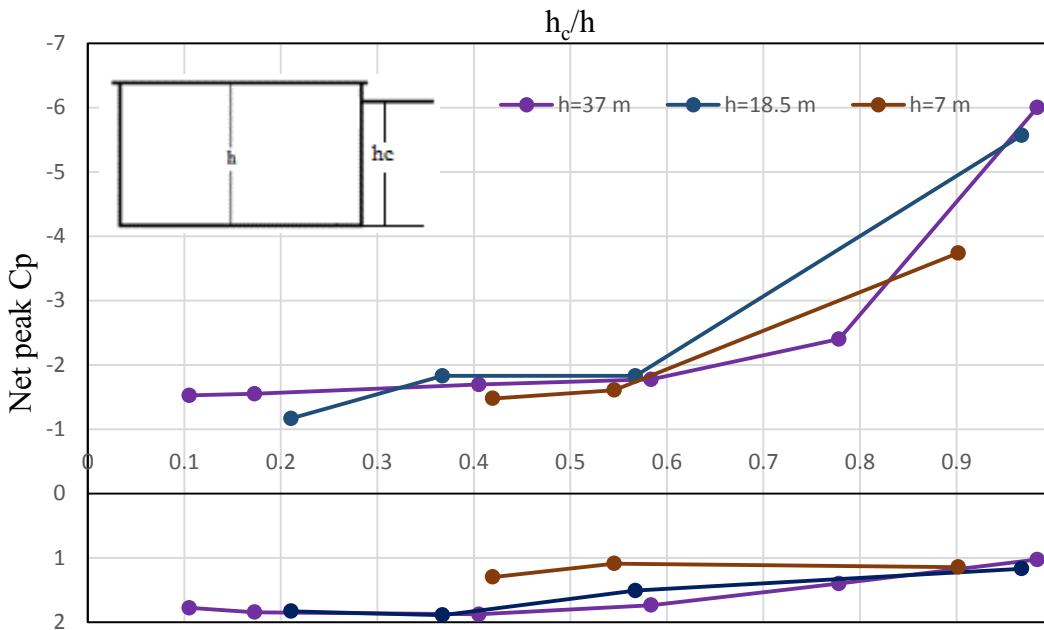
Figure 5.3 Net peak Cp values with respect to hc/h for different building height

82

5.3 Effect of wind direction on net mean and peak Cp values on canopies

Wind direction can affect values of peak positive and peak negative Cp on attached canopies. Wind direction for peak positive and negative Cp also depends on canopy's vertical position (close to the roof or close to the ground or at mid height). Figure 5.4-5.6 show net peak positive and negative values on canopies attached to a tall building (h=37 meters) for three different widths and for three different hc/h.

Figure 5.4 represents the case where the canopy is at the top of the parent wall. In this case, net peak negative pressure on canopies varies significantly with respect to wind direction. From 0 degree to 60° wind direction, the absolute value of net peak negative Cp keeps increasing, after that, it keeps decreasing up to wind direction of 120 degrees. After that, when the canopy is in the building wake zone, net peak negative Cp values become almost constant. It is observed from Figure 5.4 that the wider canopy attained the highest suction at 60°and narrower canopies experienced the highest suction at a wind direction of 45°. As suction results from flow separation, we can say that canopy located close to the roof experiences the most intense flow separation within 45° to 60° wind direction.

In case of net peak positive pressure (Figure 5.4), it remains constant from 0 to 60°. Within this range, canopies experience very little positive pressure. After 60°, the positive pressure keeps increasing and the highest positive pressure is observed at 90° wind direction regardless of canopy width. After 90° wind direction, positive pressure decreases and eventually becomes almost constant.
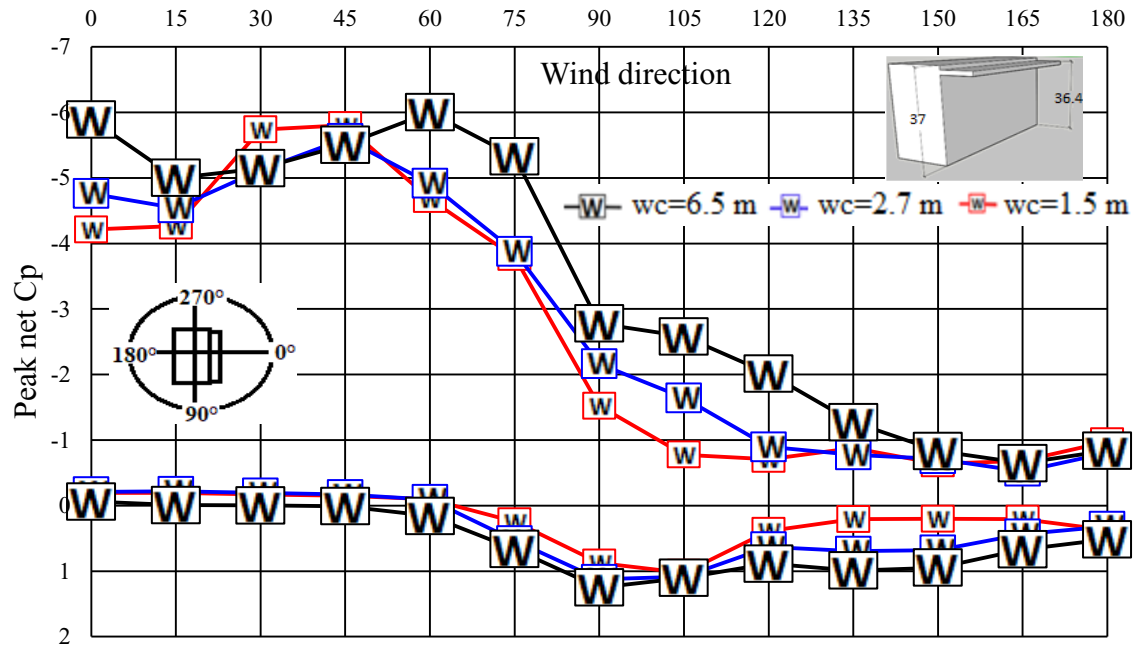
Figure 5.4 Peak net Cp values against wind direction for hc/h=0.98(h=37 m)
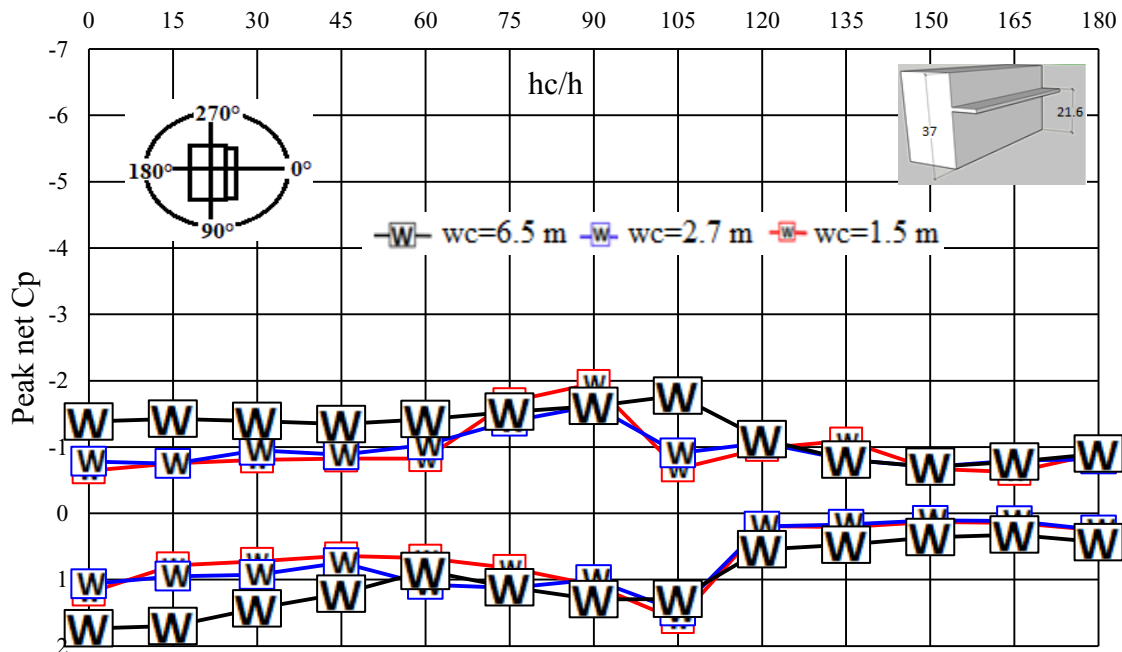
Figure 5.5 Peak net Cp values against wind direction for hc/h=0.56(h=37 m)
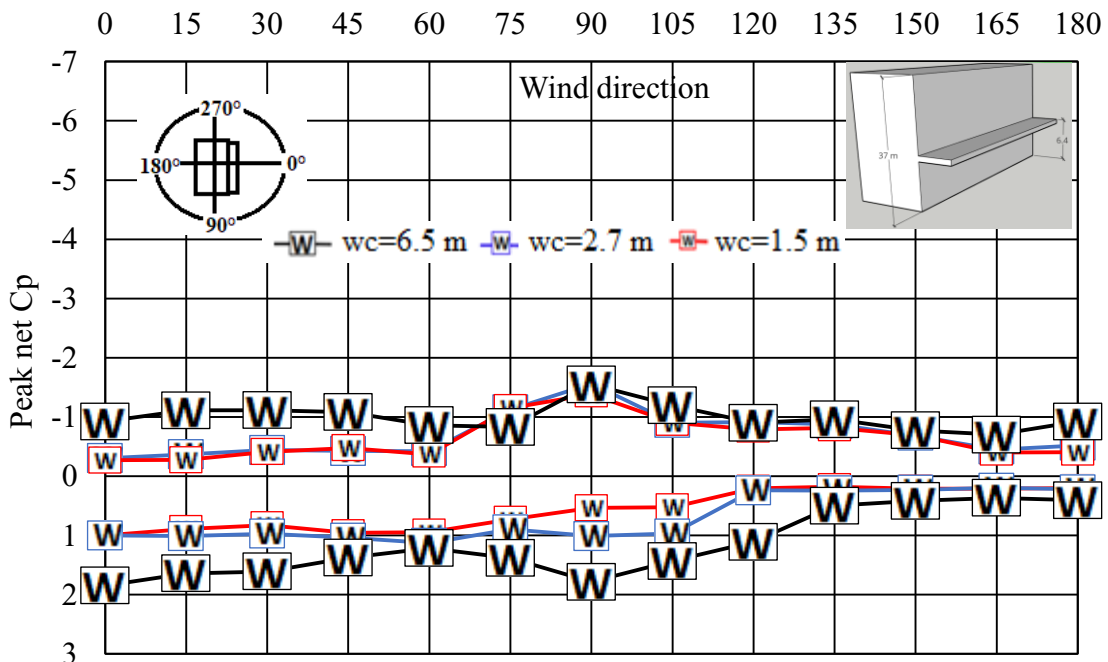
Figure 5.6 Peak net Cp values against wind direction for hc/h=0.18 (h=37 m)
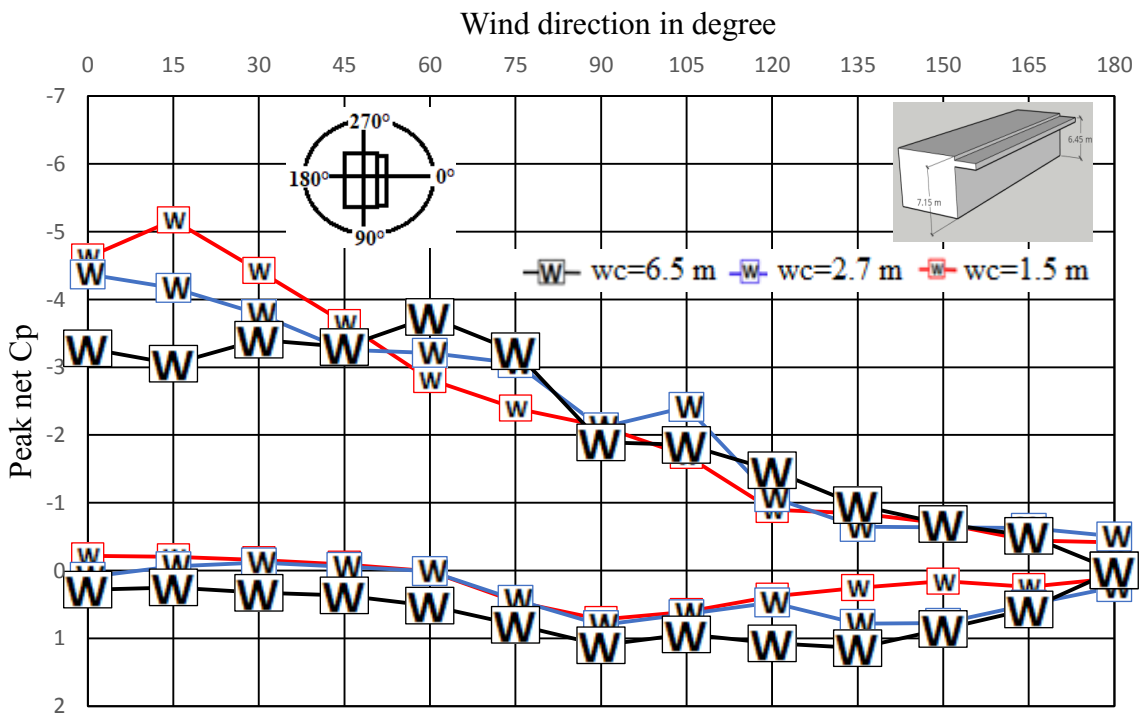
Figure 5.7 Peak net Cp values against wind direction for hc/h=0.9 (h=7 m)
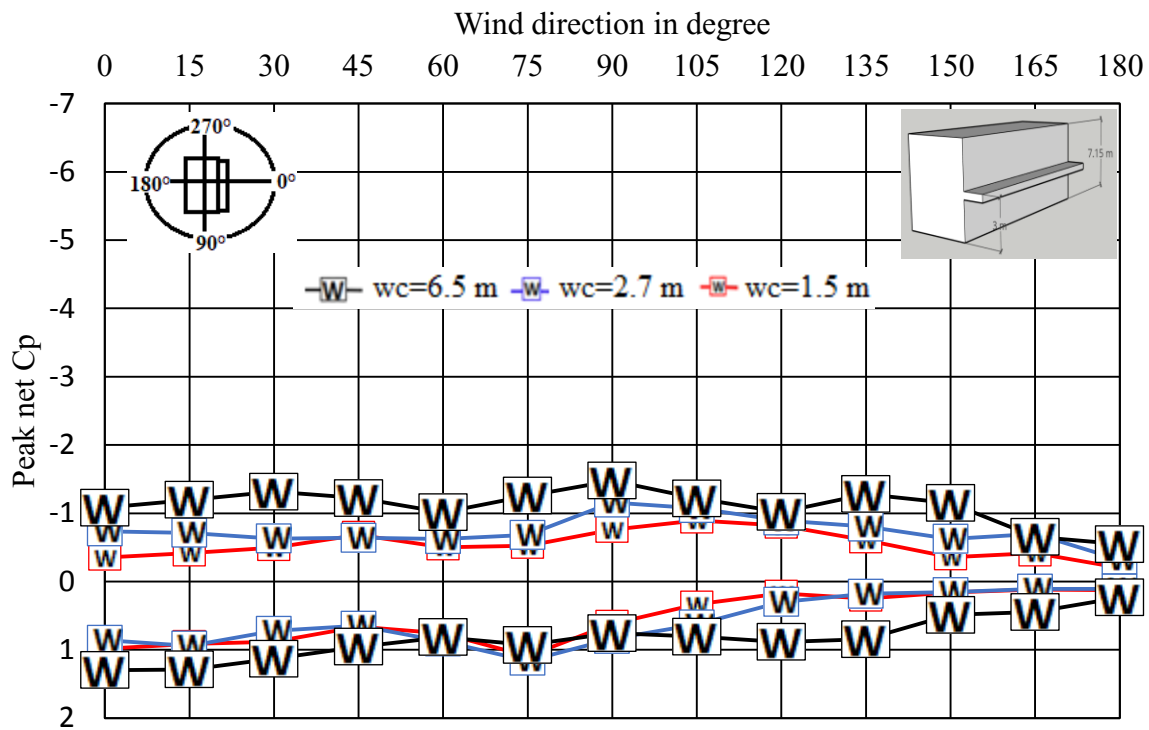
Figure 5.8 Peak net Cp values against wind direction for hc/h=0.42 (h=7 m)

Figure 5.5 represents the scenario when the canopy is situated at the mid height of the parent wall. Suction on canopies with respect to wind direction remains constant from 0 to 60°. After that, the suction increases and reaches its highest value (absolute) at 90° wind direction (w=2.7 m and w=1.5 m) and at 105° (w=6.5 m). After that, the suction on canopy decreases. The highest net peak positive pressure occurs at 0° for w=6.5 m and at 105° for w=1.5 m and 2.7 m. From 120° wind direction, both net peak positive and negative pressure remain constant with respect to wind direction.

In Figure 5.6, the net peak negative and positive Cp values have been plotted against wind direction for canopy situated close to the ground (hc/h=0.18). In case of net peak negative pressure, the observations are the same as those for Figure 5.4. So, it can be said that if canopy is located near or below the mid height of the parent wall, the most intense flow separation occurs

for a flow parallel to the parent wall. The variation of net peak positive pressure for wider canopy (w=6.5 m) is interesting. It experiences the highest pressure for a flow perpendicular to the parent building (0° wind direction in this study) and from there the pressure keeps decreasing with increasing wind direction up to 60°, then it keeps increasing up to 90°. After that, it starts decreasing up to 135°, then it becomes constant with respect to wind direction.

Figure 5.7 and Figure 5.8 show the effect of wind direction on peak net Cp values for different hc/h for low-rise building. Despite different building height, we can see the same trend for both low-rise and tall buildings for different wind directions. For example, when the canopy is close to the roof, highest (absolute value) net peak negative Cp occurs within 60° and highest net peak positive Cp is found at 90° or later. When canopy is close to the mid height, highest suction occurs at 90°

5.4 Contours of wind loads acting on canopy surfaces

Contours have been plotted for mean and peak net critical Cp values ($C_{p,n}$) on canopy for h=37m and for h=7 m. Figures 5.9-5.14 present these contours. All these contours are for the critical peak positive and negative Cp values, which means they do not represent any certain wind direction. They are the highest values (absolute values in case of negative $C_{p,n}$) regardless of the wind directions. Also, because of the symmetry, only half canopy length is presented.

Figure 5.9 and 5.10 present the contour plots of mean critical net pressure coefficient for canopy near roof level and near ground level. In Figure 5.9, the positive pressure in very little, which is anticipated as canopy is at the top of the building. The negative contours are mostly corner

oriented. On the other hand, in Figure 5.10 where canopy is near the ground, the negative

contours

wc=6.5	wc=2.7	
C_L Range: 0 to 0.4	C_L Range: 0 to 0.3	Net effect Critical mean pressure coefficient (positive)
C_L	C_L	Net effect Critical mean pressure coefficient (Negative)
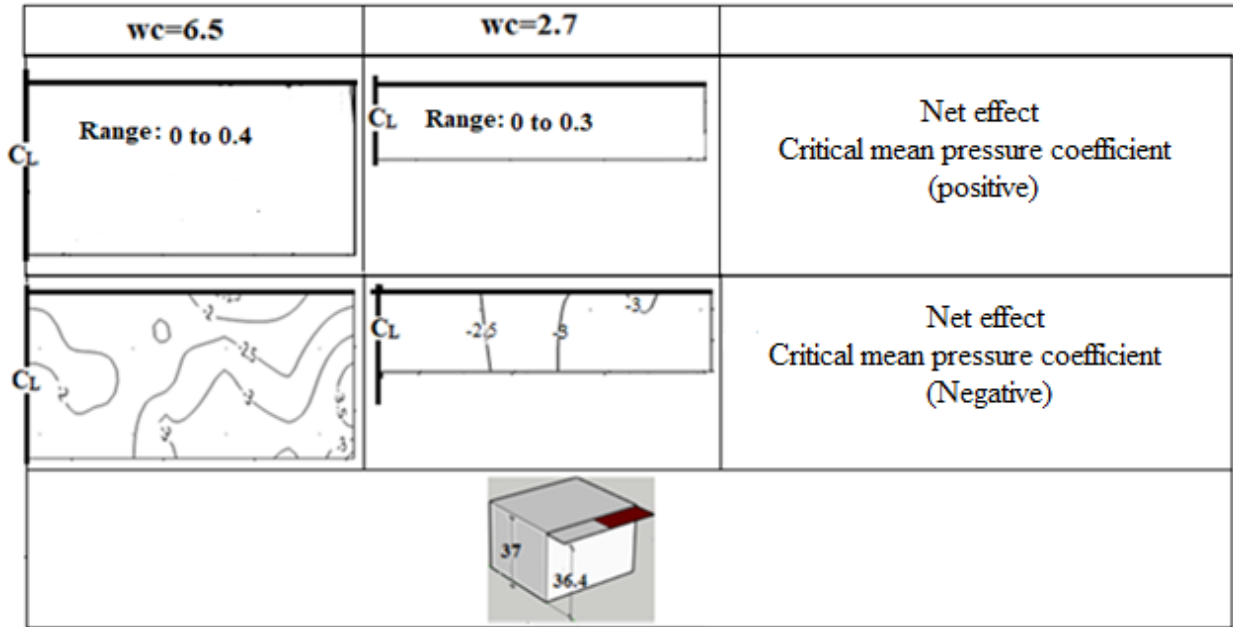
Figure 5.9 Contour plots of net critical mean loading on canopy for different widths for
hc/h=0.98 (h=37m)

wc=6.5	wc=2.7	
C_L	C_L	Net effect Critical mean pressure coefficient (positive)
C_L	C_L	Net effect Critical mean pressure coefficient (Negative)
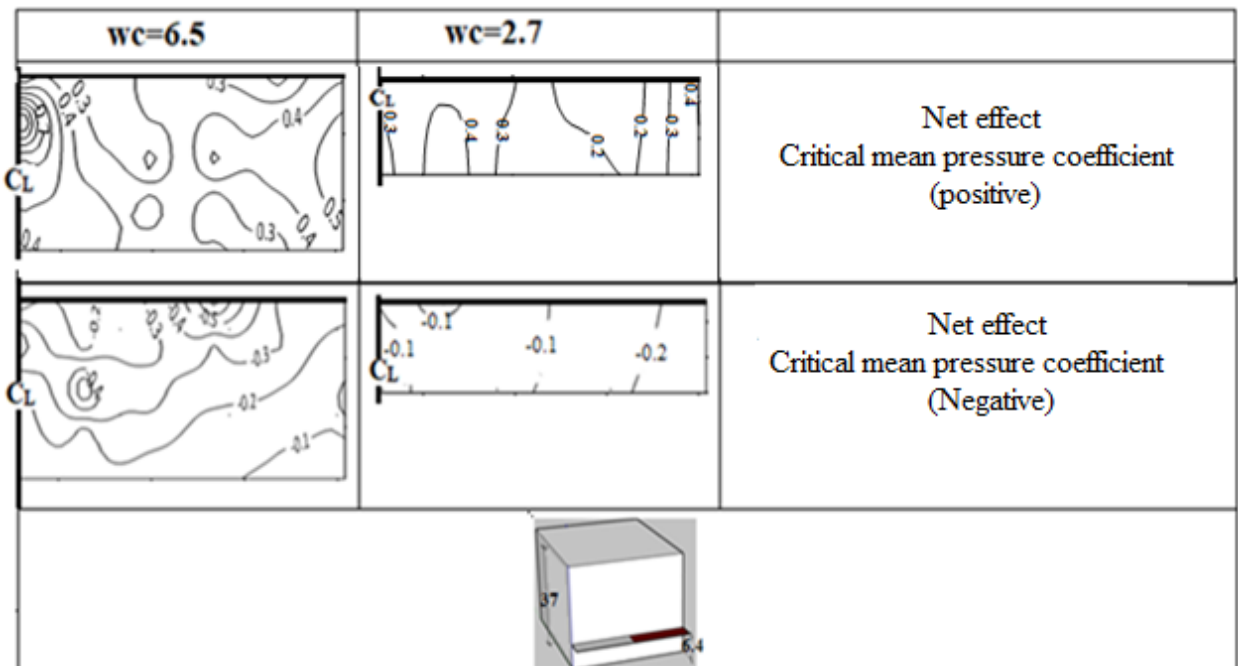
Figure 5.10 Contour plots of net critical mean loading on canopy for different widths for hc/h=0.18 (h=37m)

wc=6.5 m	wc=2.7 m	
		Net Effect Critical Peak Positive Pressure Coefficient, Cp,n
		Net Effect Critical Peak Negative Pressure Coefficient, Cp,n
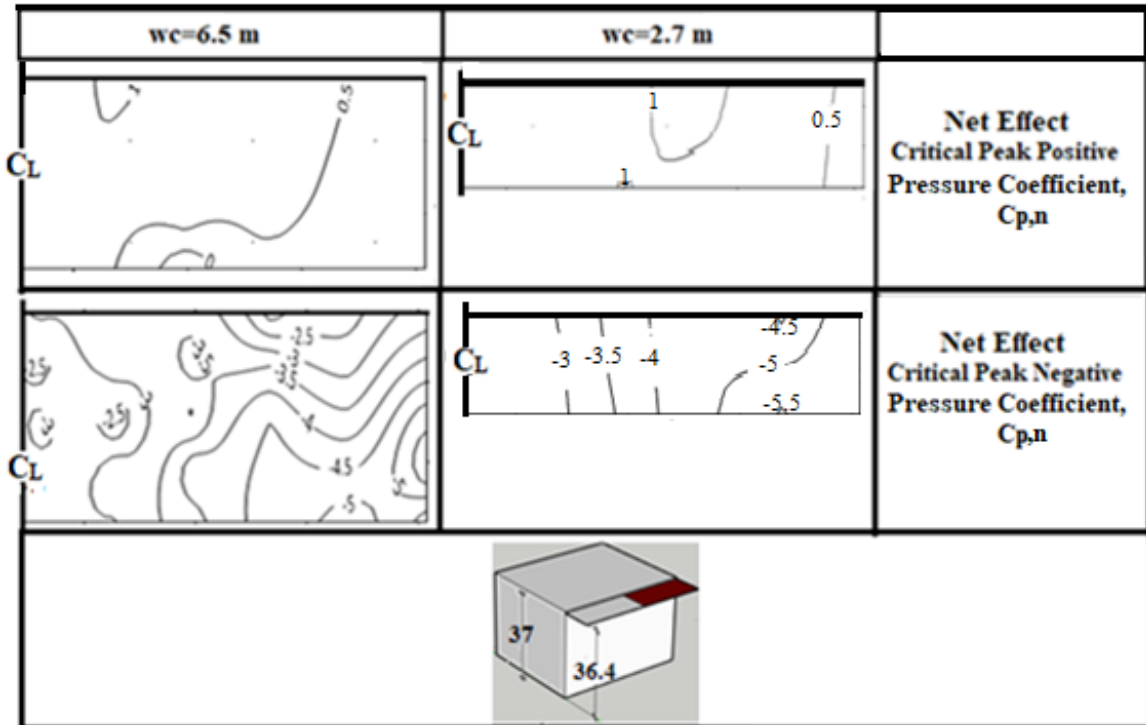
Figure 5.11 Contour plots of net critical peak loading on canopy for different widths for hc/h=0.98 (h=37m)

wc=6.5 m	wc=2.7 m	
		Net Effect Critical Peak Positive Pressure Coefficient, Cp,n
		Net Effect Critical Peak Negative Pressure Coefficient, Cp,n
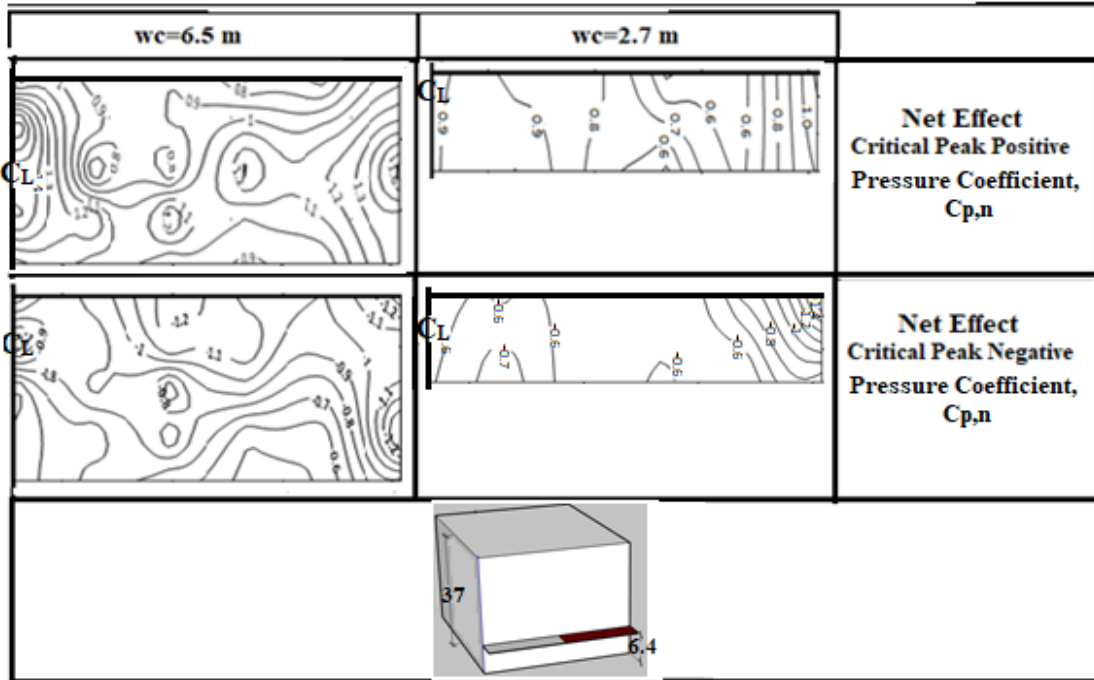
Figure 5.12 Contour plots of net critical peak loading on canopy for different widths for hc/h=0.18(h=37m)

are more prominent on the edge connected to the wall. Figure 5.11 presents contours for net critical peak loading when the canopy is at the roof level of a tall building (h=37 m). In case of peak positive, the edge connected to the parent wall is having the highest pressure for both canopy widths. In case of net peak negative pressure coefficient, the side edge and corner are having the highest suction.

In Figure 5.12, canopy attached to the same building is situated close to ground. In case of positive $C_{p,n}$, the regions close to the side edge and to center line have the highest pressure. For negative $C_{p,n}$, the side edge and inner corner have the highest suction.

Figure 5.13 presents the contours for net critical peak loading on canopies where the canopy is attached to the roof level of a 7 m high building. In case of negative $C_{p,n}$, side edge and corners are again most vulnerable. This is also applicable when canopy is at the mid height (Figure 5.14.)

In case of net peak positive pressure in Figure 5.13, the edge connected to the parent wall and the region close to this edge have more pressure than that of the edge opposite to the parent wall (for wider canopy). The trend of the positive $C_{p,n}$ is similar to the trend showed in Figure 5.12.

In general, negative pressure mainly acts at corners and side edges of canopies. On the other hand, depending on the location of canopies, positive pressure can act near the center line, side edge or the edge connected to parent wall. Thus, the side edges and corners are the most vulnerable areas of a canopy.

wc=6.5m	wc=2.7m	
		Critical net peak positive pressure coefficient, Cp,n
		Critical net peak negative pressure coefficient, Cp,n
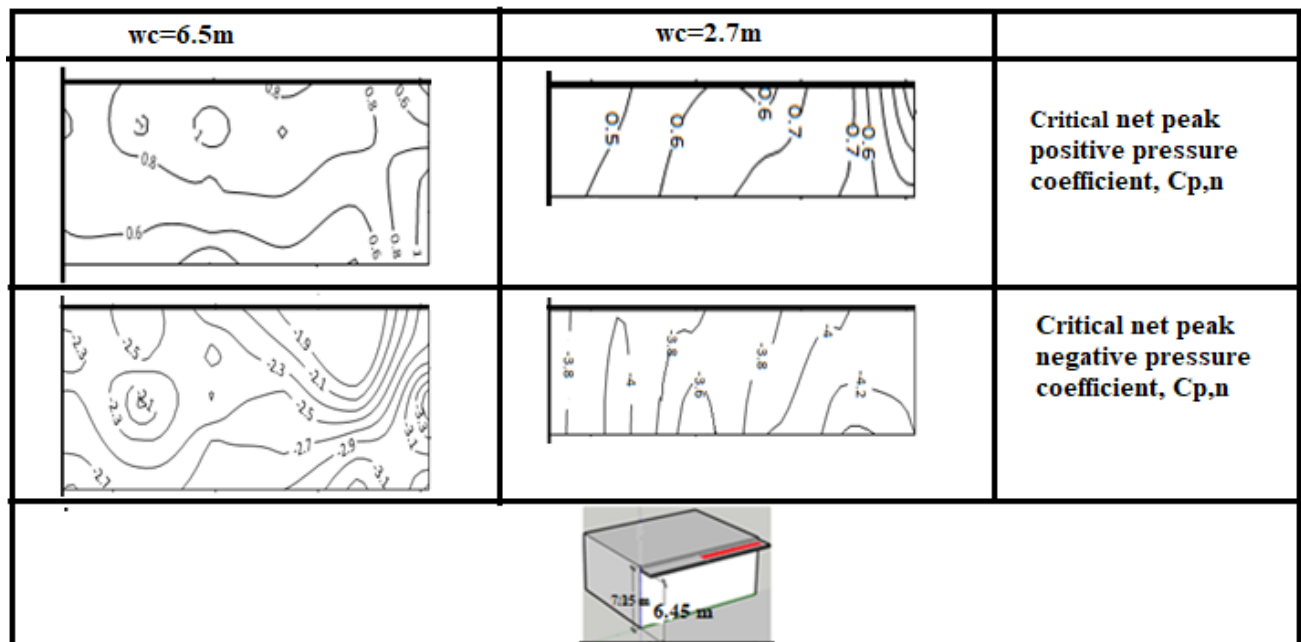
Figure 5.13 Contour plots of net critical peak loading on canopy for different widths for hc/h=0.9 (h=7m)

wc=6.5 m	wc=2.7 m	
		Critical net peak positive pressure coefficient, Cp,n
		Critical net peak negative pressure coefficient, Cp,n
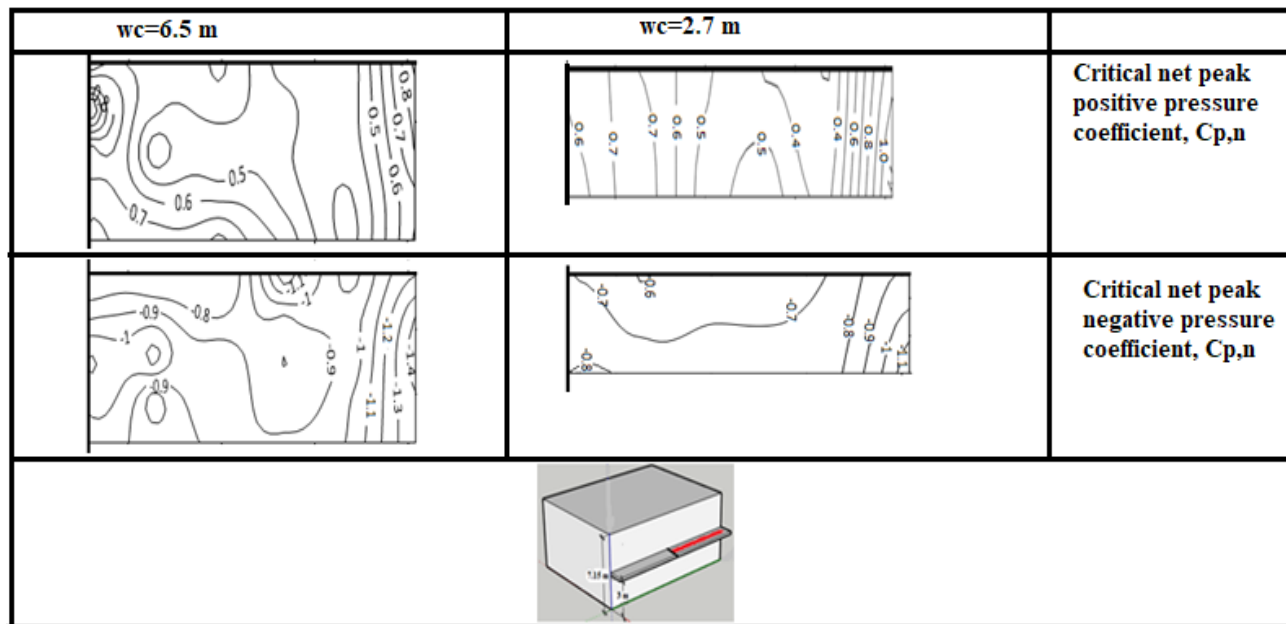
Figure 5.14 Contour plots of net critical peak loading on canopy for different widths for hc/h=0.46 (h=7m)

5.5 Effect of h_c/h and canopy width on net peak C_p values on canopies

The relevant vertical position of canopy with respect to roof height (expressed as h_c/h) is a particularly important parameter for studying wind loading on attached canopies. Positive or negative pressure on upper and lower surface of attached canopy vary greatly with h_c/h ratio. To verify the effect of canopy width, three different canopy widths were tested in this study. Figures 5.15-5.17 show the effect of h_c/h and canopy width on wind loading on canopies attached to buildings of different heights.

In Figure 5.15, only tall building (h=37 m) has been considered. It is clear that wider canopy (w=6.5 m) experienced the highest net peak positive pressure when canopy is close to the ground and narrower canopies (w=2.7 m and 1.5 m) experienced the highest net peak positive pressure

when the canopy is close to the mid height of the parent wall. In case of wider canopy, it is clear that net peak positive C_p value has an inverse relation with hc/h.

The trend for peak negative pressure is opposite. With increase in h_c/h ratio, peak negative pressure (suction) increased. Negative pressure (suction) results from flow separation. Increased velocity facilitates flow separation. So, increase in hc/h should result in increasing suction. Also, parent

Figure 5.15 Peak net Cp values with respect to canopy width and hc/h for h=37 m

Figure 5.16 Peak net Cp values with respect to canopy width and hc/h for h=18.5 m

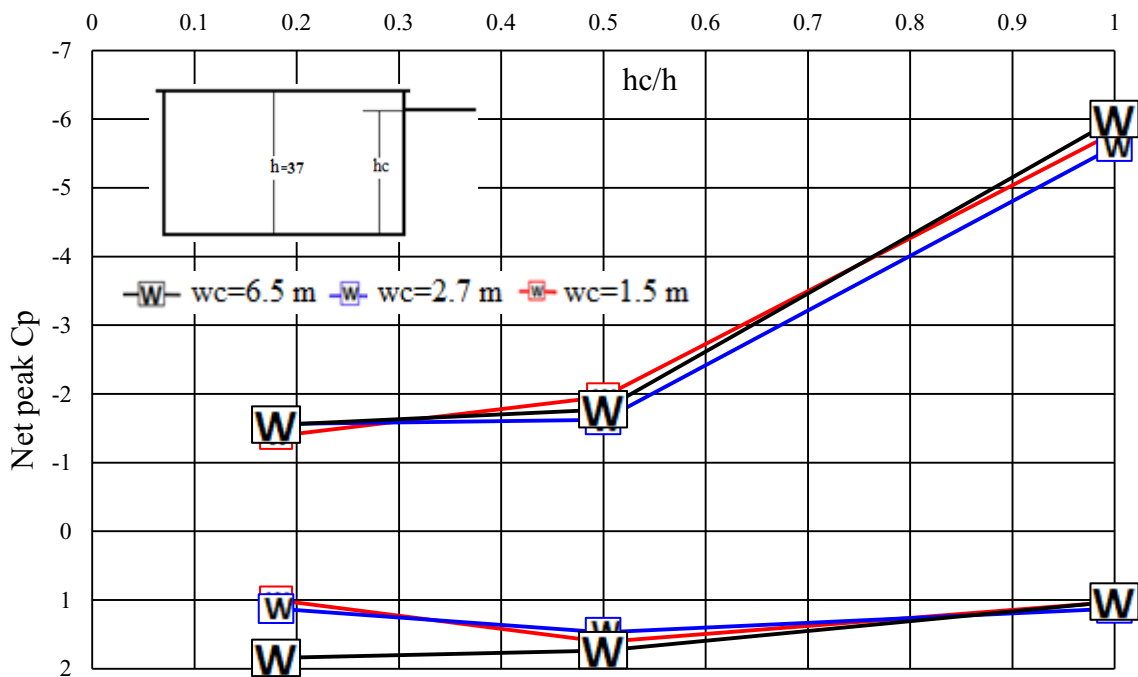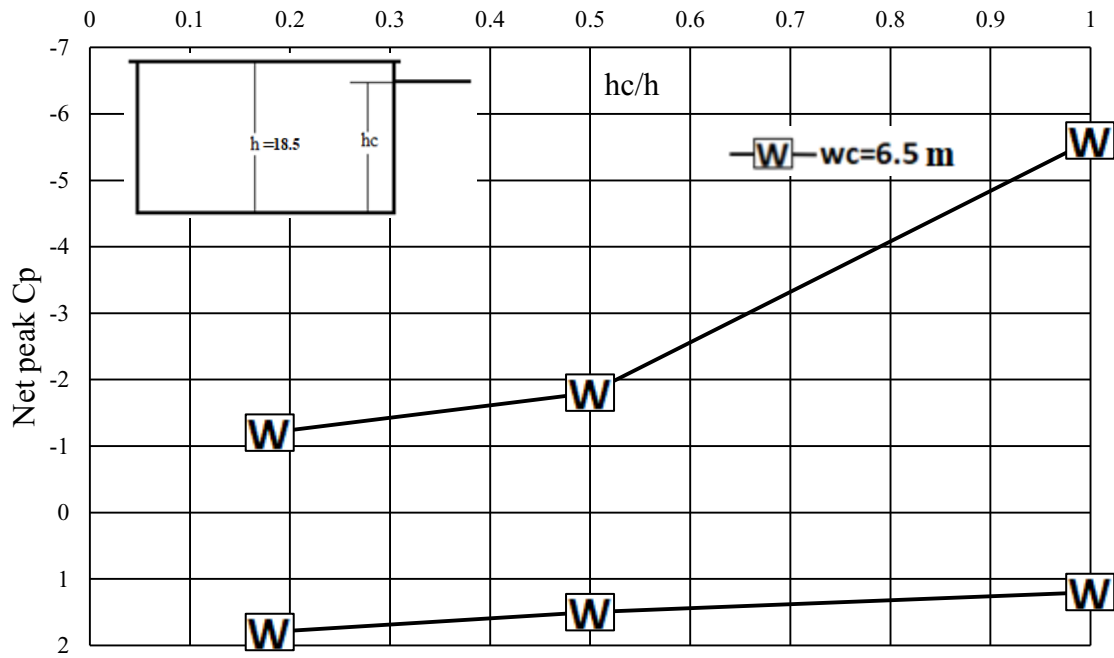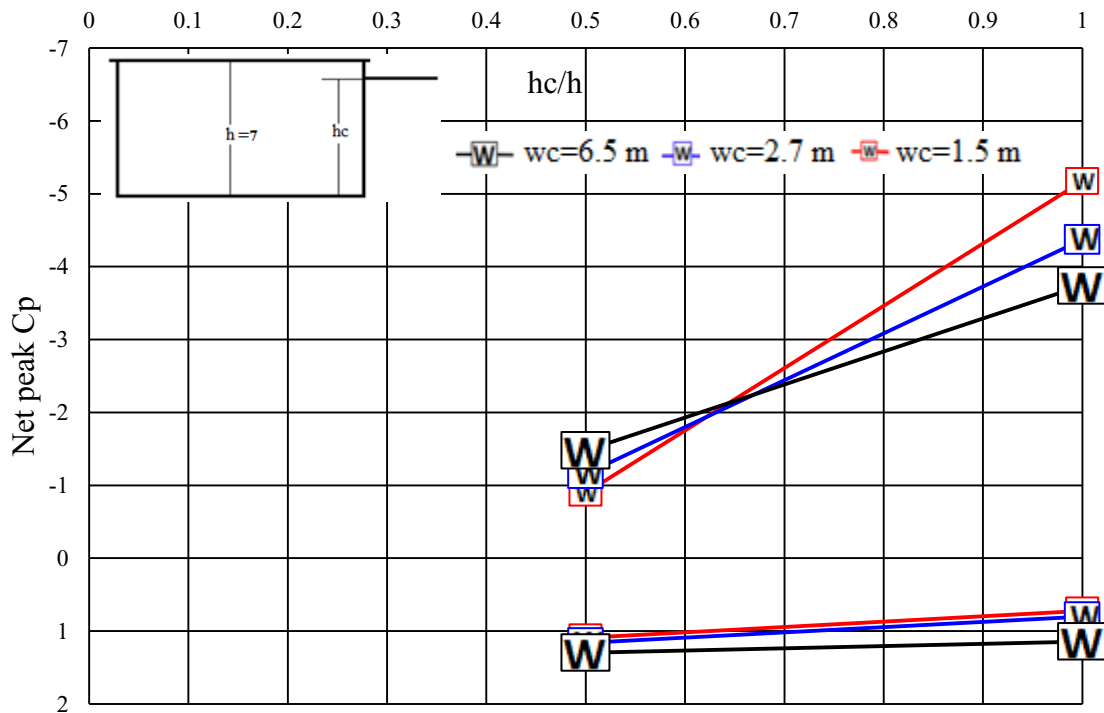Figure 5.17 Peak net Cp values with respect to canopy width and hc/h for h=7 m

94

wall causes flow stagnation which is accountable for positive pressure. But when the canopy is close to the roof, flow stagnation is not a serious issue and the most intense flow separation takes place. This leads to a sudden rise in suction on canopy. An interesting observation is, when $h_c/h \leq 0.5$, the peak negative Cp values are almost constant. But when h_c/h is getting bigger than 0.5, there is quick increase in suction and the highest suction occurs when h_c/h is close to unity. The rise in suction is almost two times. The highest value of net peak negative pressure coefficient (absolute value) is not width dependent, as observed from Figure 5.15.

In Figure 5.16, when the building height is 18.5 m, the same observations are applicable. Experimental results for only one canopy width, 6.5 m, for this building height is available.

For low-rise building, as shown in Figure 5.17, similar observations are true. Only noticeable observation is that canopy width plays a role in case of highest net peak negative (absolute value) pressure coefficients. When canopy is close to the building roof, peak negative pressure increases with decrease in canopy width. For canopy width (w_c) of 1.5 m, 34% more peak negative pressure coefficient (absolute value) is observed than that for w_c of 6.5 m.

5.6 Effect of tributary area on net peak C_p values on canopies

In the previous sections, only local pressure coefficients i.e. C_p from one pressure tap was considered. In order to understand wind loading for large areas, the area averaged values for C_p need to be considered. The area-averaging effect on peak positive and negative C_p was determined by considering single or multiple sets of pressure taps and assigning them to their corresponding effective surface areas. The area average values of C_p are important for design recommendations. In general, while designing small areas (i.e. one nail) C_p from one pressure tap

i.e. 1 ft^2(0.1 m^2) is considered. For larger areas, area average C$_p$ values over corresponding area is considered. This because the area average C$_p$ values decrease with the increase in corresponding area. This phenomenon is illustrated below.

Figures 5.18-5.20 present the area average net peak C$_p$ values for three different h$_c$/h values (canopy at the top, bottom and at the middle) for h=37 m. From Figure 5.18, when the canopy is near the roof, it is easy to observe the effect of considered area for upper surface peak negative C$_p$ values. The peak negative pressure is almost 100% more for 1 ft^2 area than that of for 1000 ft^2 (92.9 m^2) area. Same statement is applicable for net peak positive Cp values with respect to tributary area.

Figure 5.18 Peak net Cp against effective area (ft^2) for hc/h=0.98 for h=37 m

Figure 5.19 Peak net Cp against effective area (ft^2) for hc/h=0.56 for h=37 m

Figure 5.20 Peak net Cp against effective area (ft^2) for hc/h=0.18 for h=37 m

In Figure 5.19, canopy is situated near the mid-height of the building. In case of net peak negative C_p, the highest value (absolute) is almost double than the lowest value. Change in net peak positive C_p values due to change in considered area is noticeable here. For peak positive C_p, there is a 200% rise in C_p value due to reduction of considered area on both surfaces.

In Figure 5.20, when the canopy is close to the ground, the variation in peak negative C_p value is more than double, almost 200%. The variation in net peak positive C_p value is around 100% due to the change in tributary area.

Figure 5.21 Peak net Cp against effective area (ft^2) for hc/h=0.97 for h=18.5 m

Figure 5.22 Peak net Cp against effective area (ft^2) for hc/h=0.57 for h=18.5 m
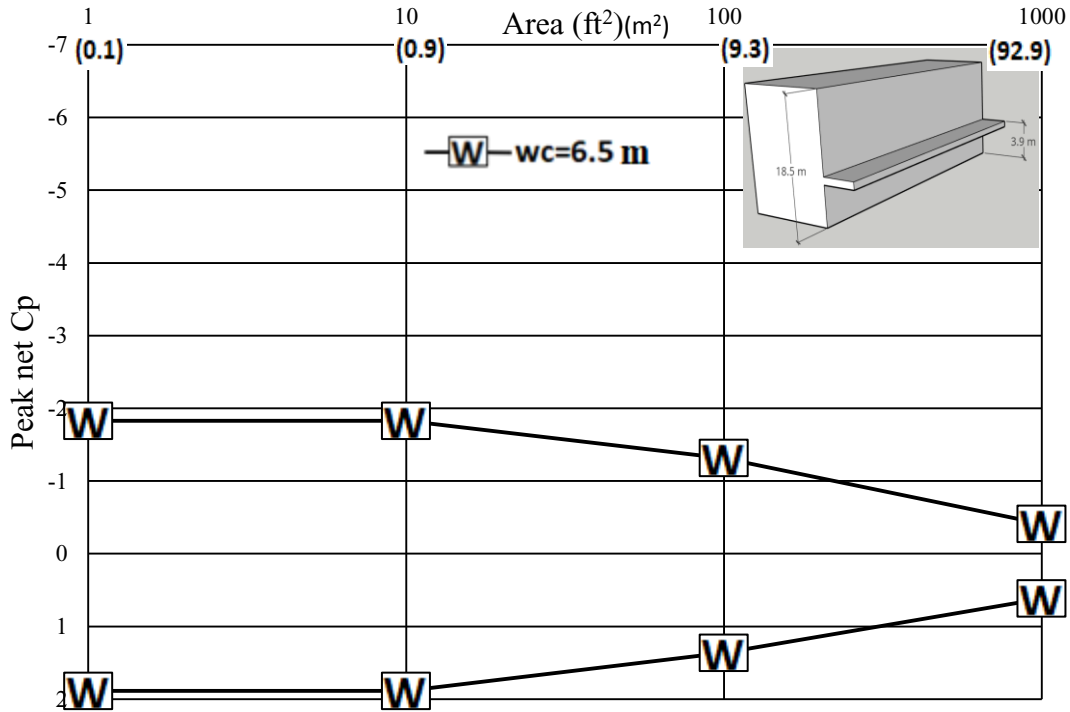
Figure 5.23 Peak net Cp against effective area (ft^2) for hc/h=0.21 for h=18.5 m

Figures 5.21-5.23 present the area average peak C_p values for three different h_c/h values (canopy at the top, bottom and at the middle) for h=18.5 m. Only one canopy width (w=6.5 m) was considered for this building height.

Figure 5.21 shows 44% increase in suction on the upper surface of the canopy when the area average is smaller. The variation in peak positive C_p is negligible when the canopy is located near the roof)

In Figure 5.22, canopy is close to the mid height of the building. In this position, the highest net peak negative Cp value (absolute value) is more than double of the lowest value (absolute). Same observation is made for net peak positive values. The same conclusions can be drawn from Figure 5.23 when the canopy is near the ground.
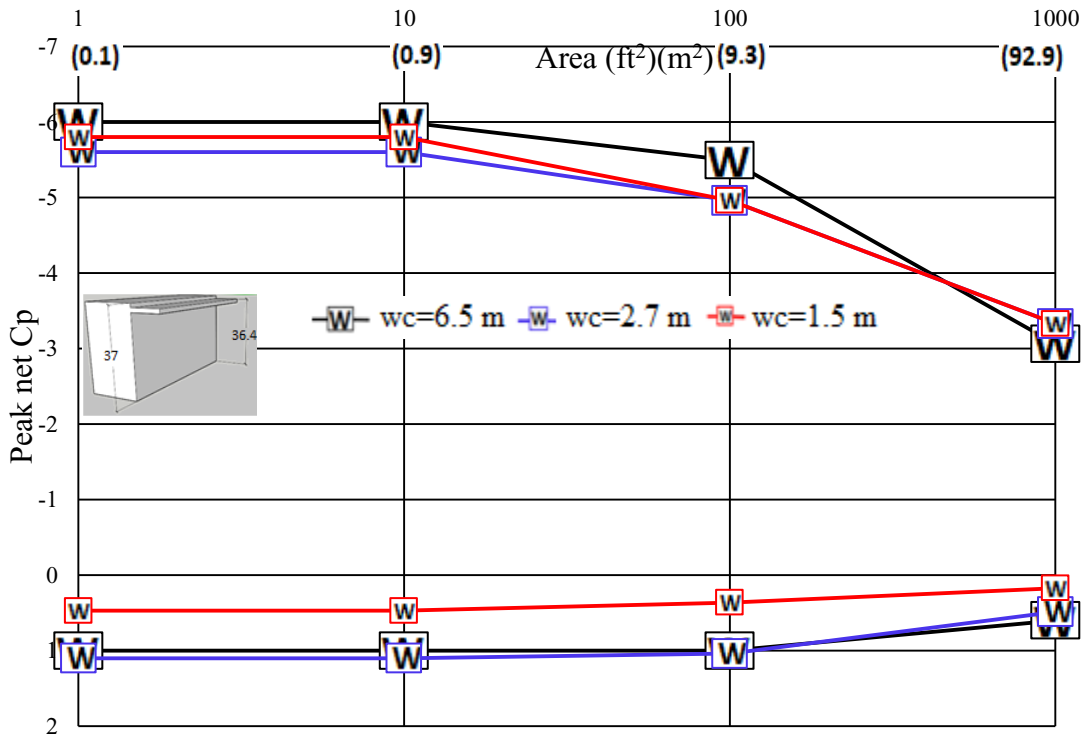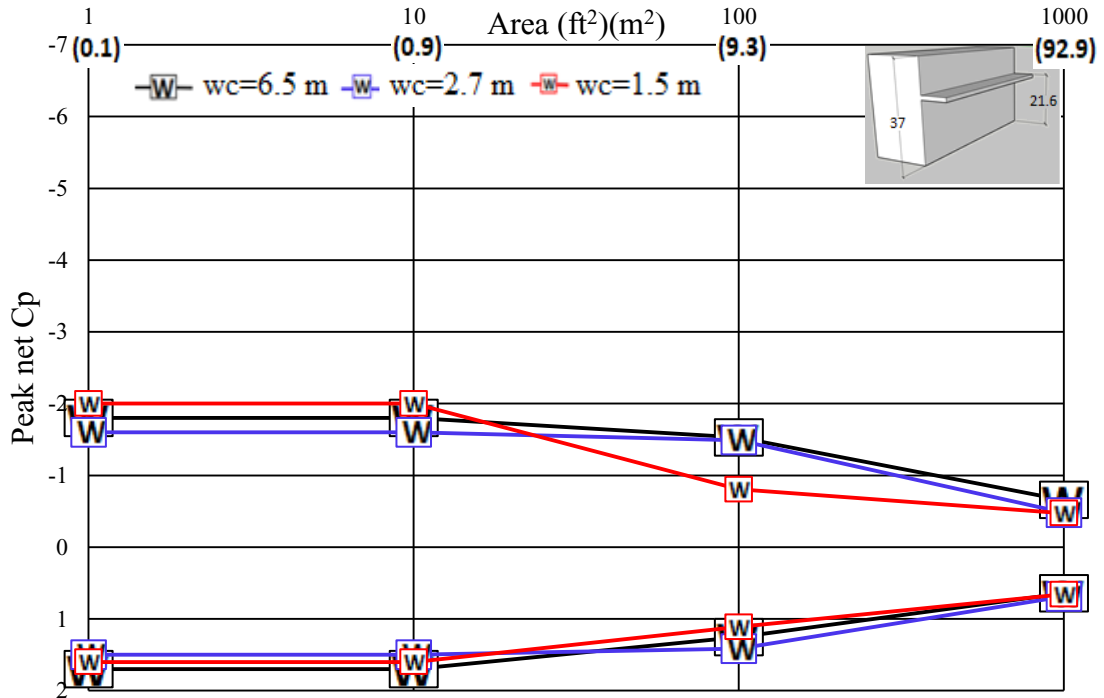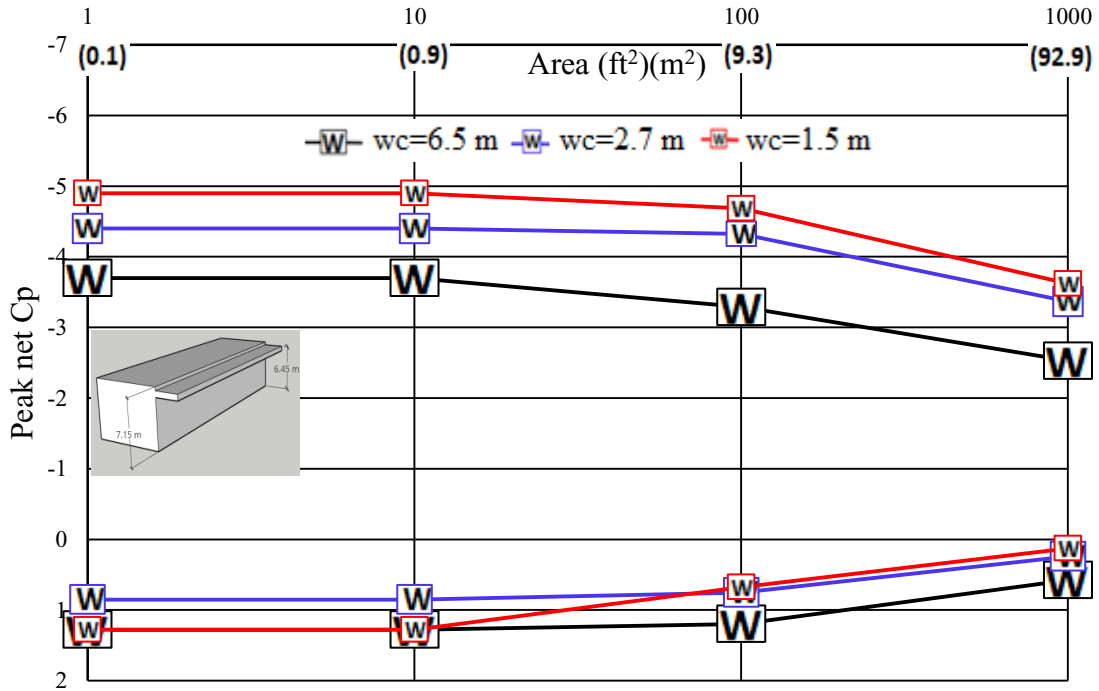
Figure 5.24 Peak net Cp against effective area (ft2) for hc/h=0.9 for h=7 m

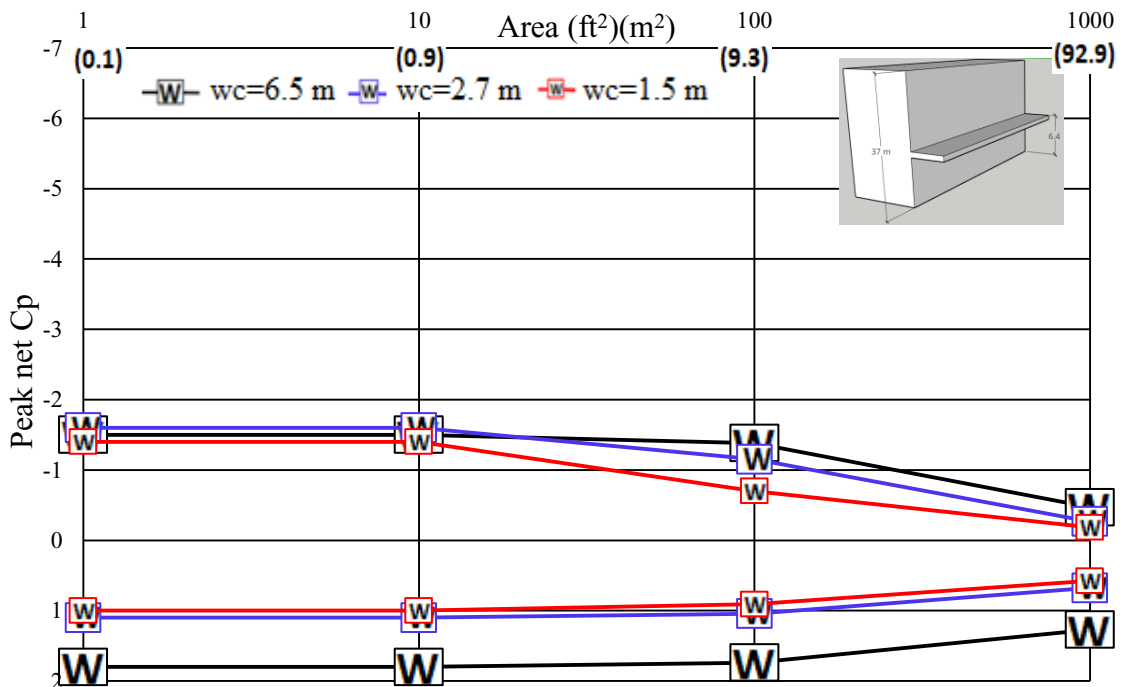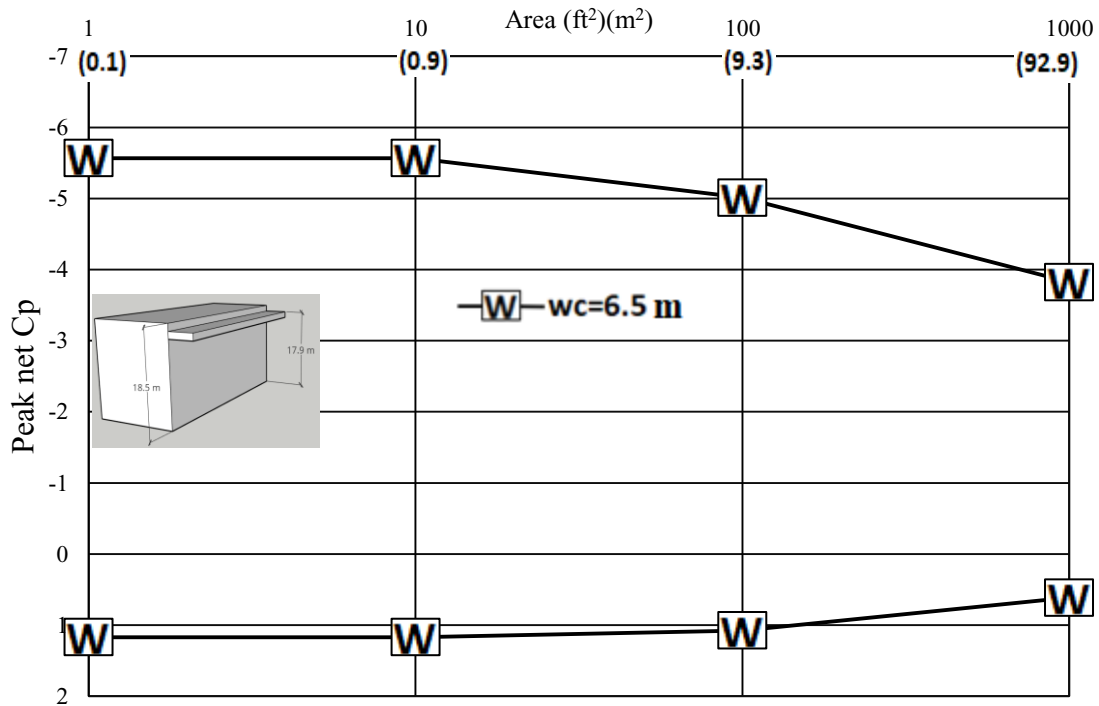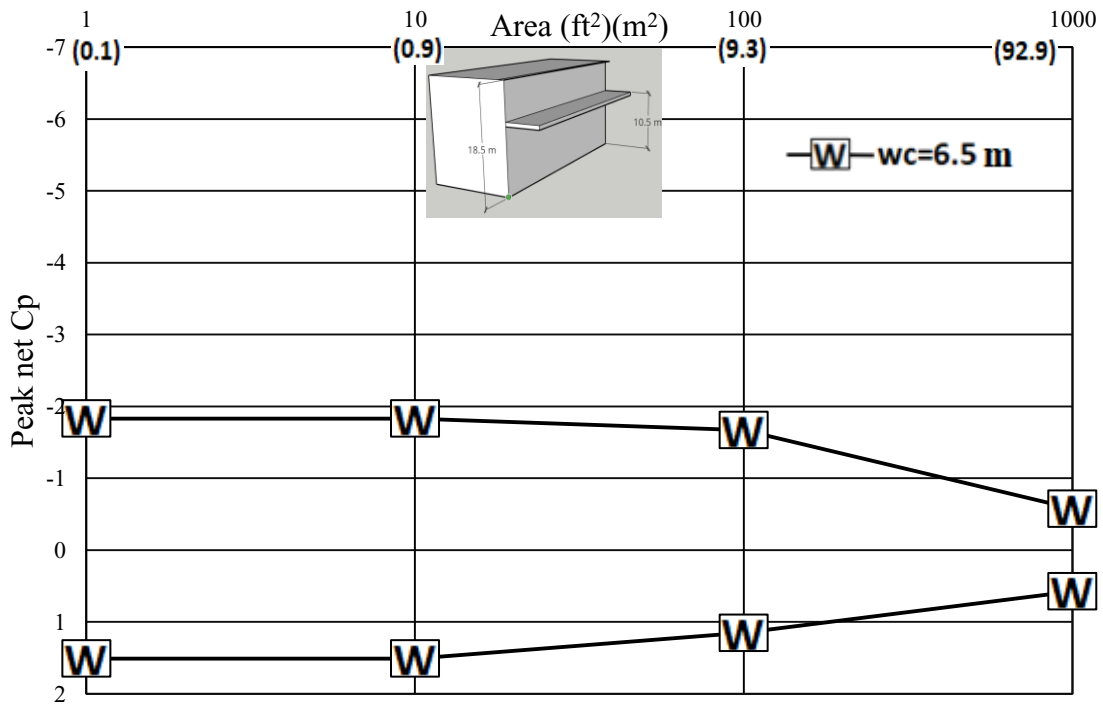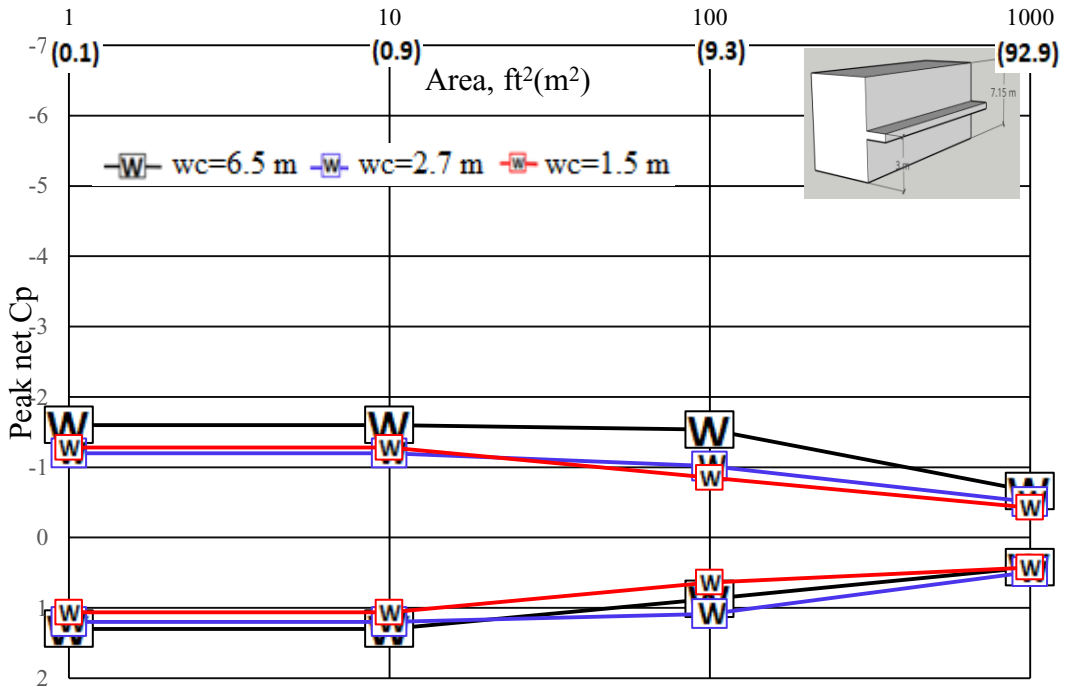Figure 5.25 Peak net Cp against effective area (ft^2) for hc/h=0.46 for h=7 m

Figures 5.24 and 5.25 present the area average net peak C_p values for two different h_c/h (canopy at the top and at the middle) for the low-rise building (h=7 m). Figure 5.24 shows that highest net peak negative C_p (absolute value) is 43% higher than the lowest net peak C_p value. In case of net peak positive C_p values, there is 100% increase due to reduced tributary area. This is also true for the net peak positive and C_p values in Figure 5.25. In fact, the increase in suction is more than 100% is Figure 5.18 due to reduced considered area.

In general, net peak positive C_p values for 1 ft^2 (0.1 m^2) is around double of the net peak positive Cp values for 1000 ft^2 (92.9 m^2). This is also applicable in case of net peak negative C_p except when the canopy is placed at the top.

Chapter 6   Towards Codification of Wind Loading on

Attached Canopies

6.1 General

One of the major aims of the study was to provide design guideline for canopies attached to building taller than 60 feet. This section provides recommendations for the wind loading design of attached canopies. The proposed pressure coefficients here presented are the results of the analyses and observations made in Chapters 4 and 5.   Comparisons between the present recommendations and the AS/NZS and the DIN design guidelines for net pressure coefficients are provided. These guidelines are the results of the previously discussed studies of Jancauskas and Holmes (1985) and Hölscher et al. (2007). Additional comparisons with the ASCE 7-16 provisions for canopies attached to buildings with height less of equal to 60 feet are provided to assess the differences that practitioners may encounter when designing canopies for taller building. It is to be noted that all pressure coefficients presented from here on have been converted to conform to a 3-sec gust averaging period for codification purposes. The conversions where approximated by use of the Durst curve for gust duration (Durst 1960).

6.2 Proposed pressure coefficient values for upper and lower surfaces

Recommended pressure coefficients for the design of upper and lower surfaces of attached canopies are presented in Figure 6.1. These pressure coefficients have been obtained from the envelopes of all experimental data obtained for upper and lower surfaces of canopies (see Figures 4.19, 4.20, 4.21, 4.22, 4.23 and 4.24). A directionality factor of 0.85 has been applied to all envelopes to account for the unlikelihood that the critical wind speed occurs at the critical

wind direction for a specific building configuration. These recommended design values are given as a function of the effective area of the canopy considered.

Figure 6.1 Proposed GCp values for upper and lower surface of attached canopy

6.3   Proposed net pressure coefficients

Net pressure coefficients for the design of attached canopies are presented in Figure 6.2. These coefficients have been obtained from the envelopes of all experimental data obtained for upper and lower surfaces of attached canopies (Figures 5.18, 5.19, 5.20, 5.21, 5.22, and 5.23). A directionality factor of 0.8 has been applied to all envelopes to account for the unlikelihood that the critical wind speed occurs at the critical wind direction for a specific building configuration. These recommended design values are given as a function of the effective area of the canopy considered.
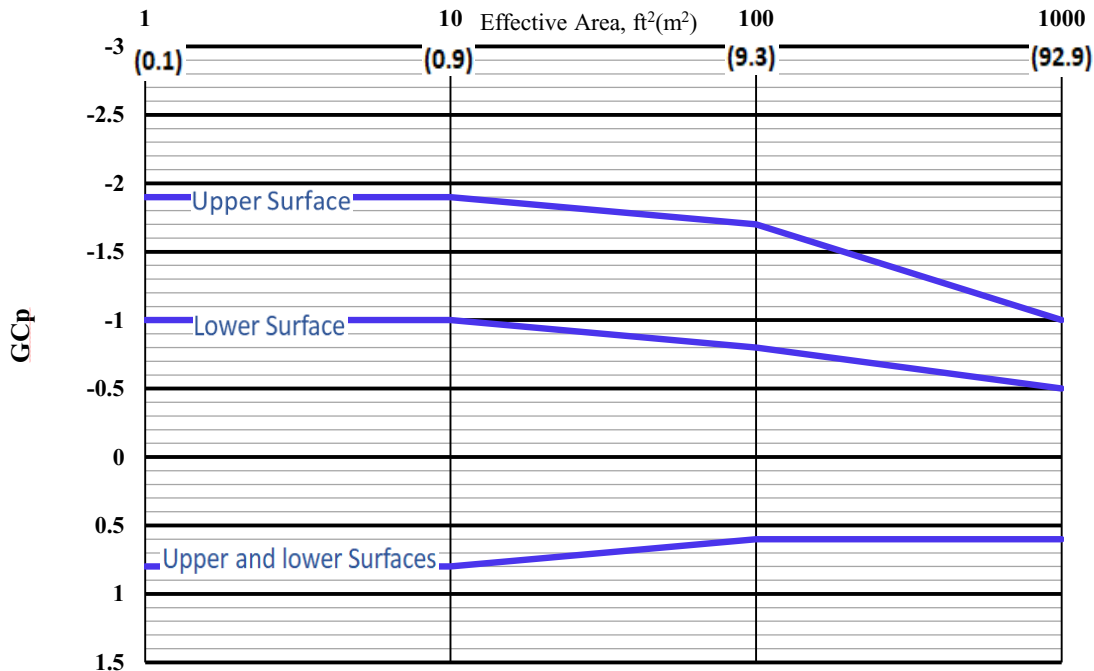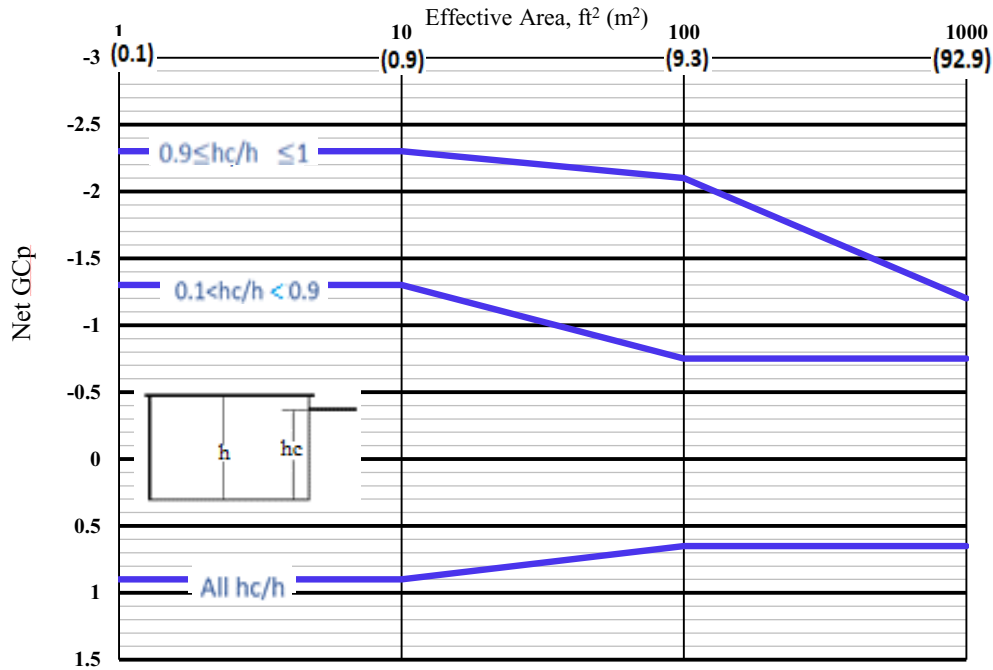
Figure 6.2 Proposed net pressure coefficients for attached canopy

6.4 Comparison with existing provisions

In Figure 6.3 and 6.4, the suggested GCp values from this study have been compared with the recommendations from AS/NZS with respect to hc/h and effective area, respectably. We can see that from hc/h=1 to hc/h=0.6, the recommendations of present study have a good agreement with AS/NZS recommendations. In case of positive pressure coefficients, a close agreement between the current study and AS/NZS is observed. From Figure 6.4, when the canopy is near the roof, we can see some agreement between the current study and AS/NZS, specially for small area. AS/NZS suggests lower net GCp values (in magnitude) for hc/h=0.5. In the case of positive GC_p, AS/NZS suggests higher positive values than the present study, especially for the small area. For larger areas, suggested GC_p values from the current study are comparable to the values provided in AS/NZS.
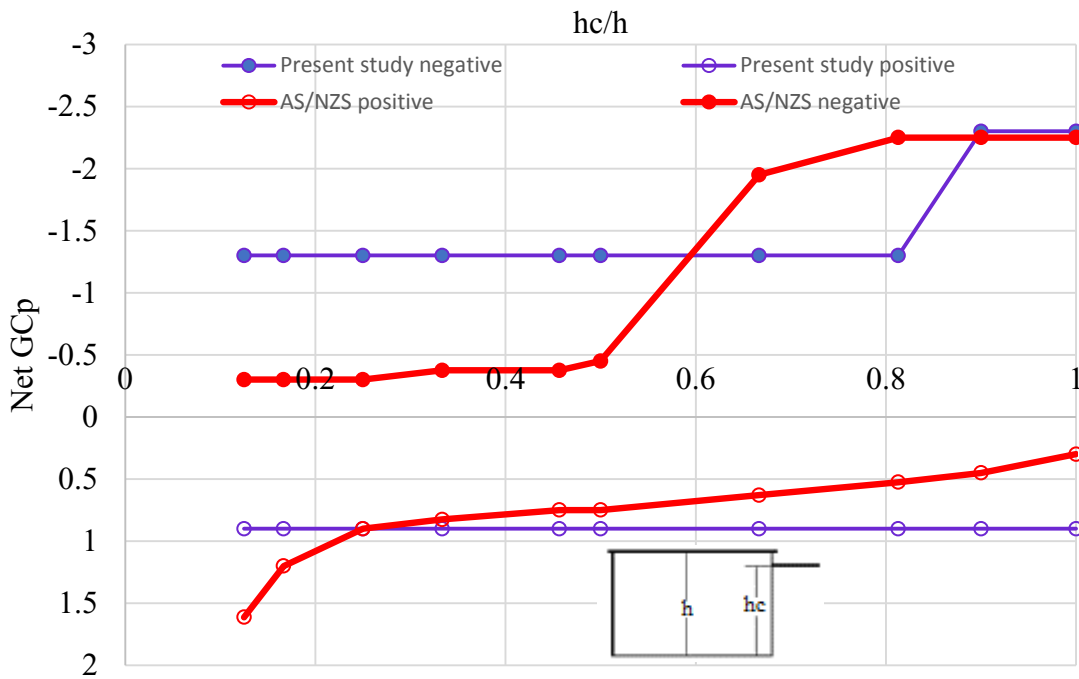
Figure 6.3 Comparison between recommendation from present study and AS/NZS recommended values with respect to hc/h
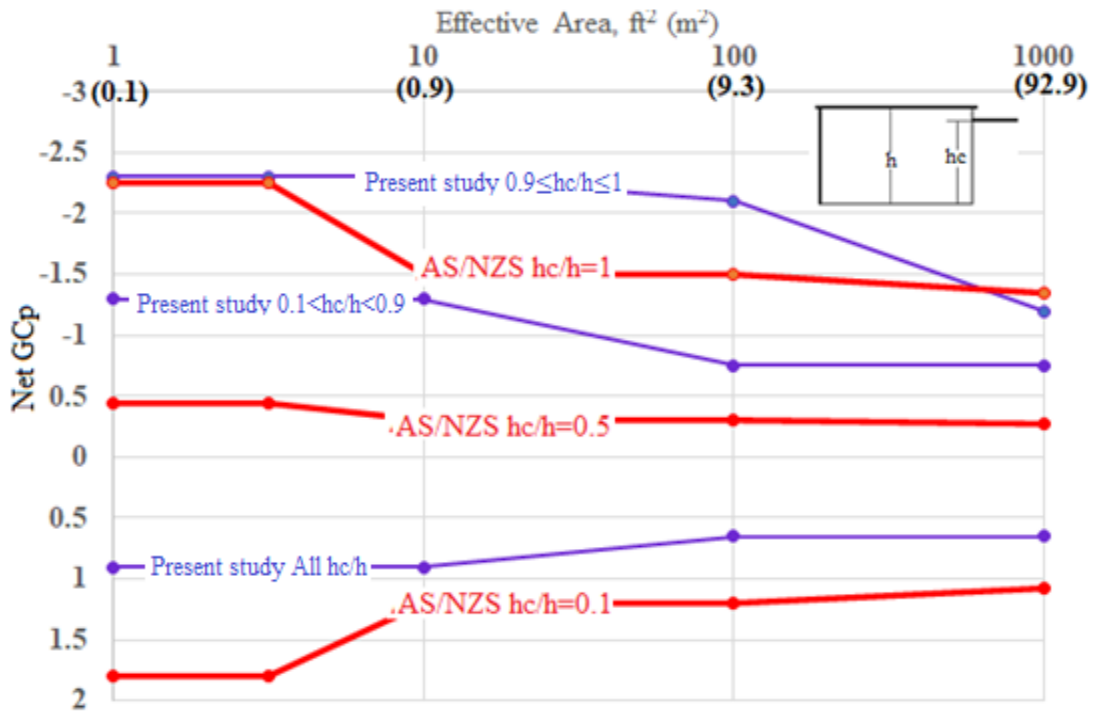
Figure 6.4 Comparison between recommendation from present study and AS/NZS recommended values with respect to effective area
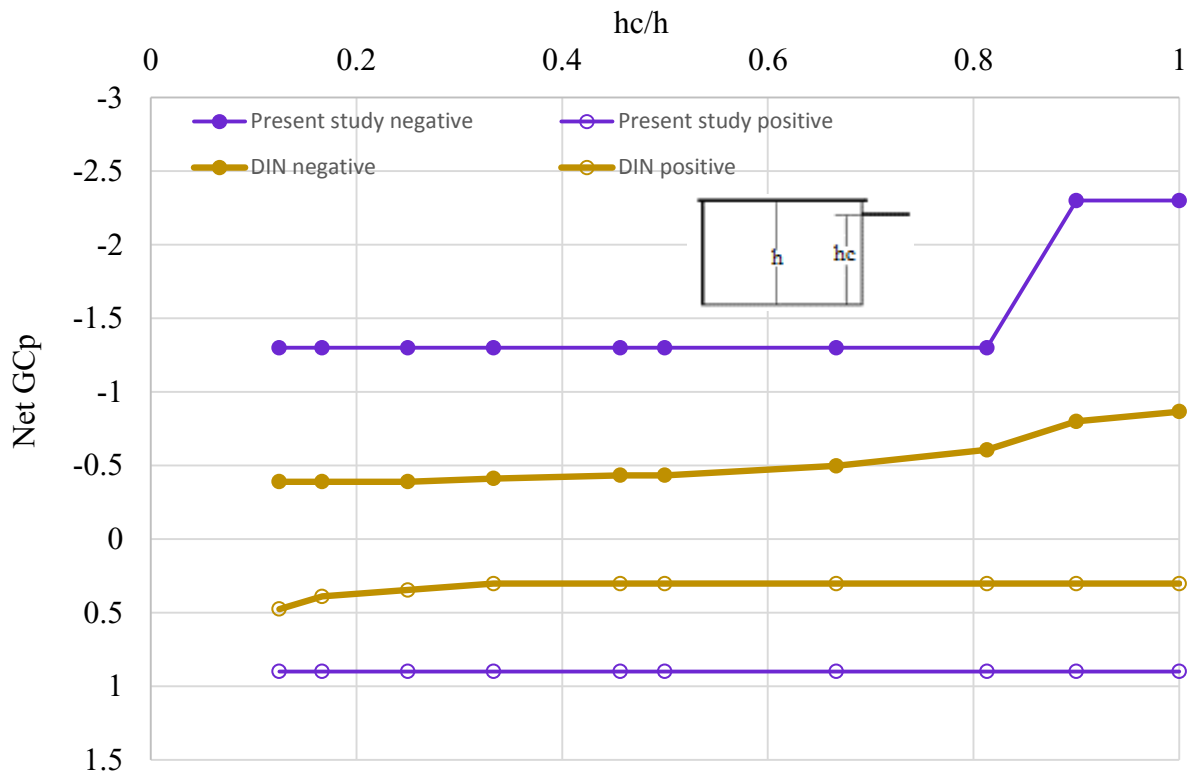
Figure 6.5 Comparison between recommendation from present study and Hölscher et al. (year) recommended values with respect to hc/h

Figure 6.5 shows net GC_p values from this study and suggestions from Hölscher et al. (2007), which is the basis for the wind loading provision for canopies in DIN. It is observed that in both cases (positive and negative) Hölscher et al. (2007) is recommending considerably lower values.

In Figure 6.6, net GC_p values recommended in the present study are compared with those from the Indian code (IS:875(Part 3), 2015). Overall, a good agreement is observed, especially when the canopy is close to the roof (hc/h>0.6). Good agreement is also observed when the canopy is near the ground. However, the present study is suggesting a lower positive net GC_p value when hc/h is close to 0.1.
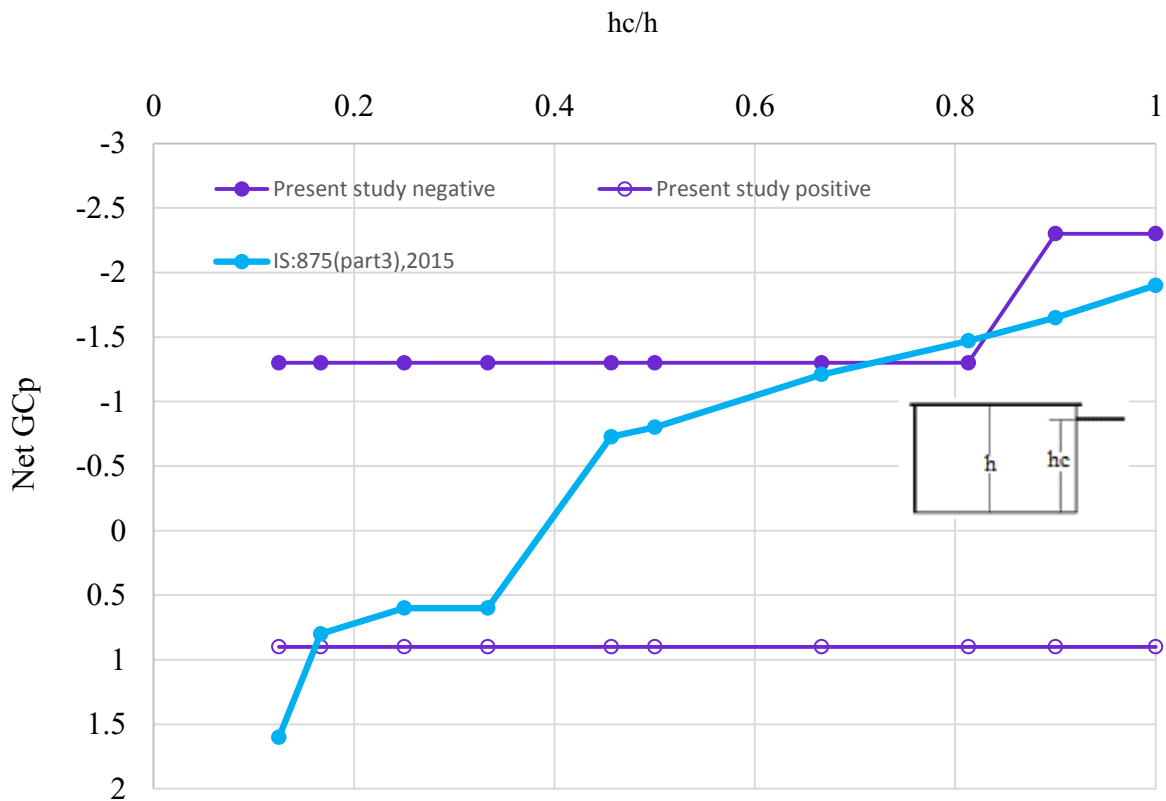
Figure 6.6 Comparison between recommendation from present study and recommendation from Indian code with respect to hc/h

ASCE 7-16 has guidelines to design canopies attached to buildings no taller than 60 feet. As present study is providing guidelines for canopies attached to building taller than 60 feet, Figure 6.7 presents a comparison between these two recommendations. It is clear that ASCE 7-16 provisions are not adequate for canopies attached to buildings taller that 60 feet. Net negative GC_p values for attached canopies with taller buildings are higher than those for canopies attached with low-rise buildings, both when $0.1 < hc/he < 0.9$ and $0.9 \leq hc/he \leq 1.0$.
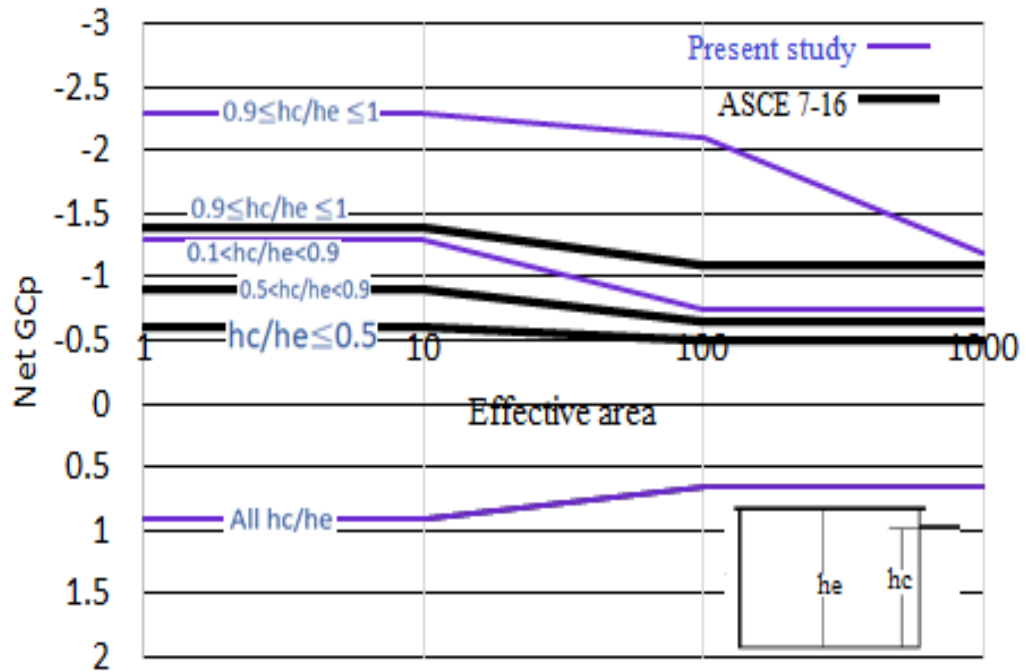
Figure 6.7 Comparison between recommendation from present study and recommendation from ASCE 7-16 with respect to effective area

Chapter 7   Summary, Conclusions and Recommendations

7.1 Summary

Wind tunnel experiments were conducted on a total of 24 different configurations to observe and study the effect of wind loading on attached canopies. The effect of several major parameters such as building height, wind direction, hc/h (canopy height to building eave height ratio), canopy width and effective area on pressure coefficients were examined. It was found that the peak pressure coefficient can be obtained from different wind directions depending on the geometric configuration of the building and canopy. Both local and area-averaged pressure coefficients were calculated. Net pressure coefficients (Cp,n) along with pressure coefficients acting on upper and lower surfaces (Cp,upper and Cp,lower) of the canopies were calculated. All pressure coefficients were analysed against the above-mentioned parameters to understand the trends and relationships that they exhibit with each other. Contours of net pressure coefficients and pressure coefficients on the upper and the lower surfaces were presented to provide a better understanding of the flow patterns occurring around the canopy. Finally, recommended design guidelines for canopies attached buildings taller than 60 feet were provided based on the results from the tests. The recommendations of the present study were also compared with the recommendations of AS/NZS 1170.2:2011, Indian Code (IS:875(part 3),2015), DIN EN 1991-1-4/NA:2010-12 and ASCE 7-16.

7.2 Conclusions

The findings of the present study can be summarised as follows:

-Building height plays an important role in case of peak negative pressure for upper surface of canopy. The lower surface experienced almost same peak negative C_p values regardless of building height or h_c/h ratio. For the positive peak values of C_p, for a certain value of h_c/h, canopies attached to taller buildings had higher values than canopies attached to low-rise buildings. In case of relatively taller buildings (h=18.5 m and 37 m), both net mean and peak negative C_p values were close. But canopies attached to lower buildings (h=7 m) were observed to experience about 50% of the suction experienced by canopies attached to taller buildings.

- The study showed that lower surfaces experienced the highest peak positive pressure at 0° or 15° wind angle and the highest peak suction was at 90° wind direction. This was true for the upper surface except when the canopy was near the roof. At this position, upper surface felt highest suction between 15° to 105° wind direction, depending on building height and canopy width. When the canopy was close to the roof, highest (absolute value) net peak negative C_p occurred within 60° and highest net peak positive C_p was found at 90° or higher. When the canopy was close to the mid height, highest suction occurred at 90°. It can be said that if canopy is situated near or below the mid height of the parent wall, the most intense flow separation occurs for a flow parallel to the parent wall.

- The negative pressure mainly affected the edges or the corner areas. The location of positive pressure was found to be a function of on canopy's vertical position. When the canopy was near the roof, the side and front edges of the canopy were most vulnerable due to positive pressure. In other cases, the areas near center line or near to the edge were most vulnerable.

- The relevant vertical position of the canopy with respect to roof height (expressed as h_c/h) was particularly an important parameter for studying wind loading on attached canopies. Net peak negative pressure coefficient increased with increase in h_c/h and net peak positive pressure

111

generally decreased with increase in h_c/h. Positive pressure on upper and lower surface of canopies, respectively, increased and decreased with decrease h_c/h.

-Canopy width was not found to be a critical parameter. However, for low-rise buildings when the canopy is placed at the top of the building, narrower canopies experience more suction than the wider canopies. This observation is also true for peak negative pressure coefficient on the upper surface of the canopy.

- In general, the variation between the highest and the lowest values of peak positive and negative pressure due to change in tributary area was almost double. The upper canopy surface was observed to undergo more than 100% variation between the highest and the lowest value of peak negative C_p (absolute value) when the canopy was close to the roof or near the ground.

7.3 Recommendations for future studies

The following recommendations can be considered in future studies:

- The canopy used in this study was placed along the full length of the parent wall. Canopies with different lengths can be considered in future studies. It will allow to examine the effect of canopy length to parent wall length ratio on pressure coefficients. Also, there may be some cases where canopy is attached to more than one wall of the parent building. This may be worth studying in the future.

- Canopies attached to buildings with different shapes should also be studied to establish any potential difference in findings due to the change in building shape.

- In this study, canopies tested were horizontal. In future studies, canopies with some slope should be tested to check whether there is any significant change in pressure coefficients.

References

AS/NZS 1170.2. Australian/New Zealand Standard for Structural Design Actions, part 2: Wind Actions. Sydney, New South Wales, Australia: Standards Australia and Standards New Zealand; 2011.

ASCE/SEI 7-16. Minimum Design Loads for Buildings and Other Structures. Structural Engineering Institute of ASCE, Reston, VA; 2016.

Candelario, J.D. Wind induced pressures on canopies attached to the walls of low-rise buildings. Master's Thesis, Concordia University, Montreal, Quebec, Canada, 2012.

Candelario, J.D, Stathopoulos, T. and Zisis, I. Wind loading on attached canopies: codification study, J. Struct. Eng., 2014; 140(5): 04014007.

Counihan, J. Adiabatic Atmospheric Boundary Layers: A Review and Analysis of Data from the Period 1880-1972. Atmos. Environ. 1975; 871-905

Davenport, A. G., Stathopoulos, T., and Surry, D. Reliability of wind loading specifications for low buildings. Proc., Int. Conf. on Structural Safety and Reliability, ICOSSAR 85, International Association for Structural Safety and Reliability; 1985.

Davenport, A. G. Past, present and future of wind engineering. Journal of Wind Engineering and Industrial Aerodynamics 2002; 90(12-15): 1371-1380.

Durst, C. S. Wind speeds over short periods of time. Meteorol. Mag. 1960; 89: 181–186.

German Institute for Standardization (DIN). Einwirkungen auf Tragwerke—teil 4: Windlasten DIN1055-4:2005-03, Berlin; 2010.

Goyal, R., Ahuja, A.K., and Prasad. J. Wind loads on buildings with attached canopies, Asian Journal of Civil Engineering 2007; 8(3): 239-246

Holmes, J. D. Wind loading of structures. Spon Press, New York; 2001.

Hölscher, N., Hubert, W., and Niemann, H. J. Normgemäße Erfassung der Windwirkungen an Vordächern. Fachteil WtG, Band 82, April, S. S2–S5; 2007.

IS: 875 (Part-3). Indian Standard code of practice for design loads (other than earthquake) -(Part 3- wind loads) for buildings and structures, Bureau of Indian Standards, New Delhi, India; 2015.

International Code Council. International building code (IBC), Fall Church, Va., 2012a.

International Code Council. International residential code (IRC), Fall Church, Va., 2012b.

Jancauskas, L., and Holmes, J. Wind loads on attached canopies. Proc., National Conf. on Wind Engineering, Texas Tech Univ., Lubbock, TX, 1985.

Jensen, M. The model-law for phenomena in natural wind. Ingenioren - International Edition 1958; 2(4): 121-128. 111

Jensen, M., & Franck, N. Model-scale tests in turbulent wind. Part II. Danish Technical Press; 1965.

National Research Council of Canada. National Building Code of Canada (NBCC), Ottawa, 2015.

Paluch, M.J., Loredo-Souza, A.M. and Blessmann, J. Wind loads on attached canopies and their effect on the pressure distribution over arch-roof industrial buildings. Journal of Wind Engineering and Industrial Aerodynamics 2003; 91: 975–994.

Roh, H.W. and Kim, H.R. Wind pressure distribution on canopies attached to tall buildings, Journal of Mechanical Science and Technology 2011; 25 (7): 1767-1774.

Savory, E., Dalley, S. and Toy, N. The effects of eaves geometry, model scale and approach flow conditions on portal frame building wind loads. Journal of Wind Engineering and Industrial Aerodynamics 1992; 41-44: 1665-1676.

Shiotani, M. Structure of Gusts in High Winds, parts 1-4, The Pysical Sciences laboratory, Nikon University, Furabachi, Chiba, Japan, 1971.

Scanivalve Corporation, ZOC 33/64Px – Electronic Pressure Scanning Module, Instruction and Service Manual

Scanivalve Corporation, DSMLINK V2.90, Installation and Operation Manual

Scanivalve Corporation, DSM 3000 – Digital Service Module, Instruction and Service Manual

Simiu, E., and Scanlan, R. Wind Effects on Structures: Fundamentals and Applications to design, 3rd Ed.,Wiley & Sons, New York., 1996.

Stathopoulos, T. & Surry, D. Scale effects in wind tunnel testing of low buildings. Journal of Wind Engineering and Industrial Aerodynamics 1983; 13(1-3): 313-326.

Stathopoulos, T. Design and fabrication of a wind tunnel for building aerodynamics. Journal of Wind Engineering and Industrial Aerodynamics 1984; 16(2-3): 361- 376.

Stathopoulos, T. Wind Loads on Low-Rise Buildings: A Review of the State of the Art. Engineering Structures 1985; 6 (2): 119-135

Stathopoulos, T. and Luchian, H. Wind induced forces on eaves of low building, Journal of Wind Engineering and Industrial Aerodynamics, 1994; 52: 249-261.

Tieleman, H. W., Hajj, M. R., & Reinhold, T. A. Wind tunnel simulation requirements to assess wind loads on low-rise buildings. Journal of Wind Engineering and Industrial Aerodynamics 1998; 74-76: 675-685.

Tieleman, H. W., Reinhold, T. A., & Marshall, R. D. On the wind-tunnel simulation of the atmospheric surface layer for the study of wind loads on low-rise buildings. Journal of Wind Engineering and Industrial Aerodynamics 1978; 3(1): 21-38.

Uematsu, Y., Iizumi, E., and Stathopoulos, T. Wind force coefficients for designing free-standing canopy roofs. Journal of Wind Engineering and Industrial Aerodynamics 2007; 95 (9-11): 1486–1510.

Uematsu, Y., Stathopoulos, T., and Iizumi, E. Wind loads on free-standing canopy roofs: Part 1. Local wind pressures. Journal of Wind Engineering and Industrial Aerodynamics 2008a; 96 (6-7): 1015–1028.

Uematsu, Y., Stathopoulos, T., and Iizumi, E. Wind loads on free-standing canopy roofs: Part 2. Overall wind forces. Journal of Wind Engineering and Industrial Aerodynamics 2008b; 96 (6-7): 1029–1042.

Wiik, T. and Hansen, E.W.M. The assessment of wind loads on roof overhang of low-rise Buildings, Journal of Wind Engineering and Industrial Aerodynamics, 1997; 67&68: 687-696.

Zisis, I. and Stathopoulos, T. Wind-Induced Pressures on Patio Covers, Journal of Structural Engineering 2010; 136 (9): 1172–1181.

Zisis, I, Raji, F, and Candelario, J. Large Scale Wind Tunnel Tests for Canopies Attached to Low-rise Buildings. Journal of Architectural Engineering 2017; 23(1): B4016005.